TECHNICAL REPORT STANDARD TITLE PAGE

1. Report No.	2. Government Accession No.	3. Recipient's Catalog No.
FHWA/TX-81/09+211-3F		

4. Title and Subtitle	5. Report Date
Field Tests and New Design Procedure for Laterally Loaded Drilled Shafts in Clay	January 1981
	6. Performing Organization Code
7. Author(s)	8. Performing Organization Report No.
Mark W. Bierschwale, Harry M Coyle, and Richard E. Bartoskewitz	Research Report 211-3F
9. Performing Organization Name and Address	10. Work Unit No.
Texas Transportation Institute The Texas A&M University System College Station, Texas 77843	11. Contract or Grant No. Study No. 2-5-77-211
	13. Type of Report and Period Covered
12. Sponsoring Agency Name and Address	Final-September, 1976 August, 1980
State Department of Highways and Public Transportation; Transportation Planning Division P. O. Box 5051 Austin, Texas 78763	14. Sponsoring Agency Code

15. Supplementary Notes

Research performed in cooperation with DOT, FHWA.
Study Title: Design of Drilled Shafts to Support Precast Panel Retaining Walls

16. Abstract

Lateral load tests were conducted on three drilled shafts in predominantly CH soil. Shaft sizes varied from 30 in. (760 mm) to 36 in. (910 mm) in diameter and 15 ft. (4.6 m) to 20 ft. (6.1 m) in length. Loads were applied incrementally at a point 2.6 ft (790 mm) above the ground surface. Duration of the tests was 57, 24 and 205 days. Measurements of lateral earth pressure at various points along the length of the shaft, displacement near the ground surface, and rotation in the plane of loading were obtained for each increment of load. Additional data on five shafts tested under similar conditions were obtained from the literature.

Based upon an analysis of the test data, the ultimate lateral load capacity of a rigid shaft was defined as the load required to produce a shaft rotation of 2 degrees. This definition was used to obtain an empirical correlation of rotation with lateral load. A correlation of the coefficient of ultimate resistance at the groundline, N_p, with soil shear strength was also made. A design procedure utilizing the two correlations was developed.

Several analytical methods described in the literature were used to calculate the capacity of the eight test shafts. The results were compared with computed capacities obtained by use of the design procedure developed for this research study.

17. Key Words	18. Distribution Statement
Design procedure, drilled shafts, field tests, lateral load, pressure cells, ultimate resistance.	No Restrictions. This document is available to the public through the National Technical Information Service, Springfield, Virginia 22161

19. Security Classif. (of this report)	20. Security Classif. (of this page)	21. No. of Pages	22. Price
Unclassified	Unclassified	129	

Form DOT F 1700.7 (8-69)

FIELD TESTS AND NEW DESIGN PROCEDURE FOR LATERALLY LOADED DRILLED SHAFTS IN CLAY

by

Mark W. Bierschwale
Research Assistant

Harry M. Coyle
Research Engineer

and

Richard E. Bartoskewitz
Engineering Research Associate

Research Report No. 211-3F

Design of Drilled Shafts to Support Precast Panel Retaining Walls
Research Study Number 2-5-77-211

Sponsored by
State Department of Highways and Public Transportation
in Cooperation with the
U.S. Department of Transportation
Federal Highway Administration

January 1981

TEXAS TRANSPORTATION INSTITUTE
Texas A&M University
College Station, Texas

Disclaimer

The contents of this report reflect the views of the authors who are responsible for the facts and accuracy of the data presented herein. The contents do not necessarily reflect the views or policies of the Federal Highway Administration. This report does not constitute a standard, specification or regulation.

There was no invention or discovery conceived or first actually reduced to practice in the course of or under this contract, including any art, method, process, machine, manufacture, design or composition of matter, or any new and useful improvement thereof, or any variety of plant which is or may be patentable under the patent laws of the United States of America or any foreign country.

ABSTRACT

Lateral load tests were conducted on three drilled shafts in predominantly CH soil. Shaft sizes varied from 30 in. (760 mm) to 36 in. (910 mm) in diameter and 15 ft (4.6 m) to 20 ft (6.1 m) in length. Loads were applied incrementally at a point 2.6 ft (790 mm) above the ground surface. Duration of the tests was 57, 24 and 205 days. Measurements of lateral earth pressure at various points along the length of the shaft, displacement near the ground surface, and rotation in the plane of loading were obtained for each increment of load. Additional data on five shafts tested under similar conditions were obtained from the literature.

Based upon an analysis of the test data, the ultimate lateral load capacity of a rigid shaft was defined as the load required to produce a shaft rotation of 2 degrees. This definition was used to obtain an empirical correlation of rotation with lateral load. A correlation of the coefficient of ultimate resistance at the groundline, N_p, with soil shear strength was also made. A design procedure utilizing the two correlations was developed.

Several analytical methods described in the literature were used to calculate the capacity of the eight test shafts. The results were compared with computed capacities obtained by use of the design procedure developed for this research study.

KEY WORDS: Design Procedure, Drilled Shafts, Field Tests, Lateral Load, Pressure Cells, Ultimate Resistance.

SUMMARY

This report presents the results obtained during the fourth year of a four year study on drilled shafts that are used to support precast panel retaining walls. A summary of data from the two previous tests conducted for this study is included. The objective of the study was to develop criteria for the design of foundations for this purpose.

A drilled shaft sustaining a lateral load may behave as either a flexible or rigid foundation member. During the first year it was determined that many drilled shafts that are used in this manner can be designed or analyzed as rigid structural members. The first part of this report discusses the characteristics and behavior for both flexible and rigid shafts in addition to briefly summarizing research which has been undertaken in recent years relating to the design of rigid shafts.

During the final year of this study, a lateral load test was conducted on a 2.5 ft diameter by 15 ft deep instrumented drilled shaft founded in a clay soil. During this test, long-term or sustained lateral loads were applied to the test shaft. The purpose of this phase of the study was to determine if the application of long-term sustained loads would result in excessive time-dependent deformations. For each increment of the applied lateral load the shaft rotation, soil resistance, and lateral deflection were measured.

Using the results of the three field load tests conducted during this study and five load tests reported in the literature, the ultimate capacity for rigid shafts was defined as the load which corresponds to a shaft rotation of 2 degrees. Based upon this definition, an empirical correlation was derived relating lateral load to rotation. This correlation enables the engineer to predict a load-rotation curve for a

particular size shaft up to a rotation of 2 degrees. Also, using the results of the eight load tests, various analytical methods were employed to compute the capacity of the shafts. Comparisons were made between measured field lateral capacities at 2 degrees of rotation with those predicted by the analytical methods. Based upon these comparisons and a correlation developed relating soil shear strength to the ultimate resistance coefficient, N_p, at the groundline, a recommended design procedure for rigid laterally loaded drilled shafts was formulated.

Use of the recommended design procedure results in excellent agreement between measured and predicted ultimate lateral capacities, and predicted and measured rotations between 0 and 2 degrees. In addition, the procedure allows the engineer to design a shaft such that the amount of rotation may be limited to a specified amount.

IMPLEMENTATION STATEMENT

A recommended procedure has been developed for the design of rigid laterally loaded drilled shafts founded in clay and used to support precast panel retaining walls. However, the procedure can be employed for other highway industry related applications. This procedure was developed from the results of eight field load tests conducted on shafts similar to those that would be used in practice. Based upon these load test results, the ultimate capacity of a drilled shaft was defined as the lateral load corresponding to a shaft rotation of 2 degrees. Using this definition, an impirical correlation was derived relating ultimate load to shaft rotation. An important feature in the design of retaining walls, as well as other structures, is the allowable amount of rotation. Recognizing this fact, it appears that drilled shafts for this purpose may be realistically designed on the basis of a limiting value of rotation in conjunction with a required lateral load. The design procedure presented herein enables the engineer to design the shaft such that the amount of rotation may be limited to a specified amount. It is recommended that this design procedure be implemented by the sponsoring agencies.

ACKNOWLEDGEMENTS

Funding for this research study was made possible through cooperative sponsorship by the Texas State Department of Highways and Public Transportation and the Federal Highway Administration. The support provided by these agencies is gratefully acknowledged.

Sincere appreciation is expressed to all persons who participated in or contributed to the research. Special thanks are given to the following people for their service to the study. H. D. Butler of the Bridge Division was the contact representative and Robert Long of the Materials and Test Division was the assistant contact representative for SDHPT. Charles Duncan served as the contact representative for FHWA. Research Assistants Vernon Kasch, Leon Holloway and Mark Bierschwale rendered invaluable assistance by conducting the field tests and writing the reports. Gratitude is expressed to Bill Ray, Eddie Denk and the personnel of the TTI research support group who constructed the loading facility and tests shafts which were the core of the research. The contributions of all persons who were either directly or indirectly associated with the research study are gratefully acknowledged.

TABLE OF CONTENTS

TABLE OF CONTENTS (Continued)

LIST OF TABLES

LIST OF FIGURES

LIST OF FIGURES (Continued)

LIST OF FIGURES (Continued)

INTRODUCTION

Drilled Shaft Characteristics

Drilled shafts are cylindrical foundation elements designed for the purpose of transferring loads to a depth in the soil where adequate load transfer can be obtained. In recent years, the use of drilled shafts for supporting both axial and lateral loads has increased in foundations for buildings, retaining walls, and numerous other applications in a variety of soil conditions. The drilled shaft may also be termed a drilled pier, a caisson, a bored-pile, or a cast-in-place pile.

A drilled shaft obtains its axial bearing capacity from a combination of frictional resistance on the side of the shaft and end bearing resistance. The ratio of frictional to end bearing resistance is governed by soil conditions at the site and the drilled shaft geometry. The bottom of the shaft may be enlarged or underreamed, either to increase the bottom bearing area or to resist uplift. Drilled shafts are analyzed for axial capacity with the static equations which are used for driven piles. However, the effects of such factors as placement of fresh concrete and stress relief due to excavation can significantly influence the properties of the soil in the vicinity of the shaft. Fortunately, research has been conducted and design methods developed which take into account the various

---

Numbers in parentheses refer to the references in Appendix I.

uncertainties involved (29).

The lateral resistance of drilled shafts is governed by several factors, one of the most important being the ratio of structural stiffness to soil stiffness. The relative stiffness of the soil with respect to the foundation element controls the mode of failure and the manner in which the shaft will behave under an applied lateral load. Applied lateral loads are resisted by the lateral earth pressure developed in the supporting soil along the length of the shaft. By using a drilled shaft foundation, the design engineer can take advantage of the lateral soil resistance and make more efficient use of the soil in the foundation design as compared with other types of foundations.

The design process for drilled shafts has three integral parts. The first part involves conducting an adequate subsurface exploration program in order to establish the technical and economic feasibility of using drilled shafts and the characteristics of the supporting soil. The second part involves selecting the allowable working load to be used in design, the size and type of drilled shaft, and the methods to be used in construction and installation. Finally, the design or construction procedure is modified and revised, if necessary, according to the actual conditions encountered during the installation process.

Piles and drilled shafts serve essentially the same function, the only major difference being the method of installation. Piles are usually installed by driving the structural member and displacing the supporting soil. The drilled shaft, on the other hand, is constructed

by drilling a cylindrical hole, or a cylindrical and underreamed hole, into the soil and subsequently filling the hole with concrete and the necessary reinforcing steel.

Compared to a spread footing, the drilled shaft usually requires less concrete and more reinforcing steel. Also, the drilled shaft requires no formwork and the reinforcing steel can be pre-fabricated. Thus, the drilled shaft is usually more economical due to reduced labor requirements.

Major economic advantages were gained during the late 1940's with the development of truck-mounted and crane-mounted drilling and excavating rigs. Mechanical rigs are capable of drilling shafts to depths greater than 100 ft (30.5 m) and up to 12 ft (3.66 m) in diameter, with enlarged bases or underreamed bells up to 25 ft (7.63 m) in diameter (40). As this new mechanical equipment became available, drilled shafts became attractive in many areas where they were not previously considered.

The relative merits of drilled shafts in comparison with other types of foundations depend not only on economics but also on several technical factors. In situations where it is not clearly evident which type of foundation is more desirable, the advantages and disadvantages of each type of foundation should be carefully considered.

Some of the advantages of drilled shafts for a foundation are (31):

1. Drilled shafts can be successfully constructed in soils where it might be difficult to install other types of foundations.
2. Soil movements during construction due to heave or vibration

are minimized.

3. Soil exposed during the construction operation and inspection can reveal whether or not the soil is consistent with that predicted by the subsurface investigation.
4. The size of the drilled shaft can be readily adjusted during the construction operation so that variations in subsurface conditions can be accommodated.
5. Drilled shafts can be built rapidly as compared to some other types of foundations.
6. Construction materials are readily available and construction equipment is generally available in all parts of the United States.
7. Pile caps can be eliminated on many jobs, leading to savings in cost.
8. Construction noise is tolerable as compared to other types of construction.

Some of the disadvantages of drilled shafts for a foundation are:

1. An excellent subsurface investigation must be carried out in order that designs are made properly and in order that the appropriate construction procedure is selected.
2. Drilled shafts of good quality are critically dependent on the construction techniques that are employed.
3. The appropriate inspection of the construction requires a considerable amount of knowledge and experience. It is normally not possible to investigate the completed shaft to see whether or not a good construction job has been obtained.

4. The shear strength of the supporting soil in general is reduced by the construction operation.
5. Failures of a drilled shaft can be expensive because a single shaft is usually designed to carry a load of large magnitude.

Behavior of Laterally Loaded Drilled Shafts

The problem of a drilled shaft subjected to lateral loading is one in a class of problems concerned with the interaction of soils and structural members. The ultimate lateral resistance of a drilled shaft is governed by a combination of the yield strength of the shaft section and by the ultimate lateral resistance of the supporting soils. Consequently, the mode of failure depends on the shaft length, the stiffness of the shaft section, and the load deformation characteristics of the soil.

The usual approach to the problem of a laterally loaded shaft is to categorize the foundation member as either rigid or flexible. However, a firm boundary does not exist between what constitutes a rigid and a flexible drilled shaft.

Pioneering work by Matlock and Reese (23) on laterally loaded piles has indicated that the definition of rigidity is related to the ratio of the flexural stiffness of the pile, EI, and the foundation soil modulus, or coefficient of lateral subgrade reaction, k. Several other methods of determining how the shaft will behave have been proposed by Broms (2), Vesic (38), Davisson and Gill (6), and Lytton (21). These methods utilize a stiffness ratio in order to determine the relative stiffness of the shaft with respect to the soil. Kasch et al.,

(20) compared the results obtained by the different methods and found the various methods yielded similar determinations. Kasch also determined values for the ratio of depth to diameter, D/B, based on a wide range of soil stiffness which would classify the shaft as rigid or flexible. Kasch concluded that in order to insure rigid behavior, the D/B ratio should not exceed about 6. However, under certain conditions a foundation can have a D/B ratio as high as 10 and still behave in a rigid manner. This exception occurs when a drilled shaft is founded in a relatively weak soil. Kasch also found that to insure flexible behavior, the D/B should be in excess of 20.

In flexible or long shafts, failure is usually structural, occurring when a plastic hinge forms at the point of maximum bending moment. The solution to the problem usually requires the use of iterative techniques because the soil response is a nonlinear function of the deflection of the shaft. Of most practical interest to the engineer is a knowledge of the deflection and bending moment. The bending moment is required in the sizing of the foundation, and the deflection is important with regard to the serviceability of the supported structure. The family of curves shown in Fig. 1(a) indicates the form of a complete solution to the problem, in addition to illustrating flexible behavior of a drilled shaft.

Equation (1) is the governing differential equation for the problem of laterally loaded deep foundations; it is well known and has been analyzed by a number of authors (9, 10, 13, 23, 30, 38):

$$EI \frac{d^4y}{dx^4} + P_x \frac{d^2y}{dx^2} - p = 0 \quad \ldots\ldots\ldots\ldots\ldots\ldots\ldots \quad (1)$$

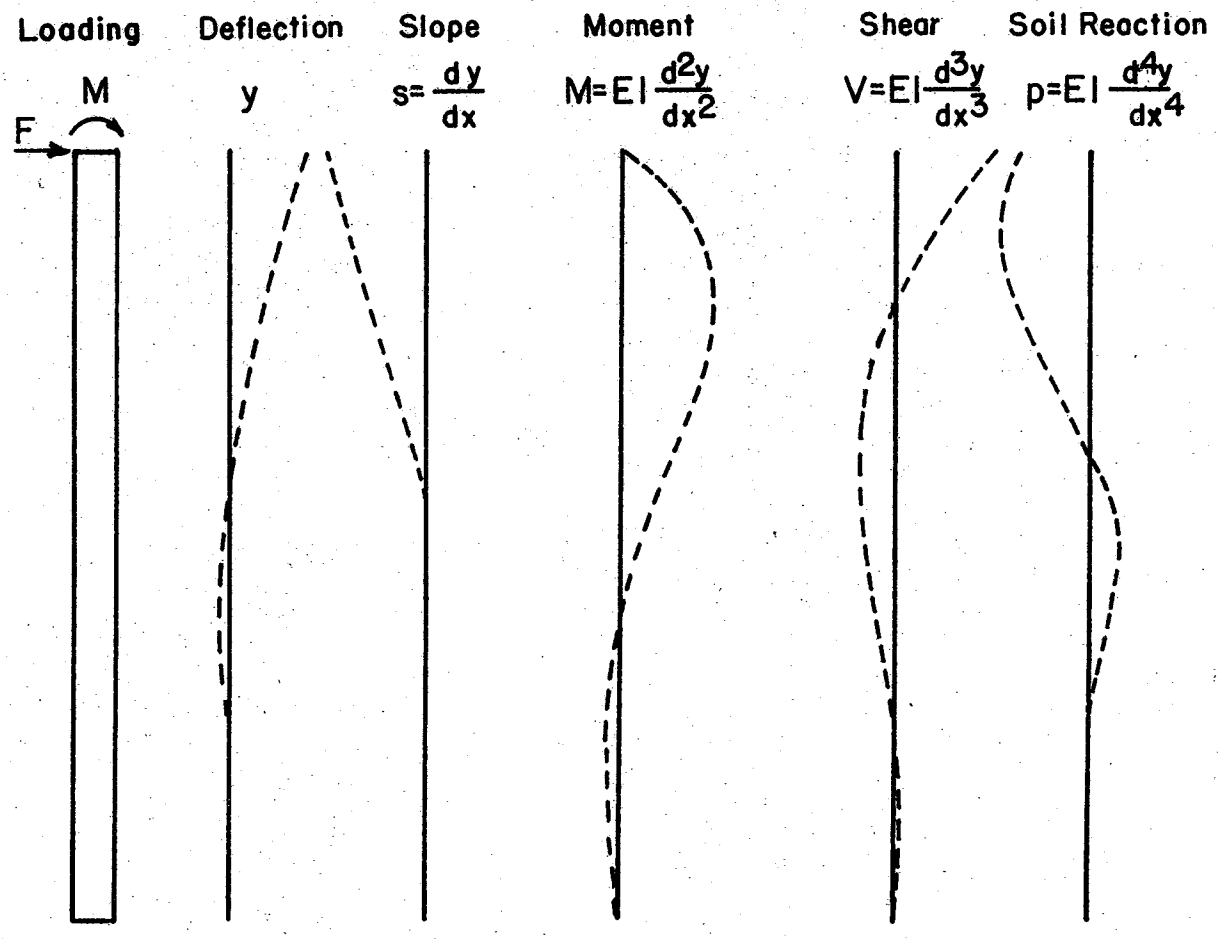

(a) Elastic Behavior of Flexible Drilled Shaft (After Welch and Reese-1972)
F = Applied Lateral Load, M = Applied Moment, EI = Flexural Stiffness of Foundation, x = Depth Below Groundline

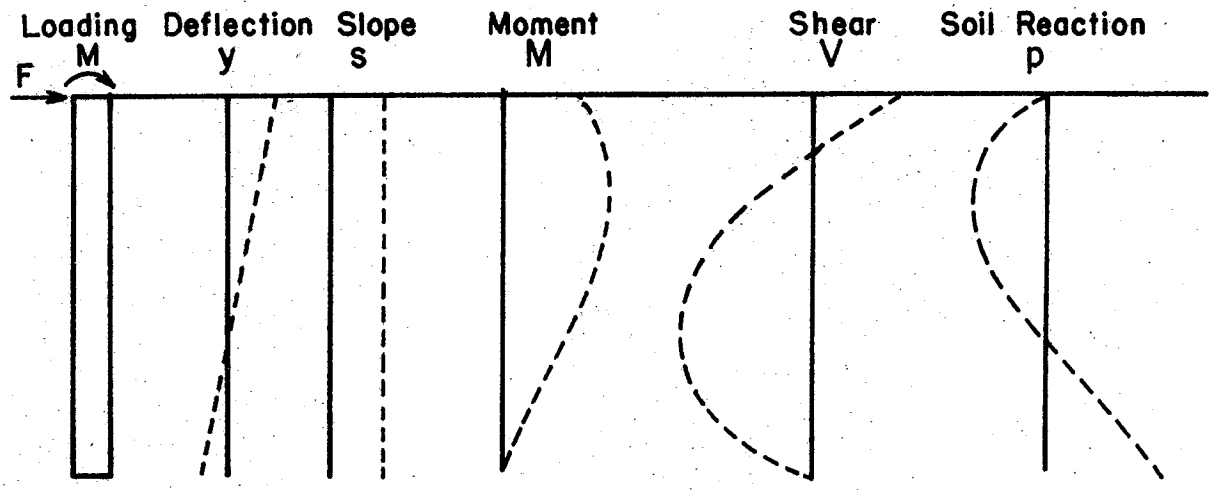

(b) Rigid Behavior of Non-Flexible Drilled Shaft (F and M same as in (a))

FIG. 1.- Drilled Shaft Behavior

where, P_x = axial load; y = deflection; x = depth below groundline; and p = soil reaction. The deflection, slope, moment, shear, and soil reaction at any point of the foundation is obtained from the solution of Equation (1). The solution can be readily obtained if an expression for the soil modulus, E_s, can be found (22, 24, 27, 28, 36). The soil modulus may be estimated best by a family of curves that show the soil reaction, p, as a function of deflection, y, as illustrated in Fig. 2. A computer solution of Eq. (1) is available with appropriate documentation from the Computing Center, University of Colorado, Boulder, Colorado. The program is entitled, "Analysis of Laterally Loaded Piles by Computer," and the Code name is COM622 (30).

Failure in rigid or short shafts takes place when the lateral earth pressure resulting from lateral loading exceeds the lateral resistance of the supporting soil along the full length of the member. The shaft rotates as a unit around a point located at some distance below the ground surface. Assuming rigid body motion, the rotation of the shaft and the displacement at the groundline define the position of the shaft. Fig. 1(b) illustrates the behavior of a rigid drilled shaft. As indicated, the load-deflection characteristics of a rigid shaft are quite different from those of a flexible shaft. The rigid shaft is assumed to be infinitely stiff, and the only motion allowed is pure rotation of the shaft as a rigid body about some point on the axis of the shaft.

It should be pointed out that absolute rigidity does not exist and bending stresses are always associated with deflections of the shaft. However, the effect of such deflections on the soil pressure decreases as the rigidity of the shaft increases (4). For the rigid shaft the resulting deflections are not significant enough to introduce error in

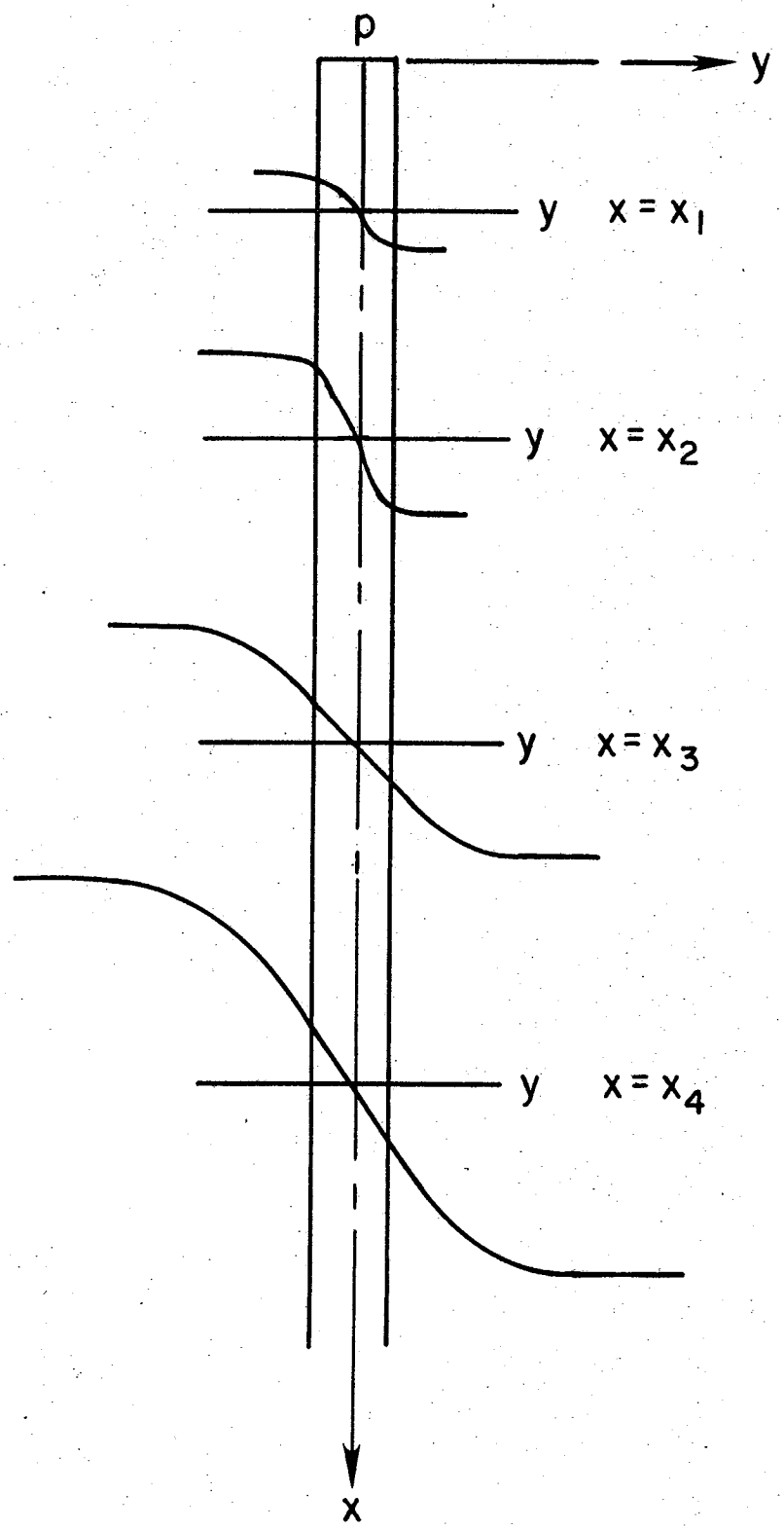

FIG. 2 — Set of p-y Curves (After Reese-1977)
p= Soil Reaction, x= Depth Below Groundline,
y= Lateral Deflection

the analysis and can be neglected.

From the results of actual load-deflection tests (14, 19, 20, 34) and several analytical approaches (4, 12), it was observed that the point of rotation does not remain at a constant distance below the ground surface but shifts to lower depths with increasing lateral load. Dunlap and Ivey (19) observed that when the strength of the soil decreases with increasing depth, the point of rotation shifts upward towards the ground surface. However, in most cases the rotation point is approximately two-thirds of the depth down from the top of the shaft.

There are a number of methods which are available for predicting lateral load behavior of rigid drilled shafts. In these methods several arbitrary assumptions are made, the most notable being that the point of rotation is constant and occurs at a depth of two-thirds the embedment depth. A comparison of the various methods is beyond the scope of this report. Detailed descriptions of the various methods can be found in references 2, 11, 16, 17, and 33.

Bhushan, Haley, and Fang (1) have advocated the use of a finite-difference method based on elastic theory, for the solution of lateral load behavior of rigid shafts. The results of this study indicated that, for deflections up to 0.5 in. (12.7 mm) the finite-difference approach produced good agreement. However, for large deflections, the prediction of actual behavior became progressively worse. Matlock and Reese (23) have reported that piles which tend to behave as rigid members cause the difference equation method used in the elastic-theory solution to become inaccurate and unstable because of the very

small successive differences which are involved.

Background and Objectives

Rigid drilled shafts are being used extensively in many types of foundations which must support lateral loads. However, little is known about the actual performance of these foundation elements under lateral loading. The existing methods for the design of laterally loaded drilled shafts generally appear to be overly conservative. The absence of reported failures tend to verify this situation. Hence, an evaluation of the field performance of rigid drilled shafts subjected to lateral loads is needed to ascertain the actual foundation behavior and to develop new design procedures.

In recent years the Texas State Department of Highways and Public Transportation (SDHPT) has developed a new concept in earth retaining wall design which utilizes drilled shafts. This new type of retaining wall consists of precast concrete panels positioned between T-shaped pilasters which are founded on drilled shafts as shown in Fig. 3. Active earth pressures acting on the precast panel wall due to backfill are transmitted to the drilled shaft through the pilasters. Consequently, both passive and active pressures may be developed in the foundation soil contacting the drilled shaft. At the present time, the magnitude and distribution of these pressures are not well known and understood, and as a result, it is probable that shafts supporting precast panel retaining walls have been overdesigned.

In 1975 Wright, Coyle, Bartoskewitz, and Milberger (41) conducted a study investigating the performance of precast panel retaining walls.

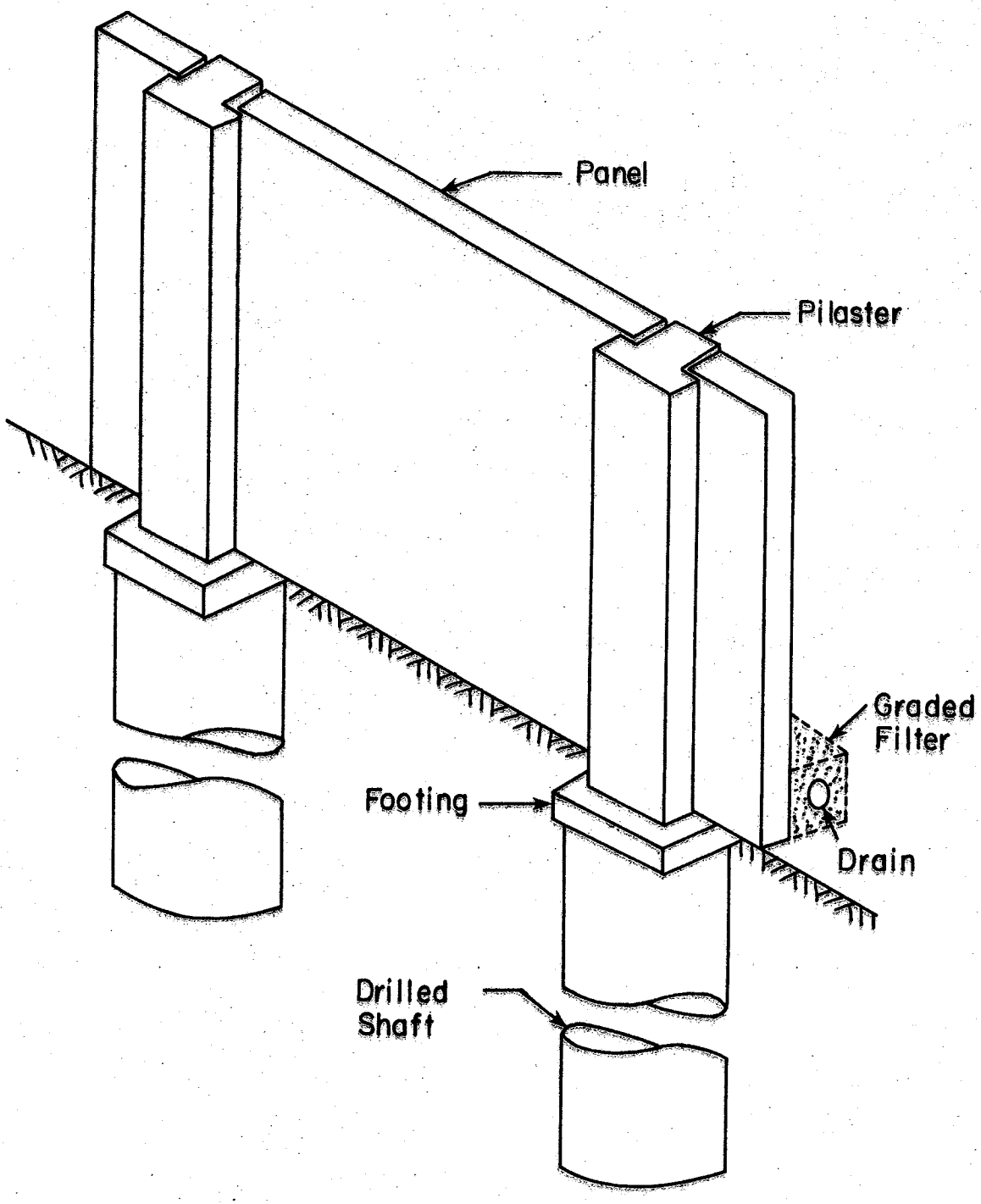

FIG. 3 – Precast Panel Retaining Wall

As a part of this research study a drilled shaft supporting a precast panel wall was instrumented with pressure cells in order to determine the practicability of installing cells and measuring lateral earth pressures. These researchers concluded that the use of pressure cells provided a reasonable method for measuring lateral earth pressure and recommended that this method be used in future research. In 1978 Ismael and Klym (15) conducted a number of tests on rigid drilled shafts, one of which was a cylindrical pier instrumented with pressure cells. A total of five pressure cells were placed in front of and in the back of the cylindrical shaft in order to obtain a complete picture of the pressure distribution along the full depth of the shaft. The use of the pressure cells proved successful and a diagram of the pressure distribution with depth was reported. Ismael and Klym also analyzed various methods for predicting the behavior of rigid shafts and discovered that certain design methods yielded conservative results. Furthermore, it was concluded that additional testing was needed in order to develop an improved design method for rigid shafts in cohesive soils.

Reese and Welch conducted two independent studies, one in 1972 (39) and another in 1975 (31). Both studies included the investigation of the behavior of drilled shafts founded in clay and subjected to short-term static lateral loads. The test shafts were instrumented with strain gages in order to measure the bending moment along the length of the shaft developed by the applied lateral loads. The soil reaction was then determined mathematically by double differentiating the bending moments. In 1979 Bhushan, Haley, and Fong (1) presented

the results of full-scale lateral load tests on 12 drilled shafts in clay. The tests included both belled and cylindrical shafts. During these tests only the lateral load and the deflection of the shafts were recorded. No effort was made in any of these studies to directly measure the soil reaction so that the distribution of the soil pressure could be determined.

In 1967 a five-year study was begun at Texas A&M University to develop a usable design procedure for drilled shaft footings for minor service structures. The study was initiated because of the belief among some SDHPT engineers that the existing design methods for drilled shafts were very conservative. In 1970, as a part of this research study, Dunlap and Ivey (19) correlated full-scale, short-term field performance tests with a theory developed earlier by Ivey (17). A design procedure was developed which allowed the selection of a particular size shaft as a function of the loads acting on the shaft and the characteristics of the soil. Soil reaction measurements were not made during this study. A later study conducted by Dunlap, Ivey, and Smith (8) investigated the long-term, sustained loading of drilled shaft footings. Only a limited amount of test data was obtained for long-term loading. However, the study resulted in considerable improvement in the existing design methods used for minor service structures.

With the advent of the new precast panel concept in retaining wall design, the SDHPT developed an increased interest in laterally loaded rigid shafts. The SDHPT recognized that improvements in design procedures may result in savings in construction costs. With this

goal in mind, a four-year research study was initiated at Texas A&M University. The study began in 1976 with the objective of developing a new design procedure for drilled shafts which support precast panel retaining walls. Kasch, Coyle, Bartoskewitz and Sarver (20) in 1977 and Holloway, Coyle, Bartoskewitz and Sarver (14) in 1978, reported the results of two short-term static tests conducted during this research study. In each test, lateral loads were applied and horizontal deflection, shaft rotation and lateral earth pressure measurements were recorded. The use of pressure cells in acquiring soil reaction measurements was successful. In both these reports preliminary design procedures for rigid drilled shafts in clay were proposed. However, one additional sustained lateral load test was needed before the final design procedure could be formulated.

During the fourth and final year of the research study the following objectives were established in order to develop a new design procedure for drilled shafts supporting precast panel retaining walls:

1. Continue to conduct a literature review in order to include any current research which might be related to this study,
2. Test one additional shaft by applying sustained lateral loads and recording resulting lateral earth pressures and shaft movements,
3. Investigate existing theories and procedures used for the design of rigid laterally loaded cylindrical shafts in clay, and
4. Correlate available test data with existing theories and procedures, and develop a new design procedure for drilled shafts supporting precast panel retaining walls.

FIELD LOAD TESTS

The prediction of the behavior of laterally loaded shafts involves the determination of the shaft-soil interaction. One approach to the determination of the shaft-soil interaction is to conduct field load tests on full-scale instrumented drilled shafts and directly measure the system interaction during testing. Field load tests were conducted during this study and the test site was located at the southwest end of the northwest-southwest runway on the Texas A&M University Research and Extension Center.

Soil Conditions

The drilled shaft which was tested during the fourth and final year of the research study was tested in the same clay soil and at the same test site used by Kasch (20) and Holloway (14) in previous studies. Soil conditions were investigated separately for each load test, due to changes in climatic conditions which produced slight variations in the soil shear strength.

Three initial soil borings and one Texas Cone Penetrometer (TCP) test were conducted by Kasch (20). The soil borings were drilled on January 7, 1977, March 15, 1977, and July 26, 1977. Undisturbed soil samples were taken with a 1.5 in (38.1 mm) thin-wall tube sampler. Results of the soil testing are logged in Figs. 4 through 6, designated B-S1, B-S2, and B-S3, respectively. A shear strength profile using the TCP test was also developed and is shown in Fig. 7. The N-values (blow counts) obtained from the TCP test were converted into undrained cohesive shear strength using a correlation developed by

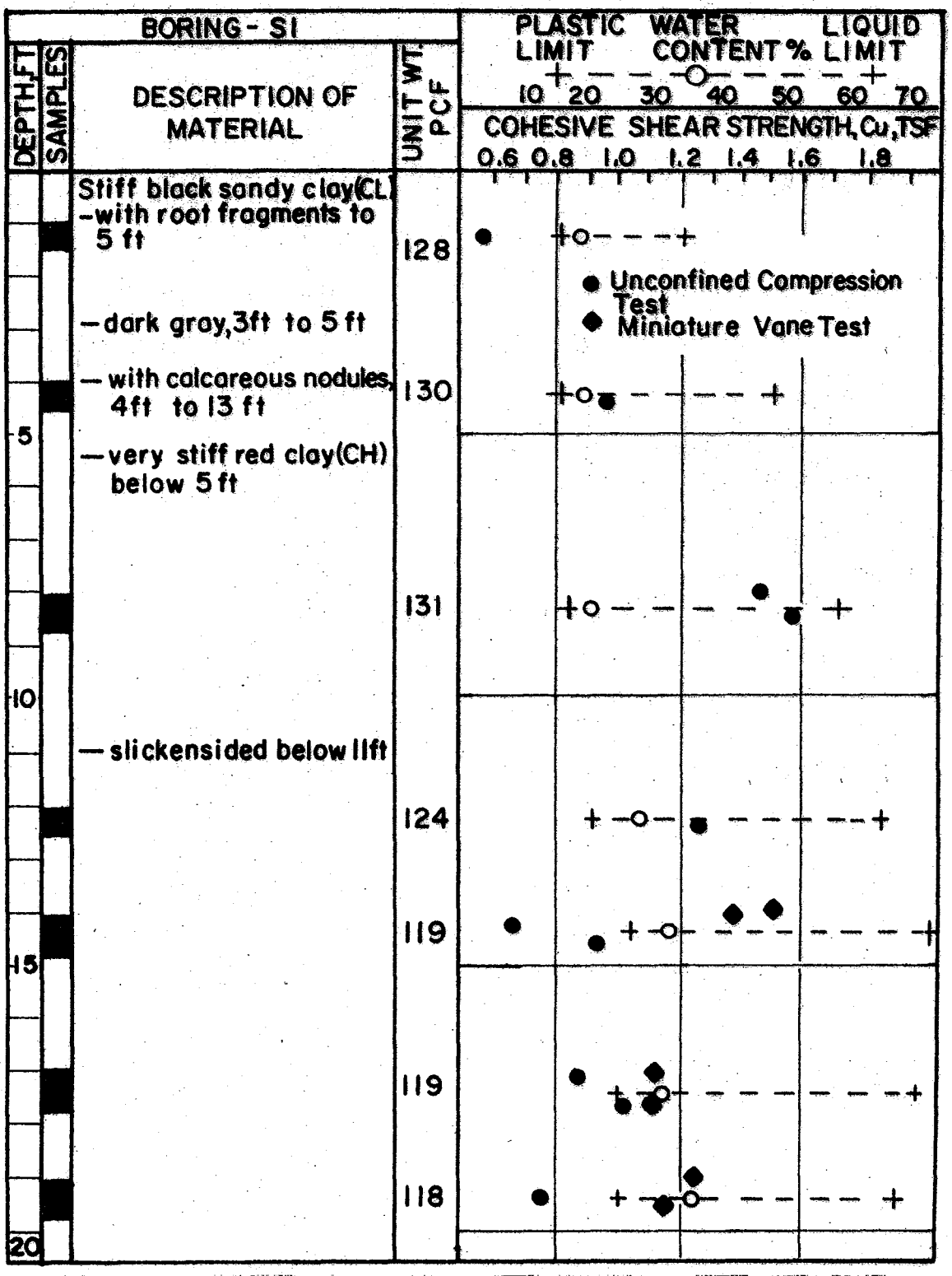

FIG. 4.– Boring – S1 (1ft=0.3048m, 1tsf= 95.8kN/m^2, 1pcf= 0.157kN/m^3)

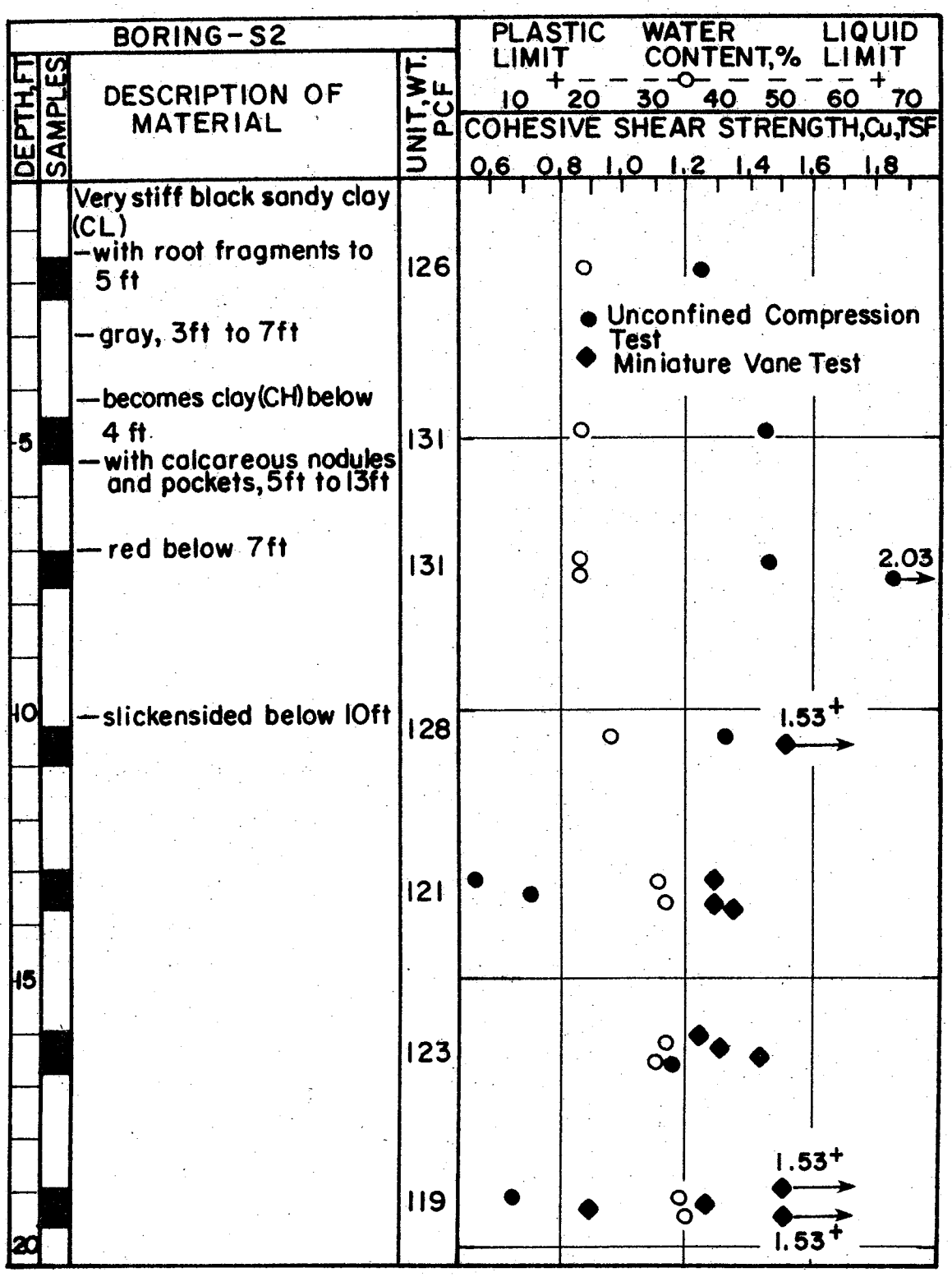

FIG. 5.—Boring — S2 (1ft = 0.3048m, 1tsf = 95.8kN/m^2, 1pcf = 0.157kN/m^3)

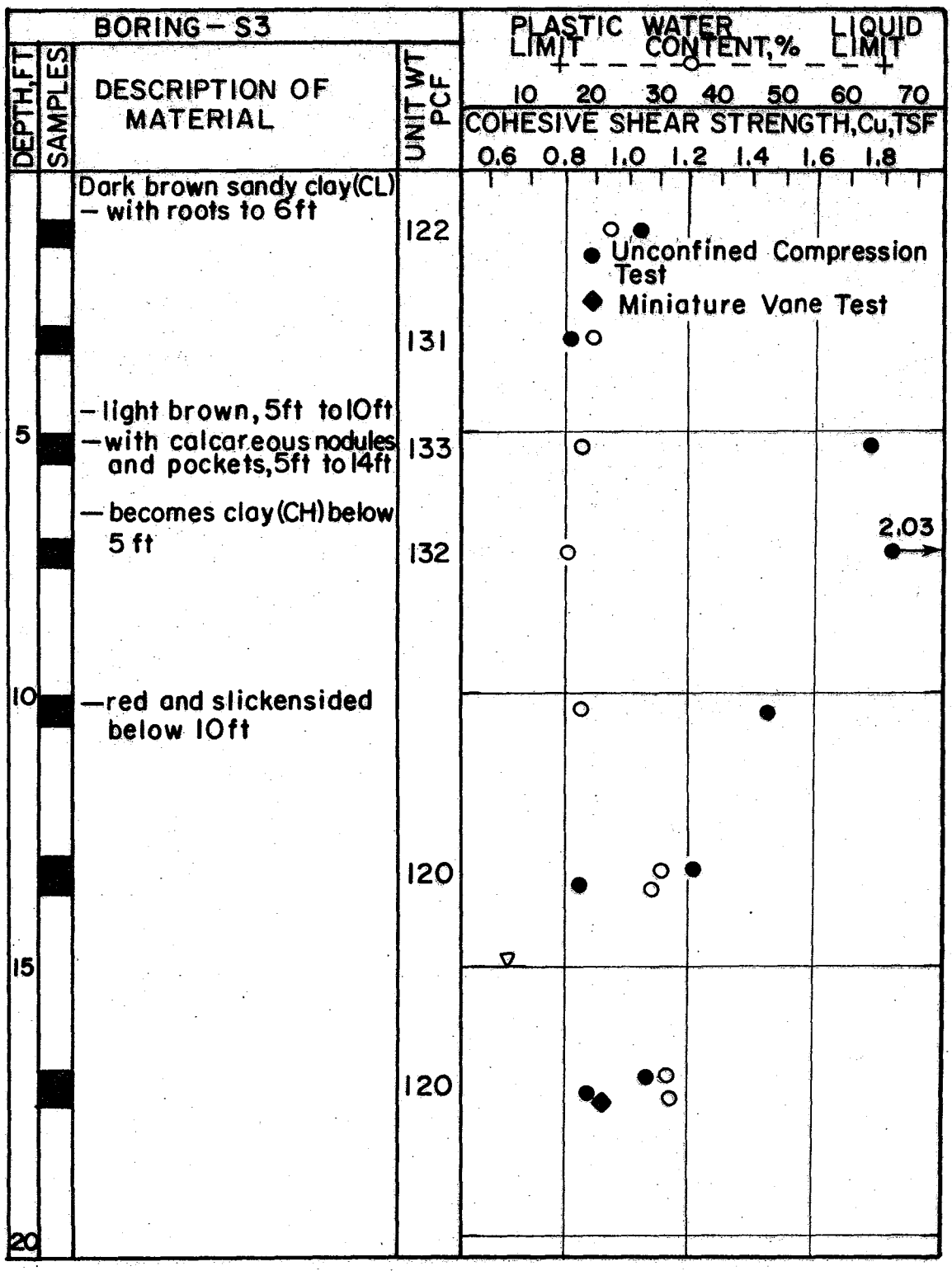

FIG. 6.– Boring – S3 (1ft = 0.3048m, 1tsf = 95.8kN/m^2, 1pcf = 0.157kN/m^3)

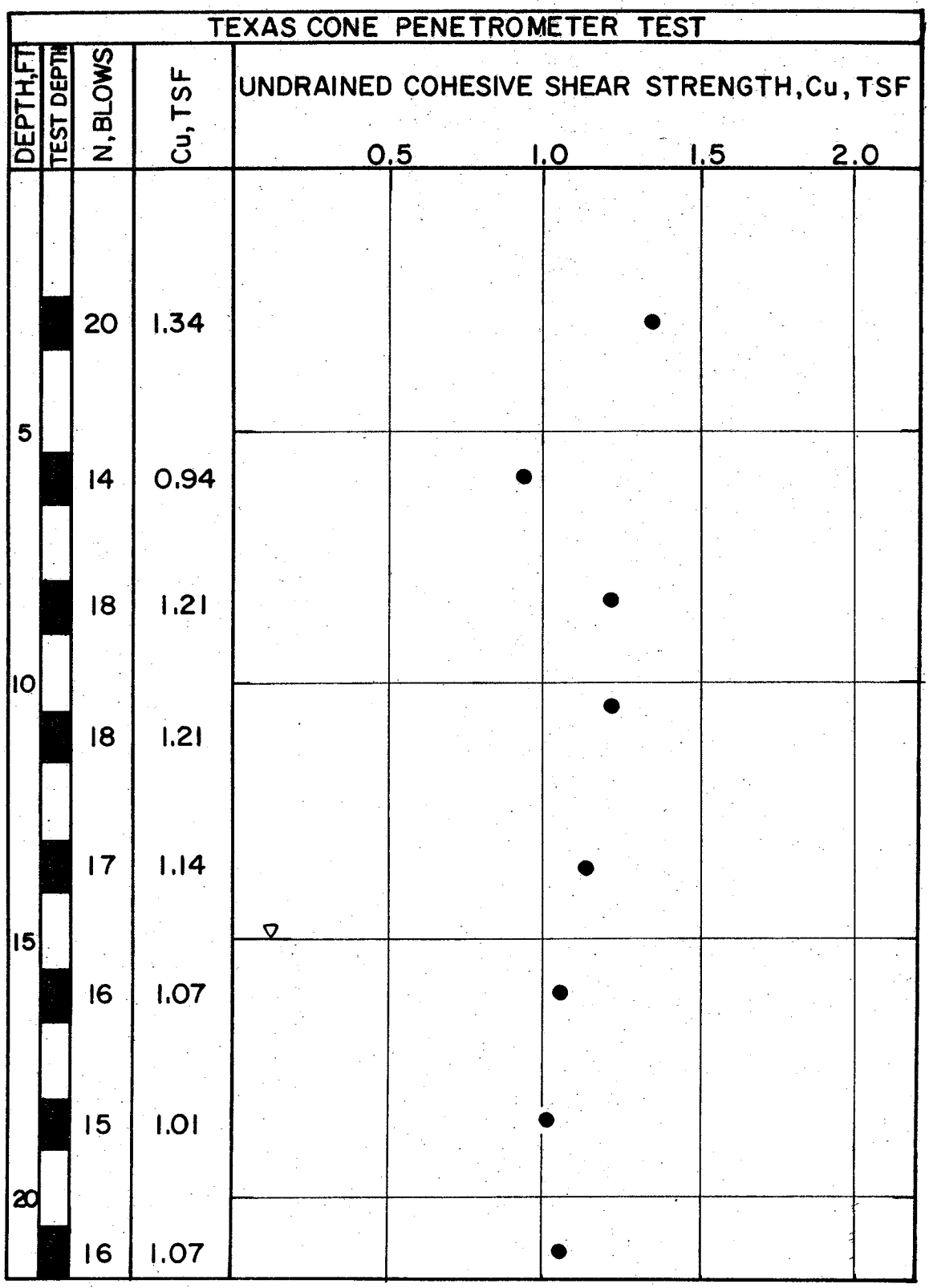

FIG. 7. — Texas Cone Penetrometer Test(1ft=0.3048m, 1tsf = 95.8 kN/m^2)

Duderstadt et al. (7). Kasch reported the average undrained shear strength to be 1.30 tsf (124 kN/m^2).

During the second year of the research study two additional soil borings were made by Holloway (14) on January 6, 1978. These borings, designated as B-S4 and B-S5, are shown in Figs. 8 and 9, respectively. Holloway reported the average undrained shear strength to be 1.40 tsf (134 kN/m^2).

On July 1, 1980,during the fourth and final year of the research, one additional boring was made which was designated B-S6 and is shown in Fig. 10. Due to the abnormal amounts of rainfall before and during the load test, the average undrained soil shear strength was reduced to 1.14 tsf (109 kN/m^2). All of the soil borings, B-S1 through B-S6, seem to indicate that the soil shear strengths at the test site are fairly uniform and consist of stiff clays with medium plasticity ranges. The boring locations with respect to test shaft locations for all tests are shown in Fig. 11.

Upon completion of boring B-S3 in July 1977, a standpipe was installed for ground water observations. A perforated PVC pipe, covered with screen wire, was placed in the borehole and surrounded with clean gravel. Kasch, in August, 1977, reported the water level to be at a depth of 15 ft (4.57 m) below the ground surface, while Holloway, in 1978, reported the water level to be located at a depth of 18.8 ft (5.73 m).

Loading System

The loading and reaction system used in performing the final field

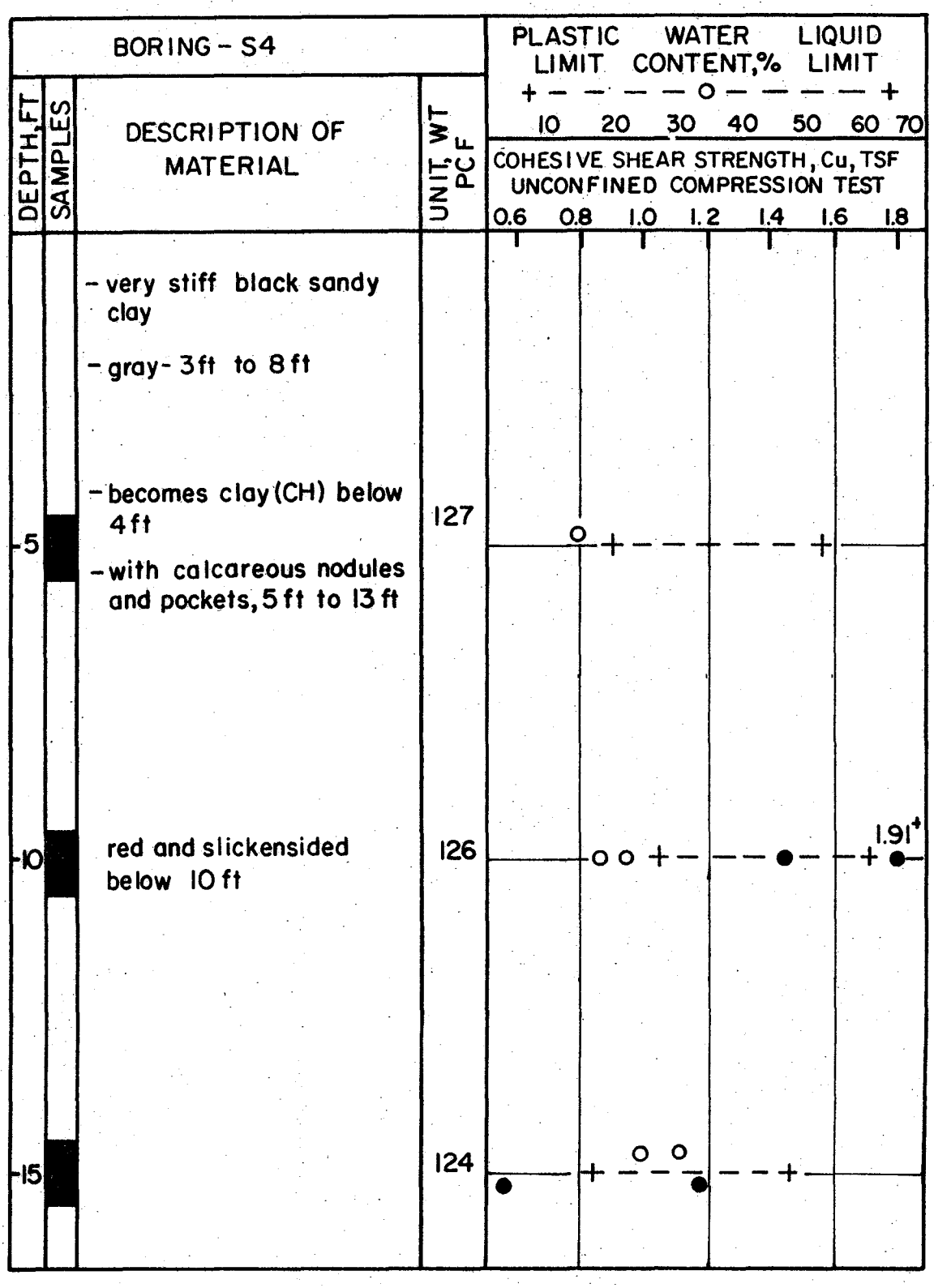

FIG. 8.— Boring — S4 (1ft = 0.3048m, 1tsf = 95.8kN/m^2, 1pcf = 0.157kN/m^3)

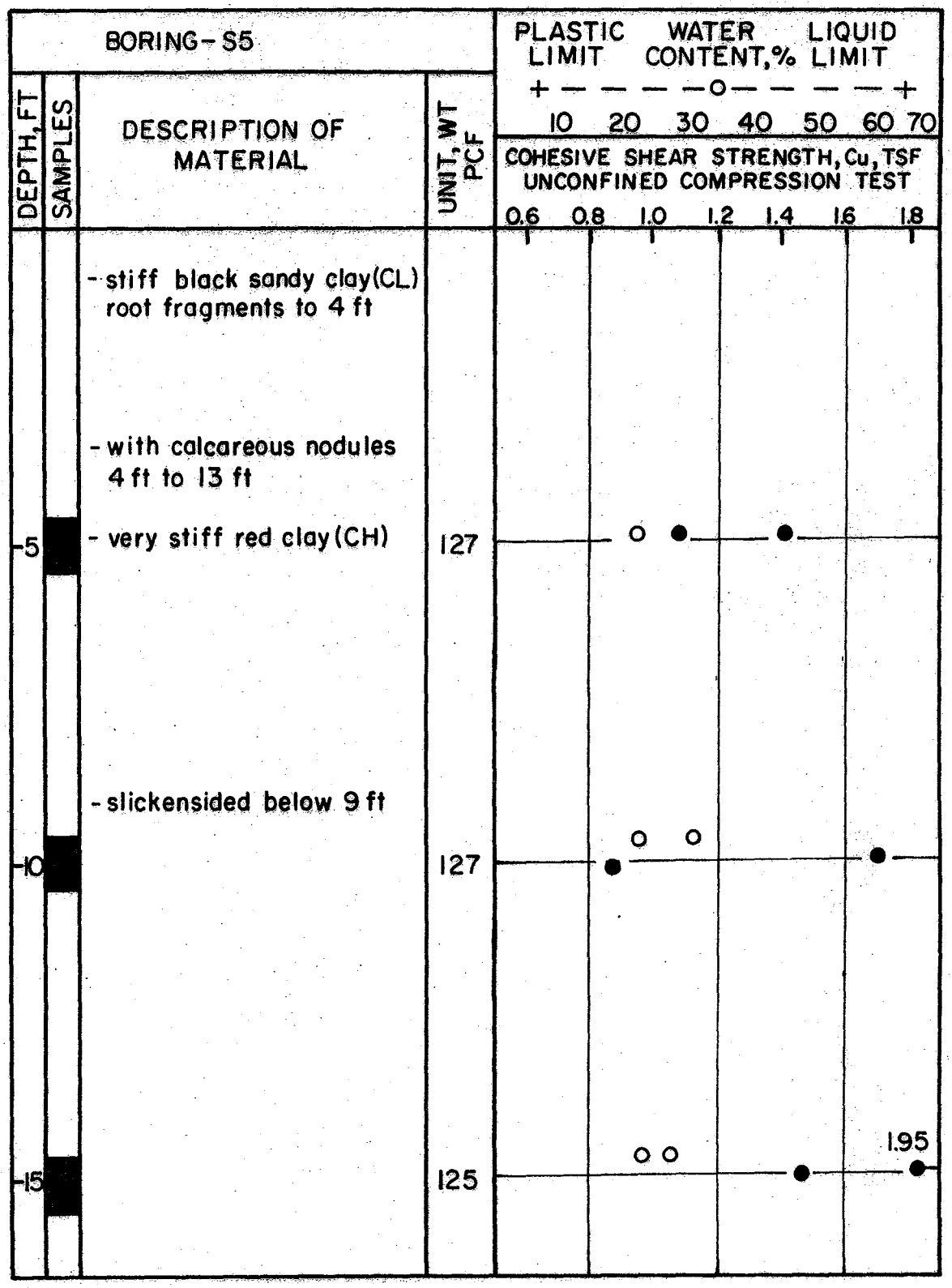

FIG. 9. — Boring — S5 (1ft = 0.3048m, 1tsf = 95.8kN/m^2, 1 pcf = 0.157kN/m^3)

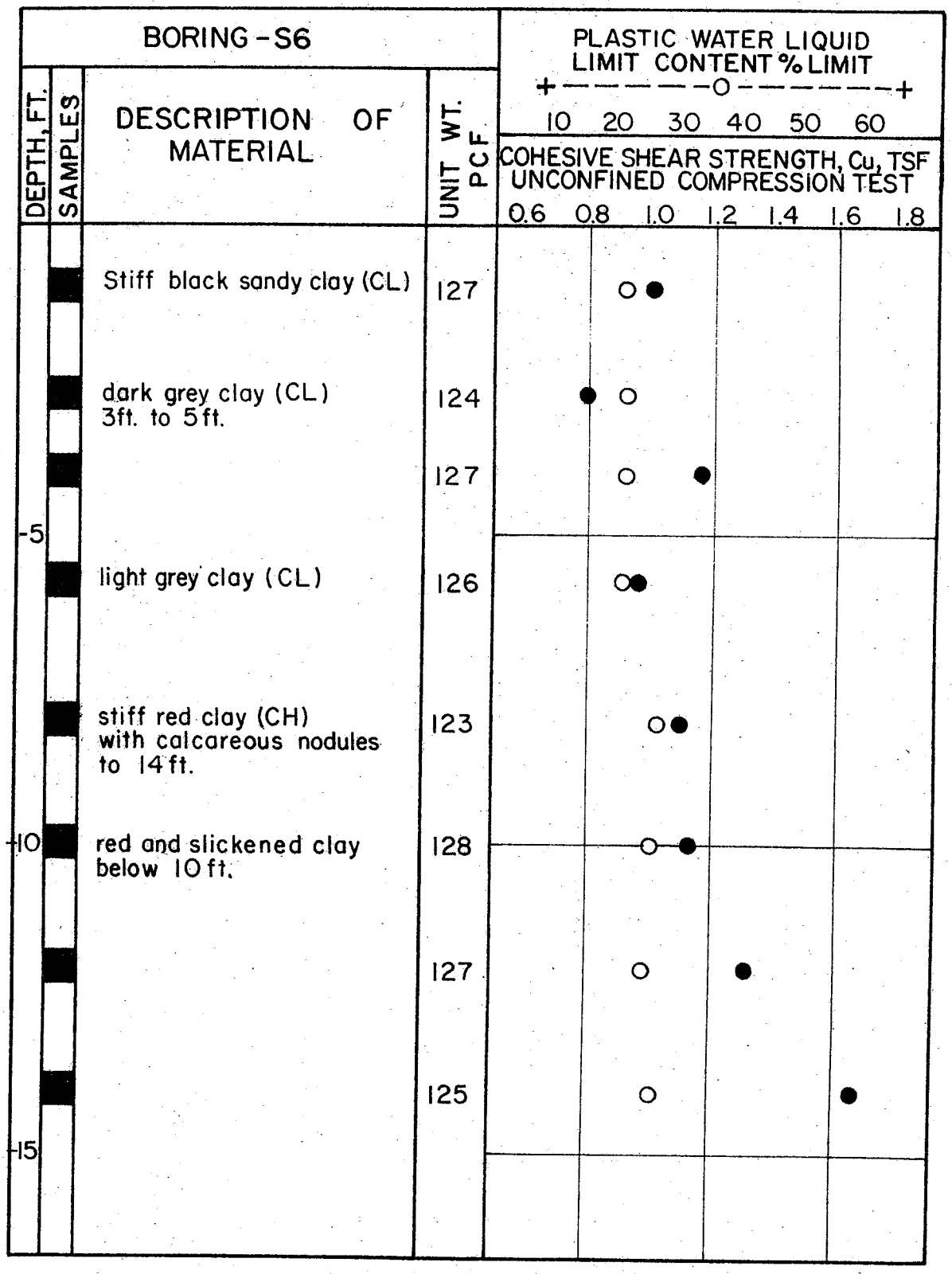

FIG. 10.- Boring - S6 (1 ft. = 0.3048 m, 1 tsf = 95.8 kN/m^2, 1 pcf = 0.157 kN/m^3)

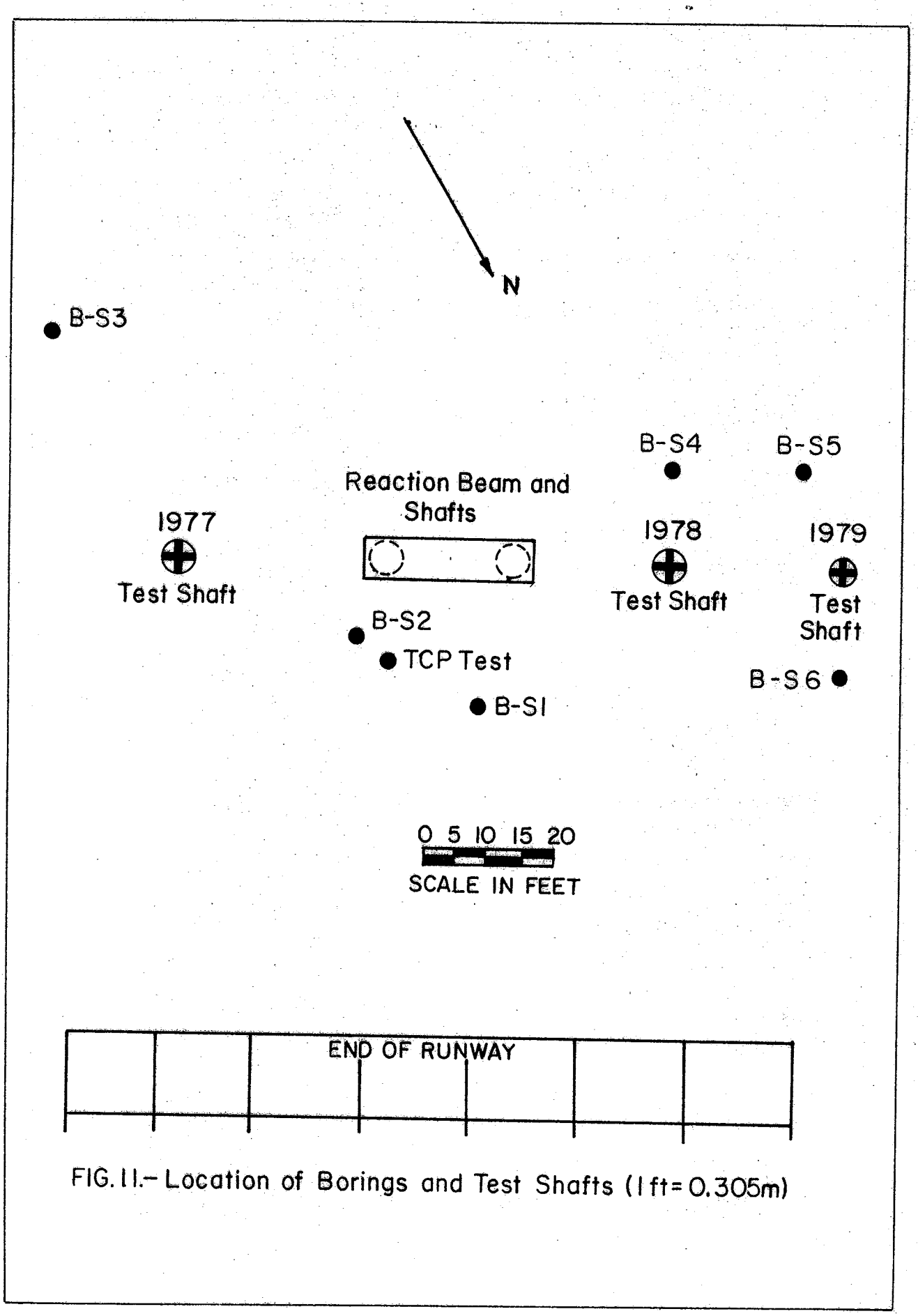

FIG. 11.– Location of Borings and Test Shafts (1 ft = 0.305m)

load test on the instrumented drilled shaft is shown in Fig. 12. The reaction pad foundation consisted of two 3 ft (0.92 m) diameter x 20 ft (6.1 m) deep drilled shafts which were connected by a 4 ft (1.22 m) wide x 3.5 ft (1.07 m) deep reinforced concrete tie beam. The lateral load was applied to the test shaft by a winch and pulley system. The winch used was a single drum, 20 ton (178 kN) capacity Garwood cable winch driven by a gasoline powered hydraulic unit. A 12:1 mechanical advantage was achieved by using two six sheave 100 ton (890 kN) capacity pulley blocks. The cable used in the loading system was a 3/4 in. (19.1 mm) 6 x 19 standard hoisting wire rope.

Bolted on the top of the drilled shaft was a 12 WF 120 steel column which was used as a link between the test shaft and the reaction system. The load applied to the shaft was measured by a strain-gaged load cell positioned between the pulley block and the steel column at a height of 2.6 ft (0.79 m) above the groundline.

The reaction system used in this particular study was a slightly modified version of the one used previously by Kasch (20) and Holloway (14). The modifications in the loading system were made in an attempt to compensate for difficulties experienced during the previous tests. The primary difficulty encountered in the test system used by Kasch and Holloway was the load variation which occurred due to a relaxation in the cables caused by temperature fluctuations. Hence, a constant lateral load had not been maintained on the shaft over an extended period of time.

In an attempt to alleviate this problem an A-frame was constructed at the edge of the reaction pad. The winch cable was placed over the

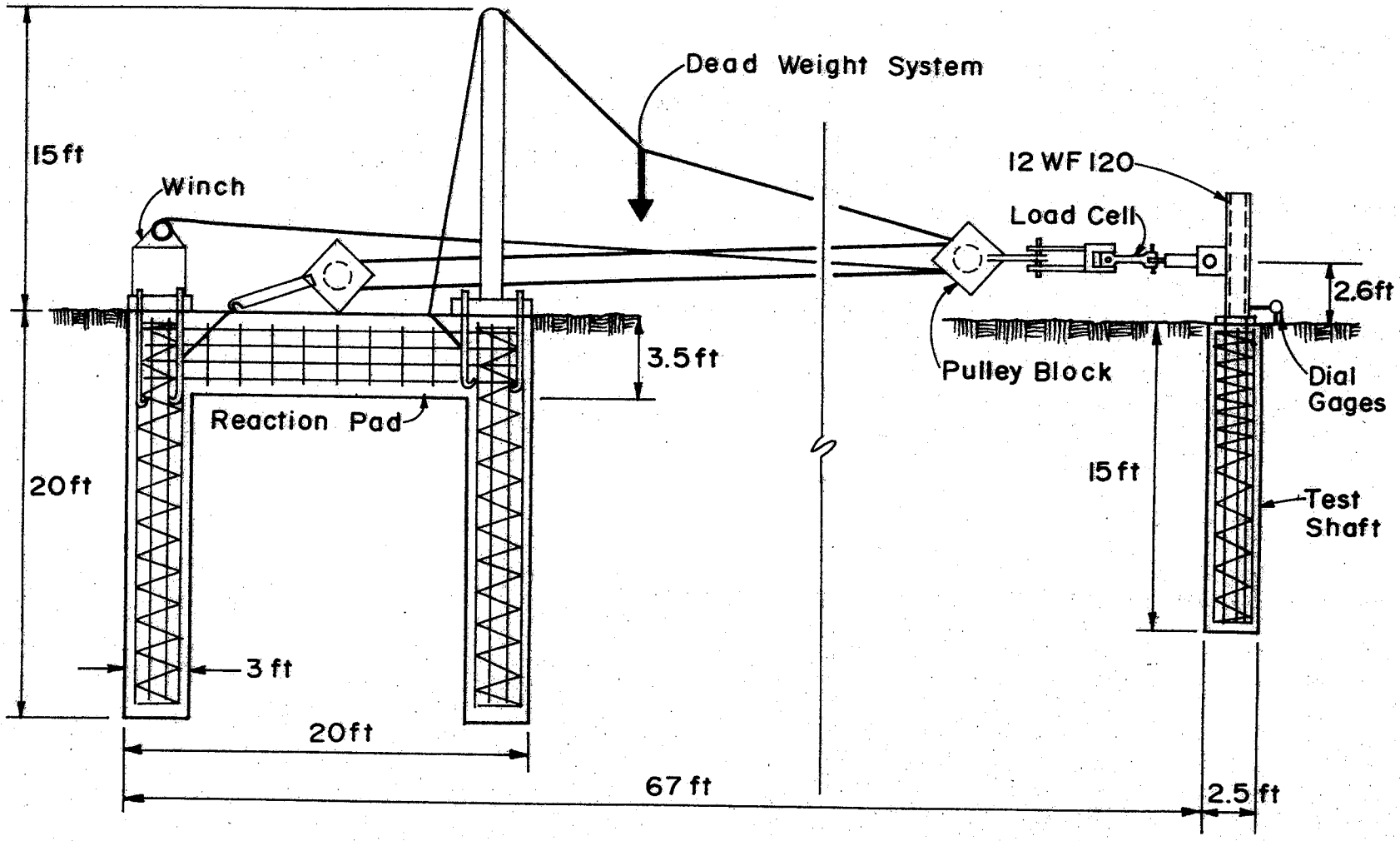

FIG. 12 - Lateral Loading System (1ft = 0.3048 m)

frame and dead-ended to the reaction pad. A dead weight was suspended from the free hanging cable incorporating the concept that the dead weight system would take up any slack which developed due to temperature related cable relaxation.

Test Shaft

The final drilled shaft tested was 2.5 ft (0.76 m) in diameter by 15 ft (4.58 m) deep. The test shaft was positioned on the center-line of the reaction pad at a distance of 67 ft (20.4 m) from the winch as shown in Fig. 11. Excluding the pressure cell instrumentation process, the procedure used in constructing the test shaft was the same as would normally be used in the field. After completion of pressure cell installation, the reinforcement cage was lowered into and positioned in the excavated hole. Ready mix concrete was then placed and vibrated directly into the hole.

The reinforcing cage used in the test shaft was constructed using two layers of longitudinal reinforcing bars surrounded by No. 3 smooth spiral reinforcing. The spiral reinforcing was spaced at a 2 in. (50 mm) pitch for the top 6 ft (1.83 m) and at a 6 in. (152 mm) pitch for the remaining length of the shaft. The outer longitudinal bars consisted of eight No. 11 (grade 60) standard reinforcing bars spaced equally at a diameter of 23-3/8 in. (59.3 cm). For the inner layer of reinforcing, twelve 1-1/2 in. (38 mm) (14S grade 60) threaded rods were used and spaced at a diameter of 19-1/2 in. (495 mm). The threaded reinforcing rods were used to enable the 12 WF 120 steel column to be fastened to the top of the test shaft. The

reinforcing steel configuration is shown in Fig. 13.

Several strength test cylinders were cast during placement of the concrete. The cylinders were cured both moist and dry to determine the compressive strength of the concrete. Based on a 28 day test, the compressive strength of the dry cured cylinders was 5200 psi (35,900 kN/m^2); the moist cured cylinders produced a 28 day compressive strength of 5300 psi (36,500 kN/m^2).

Drilled Shaft Instrumentation

Pressure cells. - Of major importance in the research study was the instrumentation of the test shaft to measure earth pressure response during lateral loading. To accomplish this, the drilled shaft was instrumented with earth pressure cells. Previous research (14, 20, 41) using earth pressure cells proved successful, and it was decided to continue to use them in this study.

The complete earth pressure measuring system consists of the Terra Tec pressure cell, the pressure lines, and the control and readout unit. A schematic of the cell is shown in Fig. 14. In principle, measured air pressure from the control unit is applied through a closed loop system inside the bellows to balance the external stress applied to the cell (3). Thus, by assuming that the internal fluid pressure is equal to the applied external stress, the pressure on the shaft is determined. A total of ten Terra Tec pressure cells were placed on the front and back of the cylindrical shaft in order to obtain a complete picture of the pressure distribution along the length of the shaft. The decision on placement of the

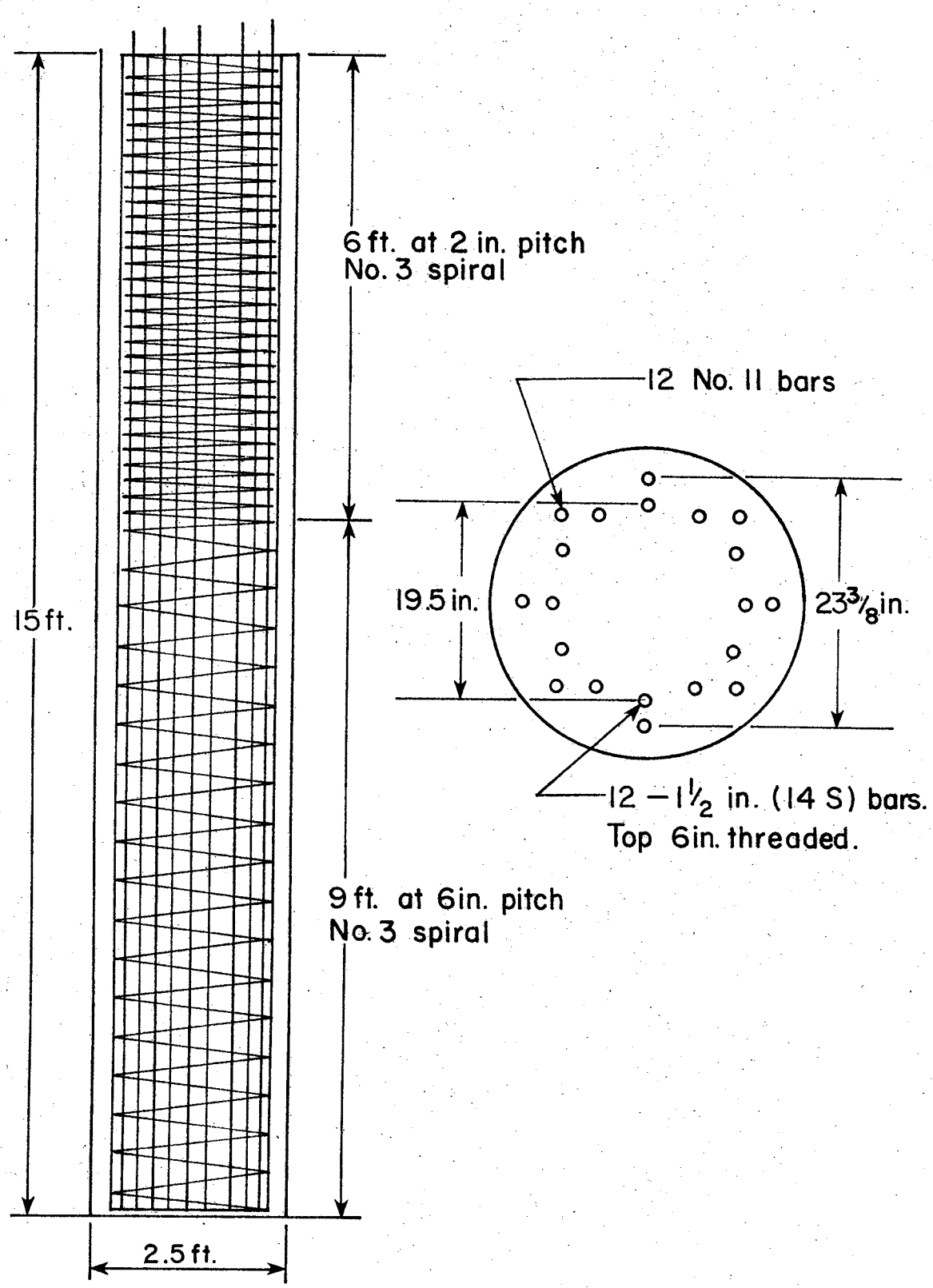

FIG. 13 – Drilled Shaft Reinforcing (1 ft. = 0.3048 m, 1 in. = 2.54 cm)

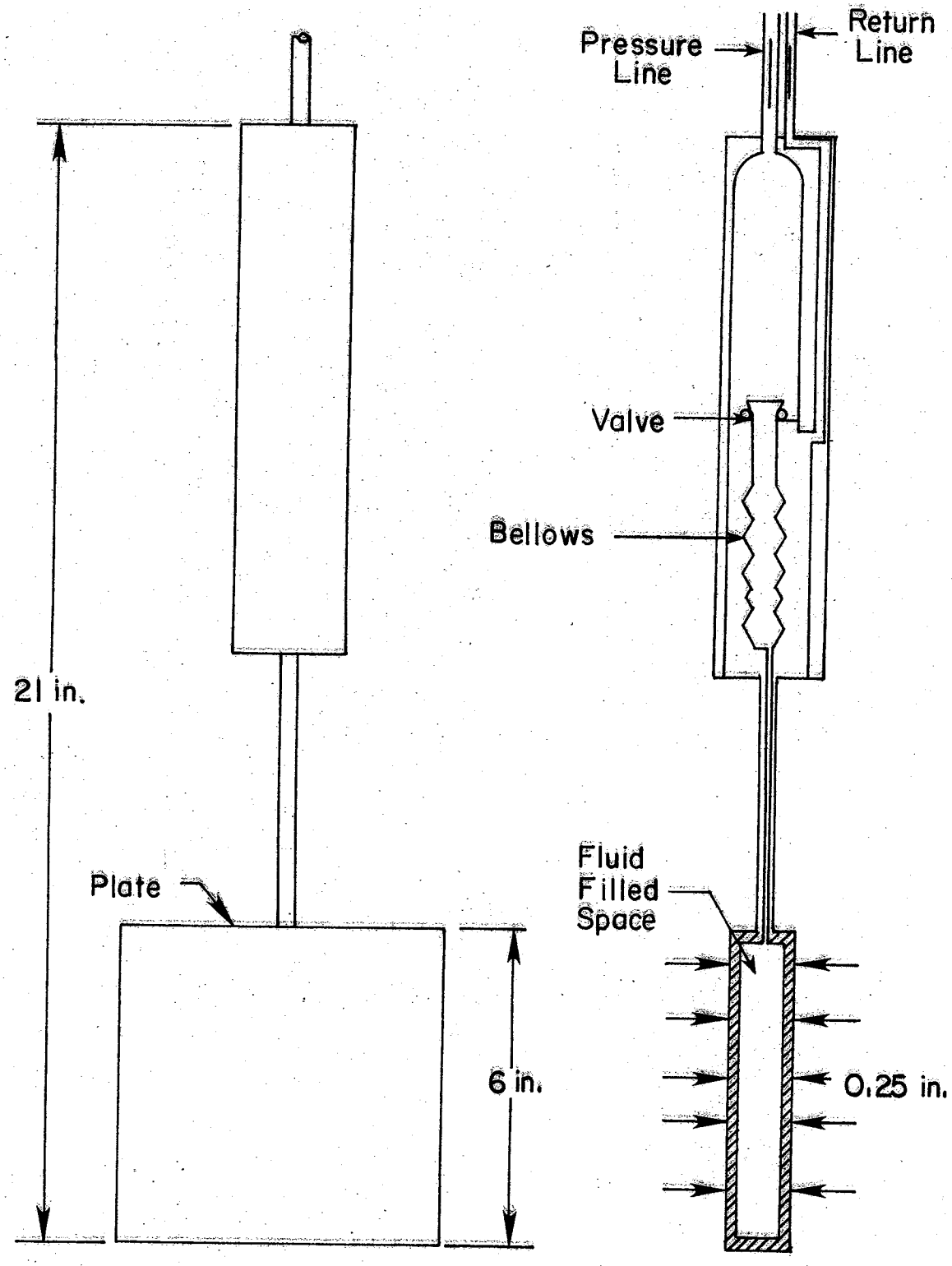

FIG. 14 - Terra Tec Pressure Cell (1 in. = 2.54 cm.)

cells was influenced somewhat by previous work conducted by Kasch (20) and Holloway (14). In both of the previous studies no soil reaction measurements were made near the groundline. Hence, for this phase of the research study, a pressure cell was placed near the groundline in an attempt to determine the magnitude of the soil reaction near the ground surface. Seven of the pressure cells were placed on the front side of the shaft in the direction of the applied load. Three cells were placed on the back side. The exact location of the individual cells is shown in Fig. 15.

Each cell was checked for malfunctions and calibrated in the laboratory before installation in the test shaft. The installation took place after excavation and before placement of the concrete. Cavities were made in the wall of the excavated hole and the pressure cells were then placed into the cavities and held in place by steel pins. The cavities were made in such a manner that the pressure cells would lie flush with the outer surface of the completed shaft.

Load cell. - A 200 kip (890 kN) capacity strain-gaged load cell was used to measure the lateral load applied to the drilled shaft. The lateral load was measured in units of microstrains with a Budd 350 strain indicator and converted to load using a predetermined conversion constant. The conversion constant was determined during calibration of the load cell prior to its installation. The accuracy of the load cell and Budd 350 strain indicator system was determined during calibration to be approximately $\pm$ 0.036 kips (0.16 kN).

Dial gages. - Lateral displacement of the drilled shaft at the groundline was measured by two dial gages located on each side of the

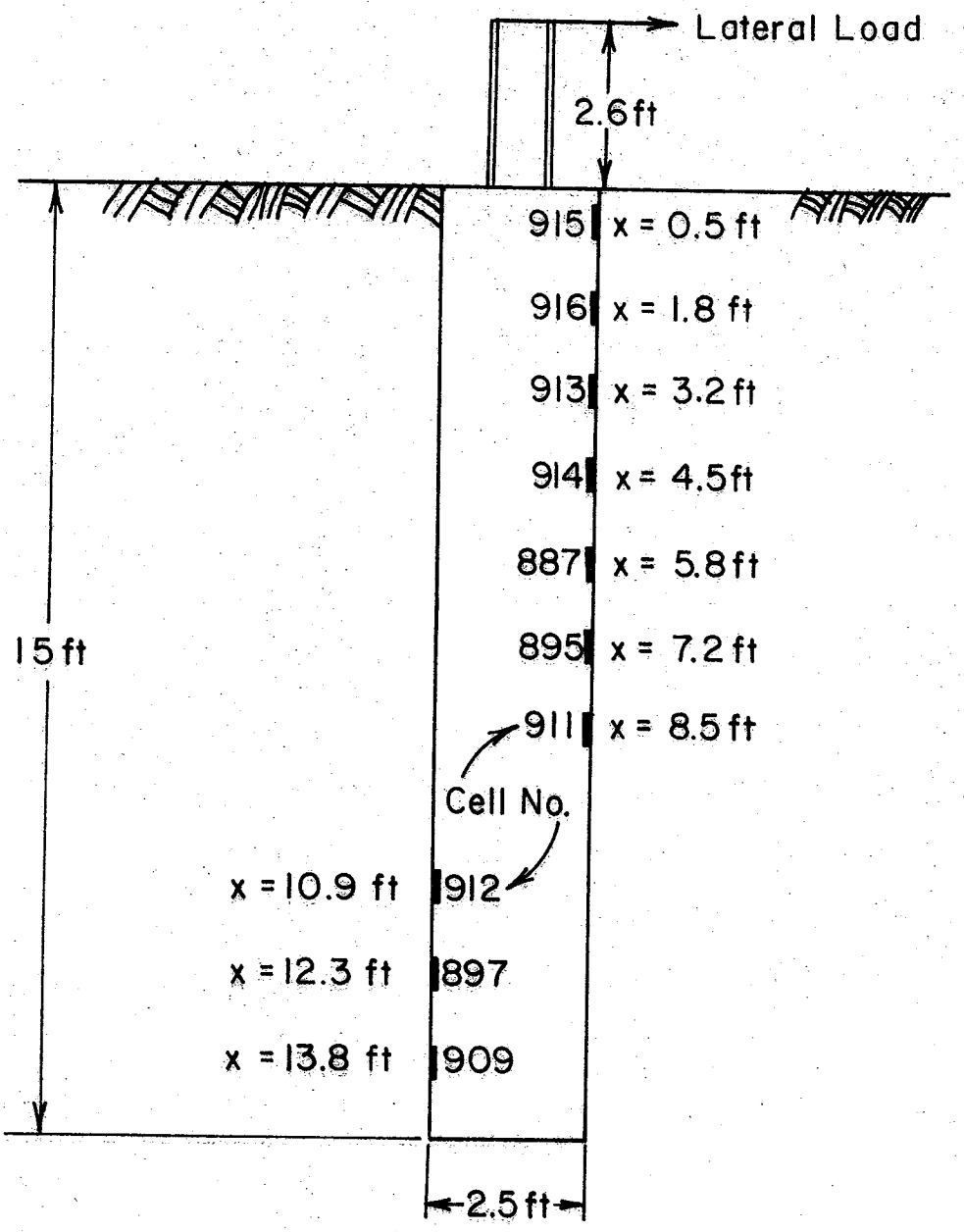

FIG. 15.— Location of Pressure Cells. x = Depth Below Groundline (1ft=0.3048m)

steel column center line. The dial gages were attached to a steel beam that was remotely supported behind the shaft as shown in Fig. 16. The accuracy of the dial gages was to the nearest ± 0.001 in. (0.03 mm).

Rotation instrumentation. - The rotation of the test shaft was measured by means of a Hilger and Watts TB108-1 inclinometer and a plumb bob apparatus. The 12 WF 120 steel column bolted to the top of the shaft was used as a reference datum for both rotation measuring devices. Using the inclinometer, rotational measurements were made by placing the inclinometer at five reference points along the flange of the steel column. The inclinometer measures the angle of tilt directly with respect to the horizontal plane. Accuracy of the inclinometer measurements are approximately ± 1 minute.

By suspending a plumb bob a fixed distance from the top of the steel column, an additional system for measuring shaft rotation was devised. Horizontal measurements from the plumb line to the five reference points on the flange of the steel column allowed the determination of the relative movement of the points. Knowing the geometry of the plumb bob system, the relative movements were converted to degrees of rotation.

Loading Procedure

All reported previous research work dealt with the behavior of drilled shafts under short-term static loads. Kasch et al. (20) in 1977, and Holloway et al. (14) in 1978, reported the results of two short-term static tests conducted during this research study. Kasch simulated the backfilling process of a retaining wall and the

Plan View

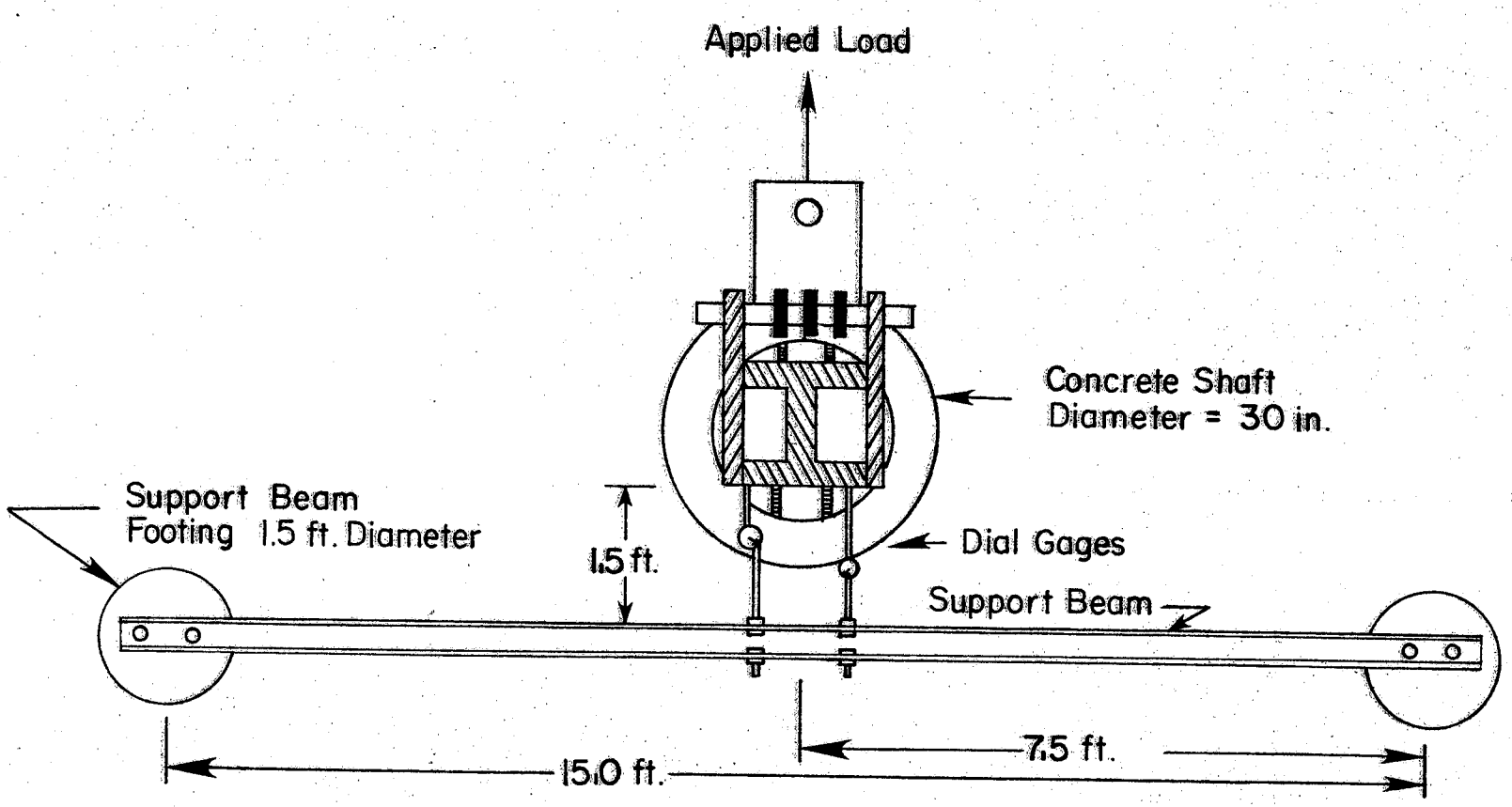

FIG. 16 — Position of Deflection Dial Gage (1 ft. = 0.3048m, 1in. = 2.54cm)

overburden pressure imposed by the backfill on the retaining wall, during a six-day period. Holloway also used a short-term loading procedure. At higher loads, it was apparent during each of the two tests that for any given load the movement was continuing for an indefinite period of time. A plot illustrating the time-dependent behavior for Holloway's test shaft is shown in Fig. 17. This time-dependent deformation behavior of a soil mass under a sustained load is usually referred to as soil creep.

In 1979 Bhushan, Haley, and Fong (1) presented the results of full-scale lateral load tests on 12 drilled shafts in stiff overconsolidated clay. The loading rate applied to the shafts was short-term; however, the effect of soil creep was observed. Although no long-term, load-deflection measurements were made, it was inferred that for loads generally less than one-half the ultimate load, deflections under sustained loading were not likely to exceed the deflection under short-term static loading by more than 20%. Until the Bhushan study, actual full-scale field testing to support the above assumption had not been performed on drilled shafts. In an earlier study conducted by Dunlap, Ivey, and Smith (8), long-term loading effects were investigated on drilled shaft footings which support minor service structures.

During the final test of this research effort, long-term or sustained lateral loads were applied to the test shaft. The purpose of this phase of the study was to determine if the application of long-term, sustained lateral loads would result in excessive time-dependent deformations.

The loading of the final test shaft began on June 13, 1979 and

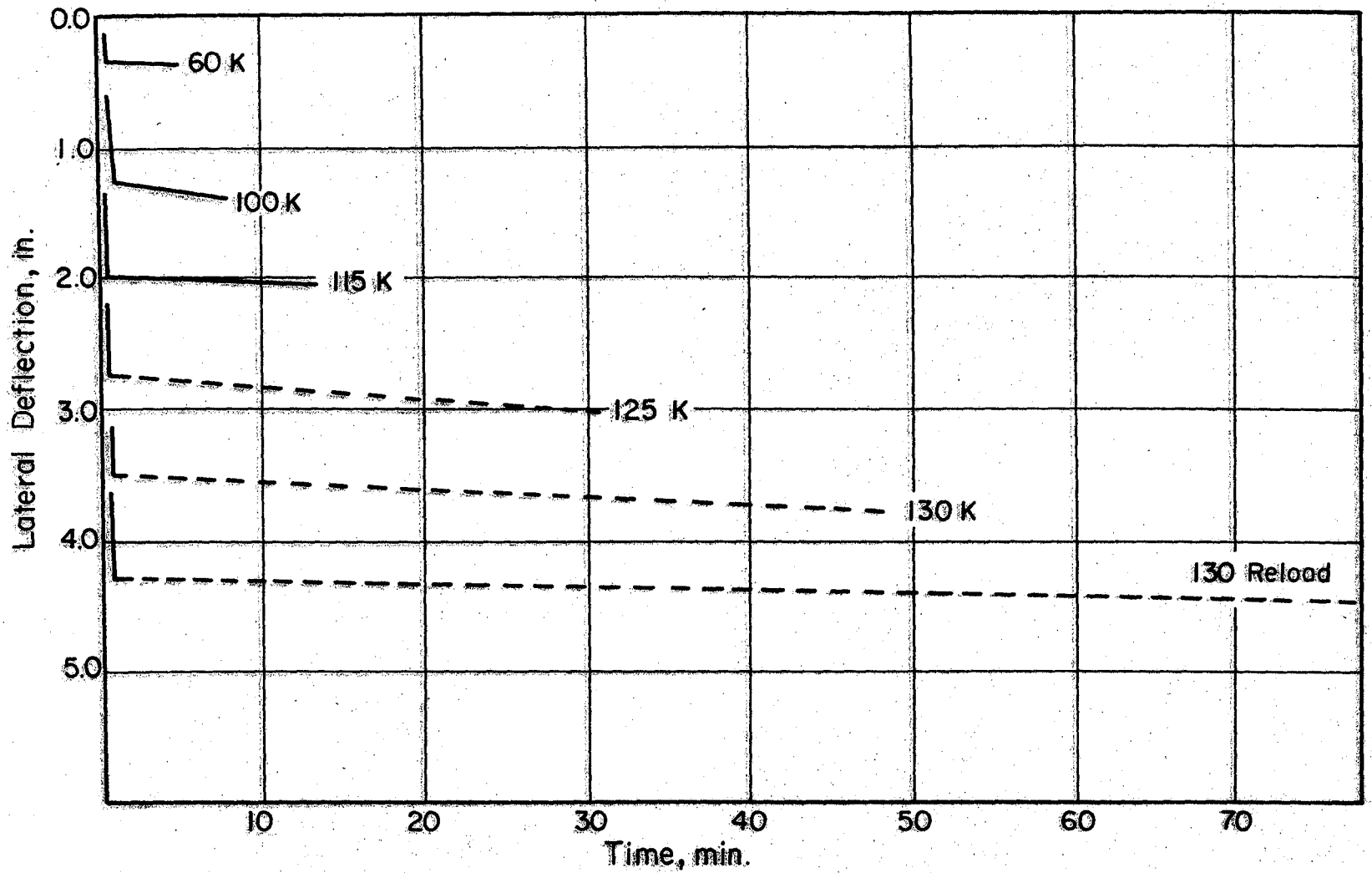

FIG. 17.– Lateral Deflection Versus Time (After Holloway et al.) (1 kip = 4.45 kN, 1 in = 2.54 cm)

continued until January 4, 1980. Initially, loads were applied by hanging weights from the suspended cable. This was done mainly to "seat" the loading system and to utilize the "dead weight" system. Thereafter, loads were applied in 2.5 kip (11.1 kN) increments by the hydraulic winch. Each load increment was maintained until the shaft movement had essentially ceased. The time usually required for shaft movement to stop was approximately one week.

Unfortunately, the "dead weight" system did not perform entirely as had been expected. Daily temperature changes caused the cables in the loading system to expand and contract, thus creating a small cyclic effect in the applied load.

When the shaft reached a rotation of approximately 1.5 degrees, the loading procedure was altered. At that time it was decided to load the shaft continuously until it was pulled out of the supporting soil.

FINAL FIELD LOAD TEST RESULTS

The results of the final lateral load test conducted during the period from June 1979 to January 1980 are presented in this section along with the presentation and analysis of deflection, rotation and soil reaction characteristics of the test shaft.

Load-Deflection and Load-Rotation Characteristics

The measured values of lateral load versus groundline deflection for both the immediate and long-term loading conditions are shown in Fig. 18. The immediate deflection values for each load increment were obtained by taking the difference between the initial dial reading before loading and the reading taken approximately 30 minutes after the load was applied. The immediate curve was then constructed by summation of the 30 minute time interval readings for each applied load increment, disregarding deflections occurring after the initial 30 minute time span. The long-term deflections were obtained in a similar manner, except that the final dial reading was taken when shaft movement had essentially stopped. The long-term curve illustrates the total amount of shaft movement. Measurements taken in this manner enabled the time-dependent behavior of the soil to be observed to some degree. However, it should be pointed out that the immediate curve does not accurately represent a true short-term loading curve which would be obtained if such a short-term load test were conducted. The immediate curve as extrapolated from the long-term load test data indicates smaller deflections for a given load then

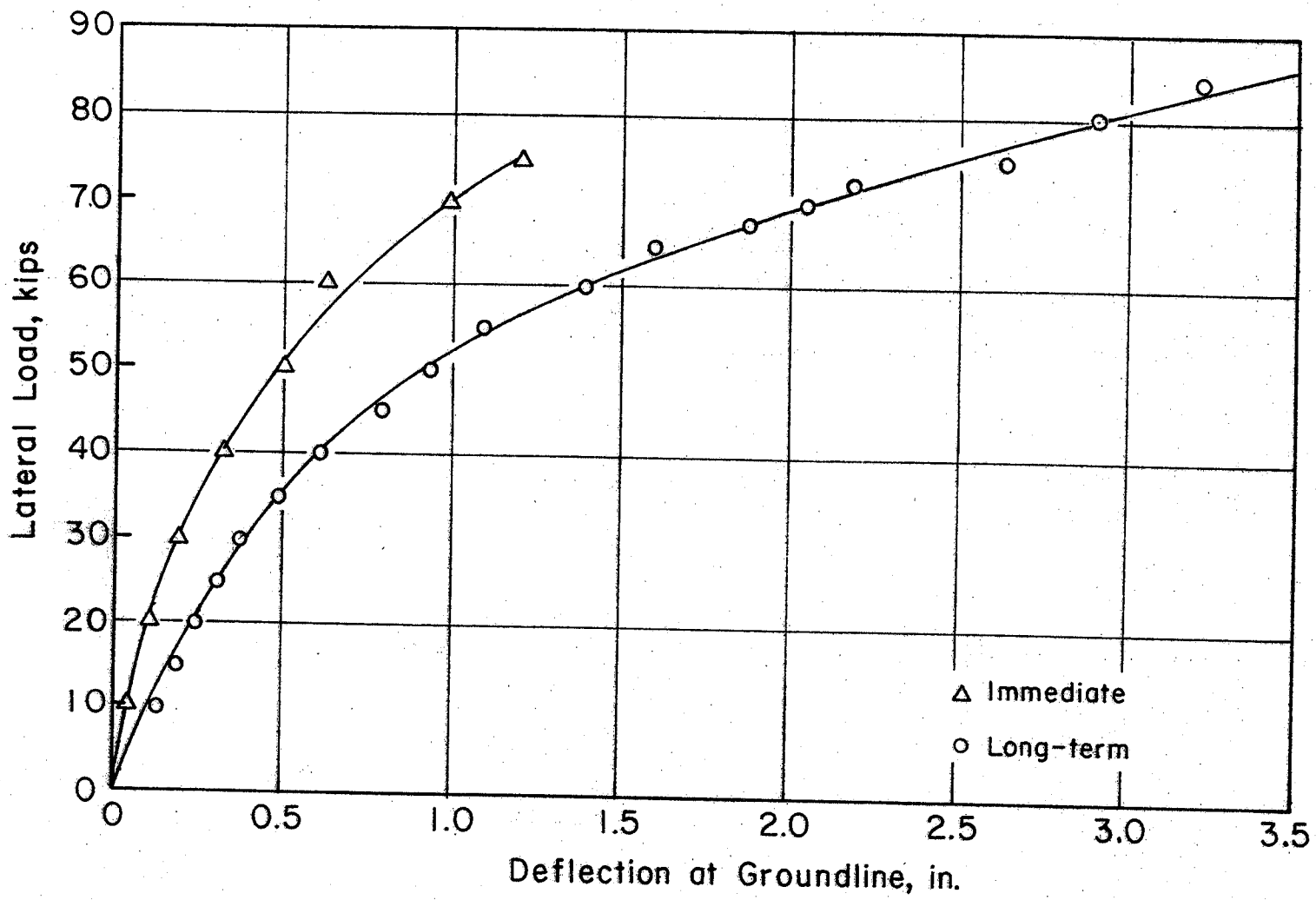

FIG. 18.— Lateral Load Versus Deflection at Groundline For Final Test Shaft (1 kip = 4.45kN, 1 in = 2.54 cm)

would be obtained in a short-term load test. Nevertheless, the test data illustrate that some amount of time-dependent deformation was present. For comparison purposes the total and immediate deflections for each load application are tabulated in Table 1.

Bhushan et al. (1) indicated from field load tests performed on 12 piers that additional deflection under constant load, except for loads near failure, increased on the order of 10% with a range of 0 to 20%. However, it should be pointed out that these load tests were conducted in very stiff clays 2.38 tsf - 2.75 tsf (228 kN/m^2 - 263 kN/m^2). In relatively soft soils the time-dependent response could be much more detrimental. Dunlap and Ivey (8) reported percentage reductions on the order of 33% to 50% long-term loads based on different soil conditions. However, these percentages were based on a limited amount of data and the values recommended are believed to be highly conservative.

The load-rotation curve for the final test shaft is shown in Fig. 19. Values of rotation were recorded in the same manner as the long-term deflection readings, that is, before and after each load increment. Referring to the load rotation curve it can be seen that the test shaft reached its maximum capacity at approximately 92 kips (409 kN), corresponding to a rotation of about 2 degrees. Similar relationships between ultimate load and rotation were reported by Kasch et al. (20) and Holloway et al. (14). These relationships for the other test shafts will be discussed in greater detail in a later section.

TABLE 1. - Deflections For Final Load Test

Load in Kips	Immediate Deflection, in inches	Total Deflection, in inches
5	0.012	0.041
10	0.043	0.133
15	0.076	0.192
20	0.111	0.247
25	0.147	0.310
30	0.193	0.375
35	0.259	0.486
40	0.324	0.611
45	0.417	0.798
50	0.497	0.930
55	0.568	1.080
60	0.629	1.308
65	0.738	1.580
70	0.973	2.045
75	1.200	2.633
80	-	2.902
85	-	3.211
90	-	3.662

NOTE: 1 kip = 4.45 kN; 1 in. = 25.4 mm

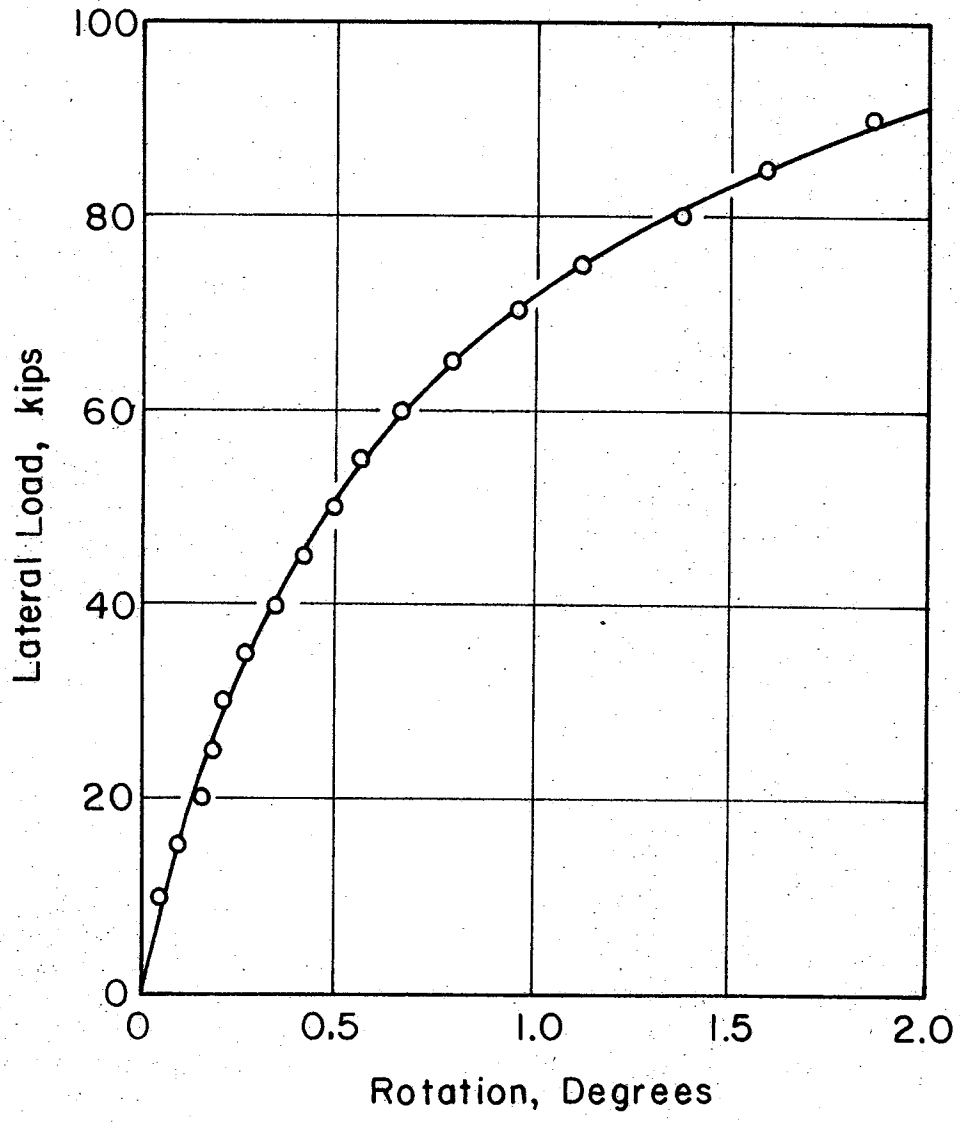

FIG. 19.– Lateral Load Versus Rotation For Final Test Shaft (1 kip = 4.45 kN)

Pressures During Lateral Loading

Throughout the entire final field-load test the soil pressures that resulted from the applied lateral loads were monitored and recorded. Initially, before the application of the first load increment, pressure cell readings were taken to establish a zero reading for each cell. Several readings were taken to insure that the cells were functioning properly. At this point, it was discovered that cell 912 produced erratic readings and was inoperative. The remainder of the cells at this stage seemed to be functioning properly.

The soil pressures that resulted from the applied lateral loads to the drilled shaft were obtained by subtracting the initial cell reading (zero reading) from the cell reading at a particular load. The soil pressures obtained for each cell throughout the test are plotted in Figs. 20 through 28.

A plot of lateral pressure versus depth for various lateral load levels is shown in Fig. 29. From this plot it is observed that the upper 4 pressure cells (915, 916, 913, 914) appear to be indicating erroneous results when compared to the pressures recorded in the lower 5 cells (887, 895, 911, 897, 909) and the results obtained from previous research (14, 15, 20).

A possible cause of the apparently erroneous data was that a mechanical defect in the pressure cells might have caused them to malfunction during the test. To investigate this possibility, the pressure cells were removed and taken to the laboratory to verify their operation after the load test was completed and the shaft was

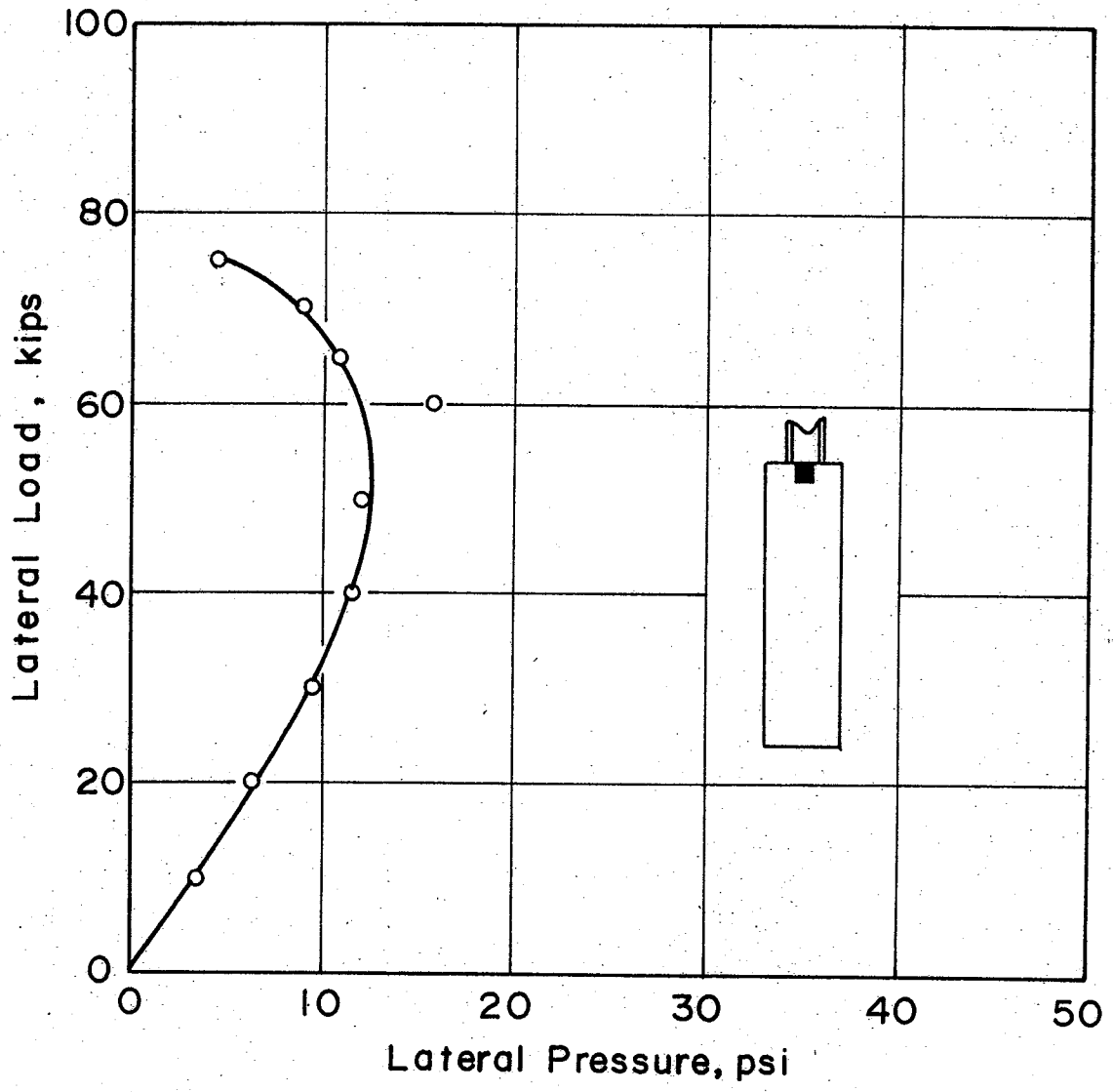

FIG. 20 – Lateral Load Versus Lateral Pressure, Cell 915
(1 kip = 4.45 kN; 1 psi = 6.89 kN/m^2)

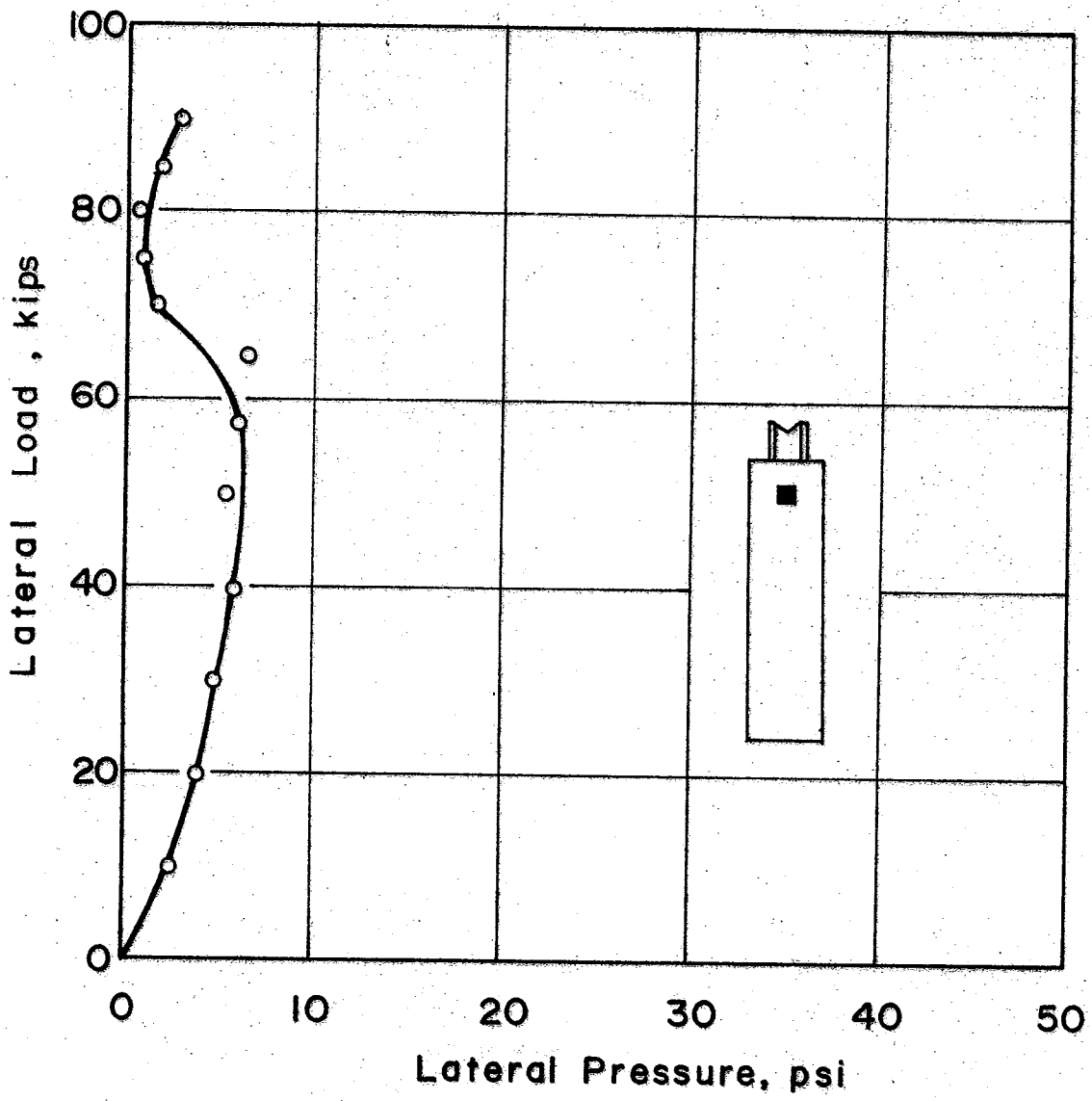

FIG. 21 – Lateral Load Versus Lateral Pressure, Cell 916
(1 kip = 4.45 kN; 1 psi = 6.89 kN/m^2)

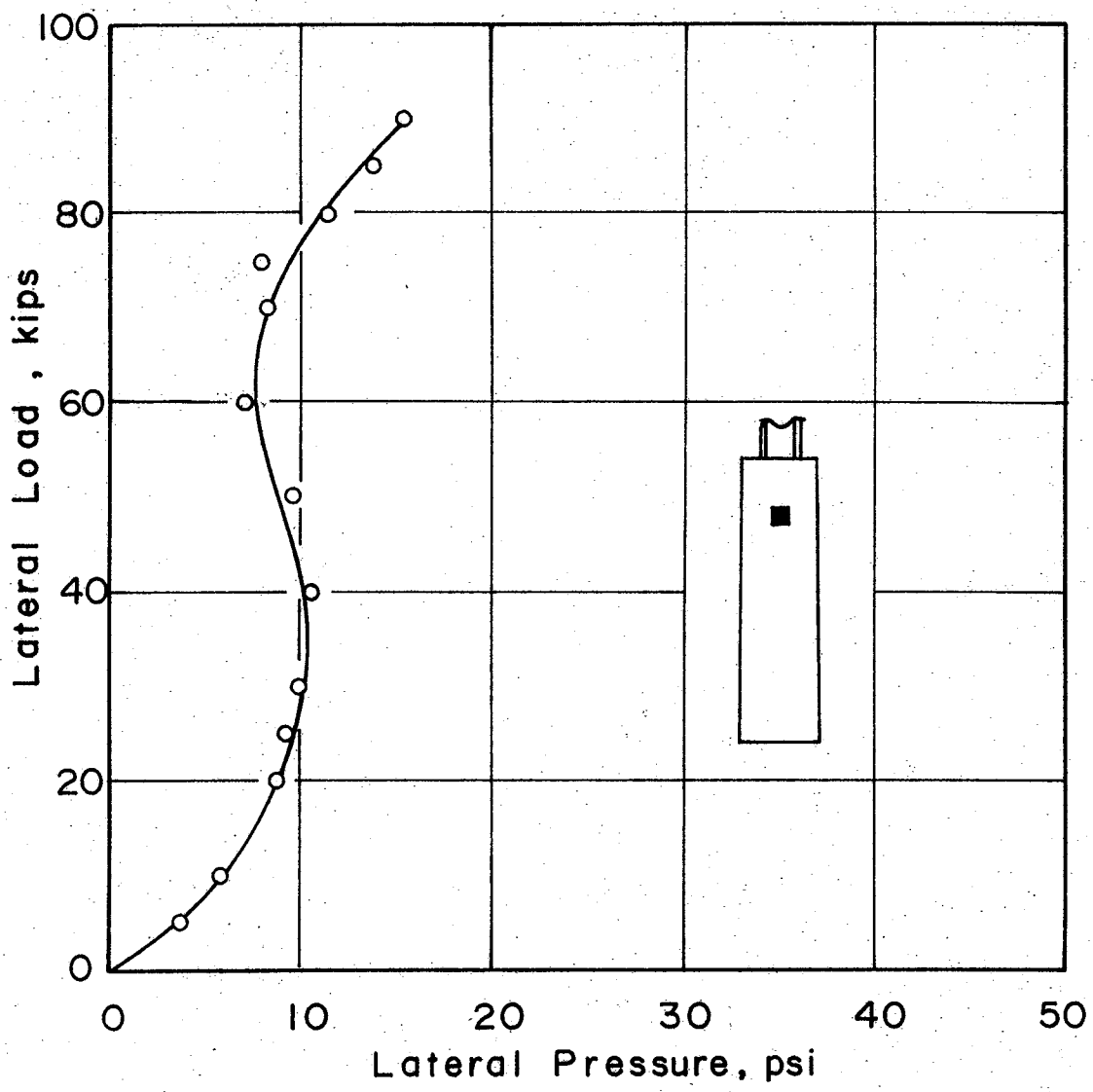

FIG. 22 - Lateral Load Versus Lateral Pressure, Cell 913
(1 kip = 4.45 kN ; 1 psi = 6.89 kN / m^2)

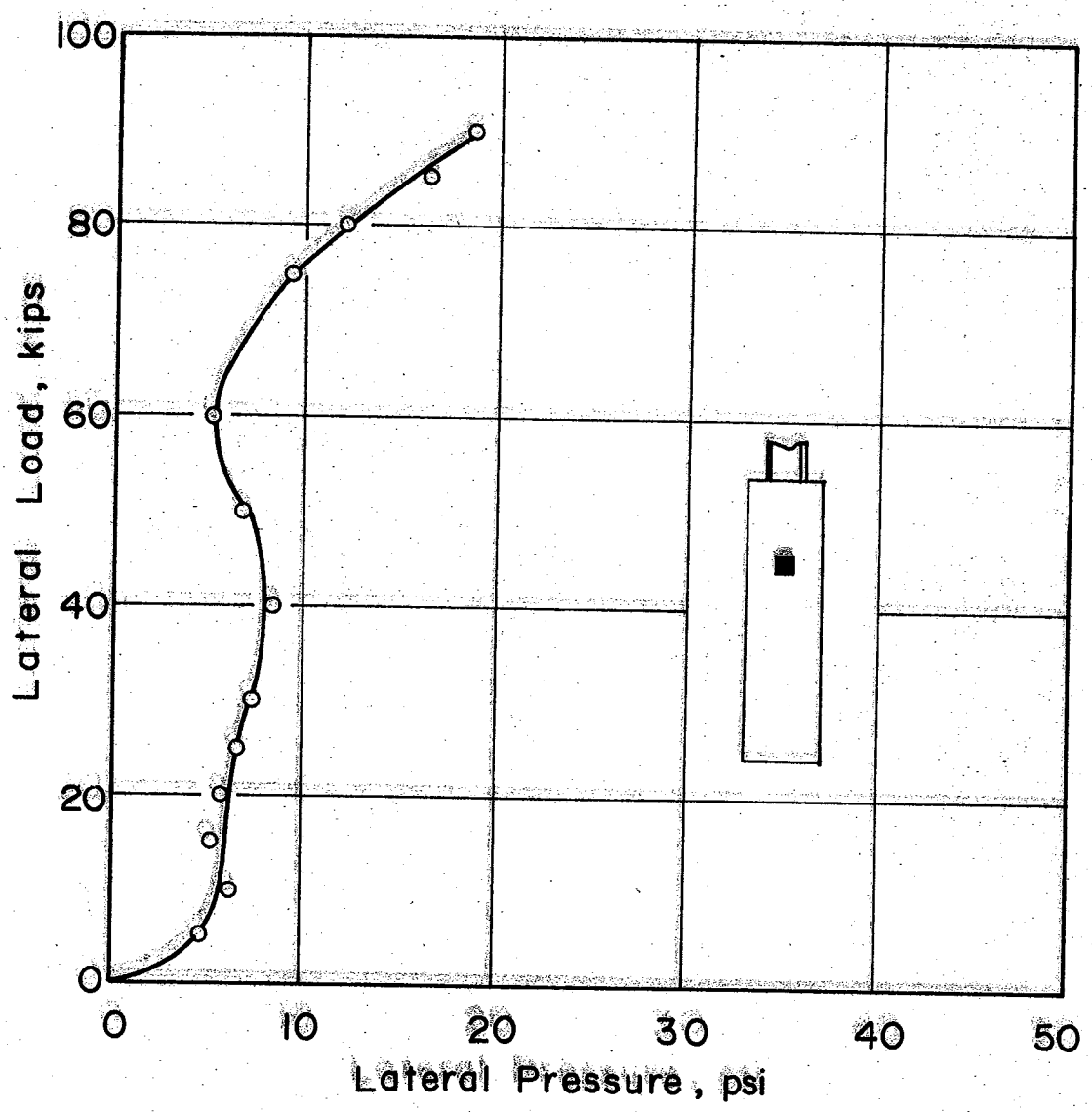

FIG. 23 - Lateral Load Versus Lateral Pressure, Cell 914
(1 kip = 4.45 kN; 1 psi = 6.89 kN/m²)

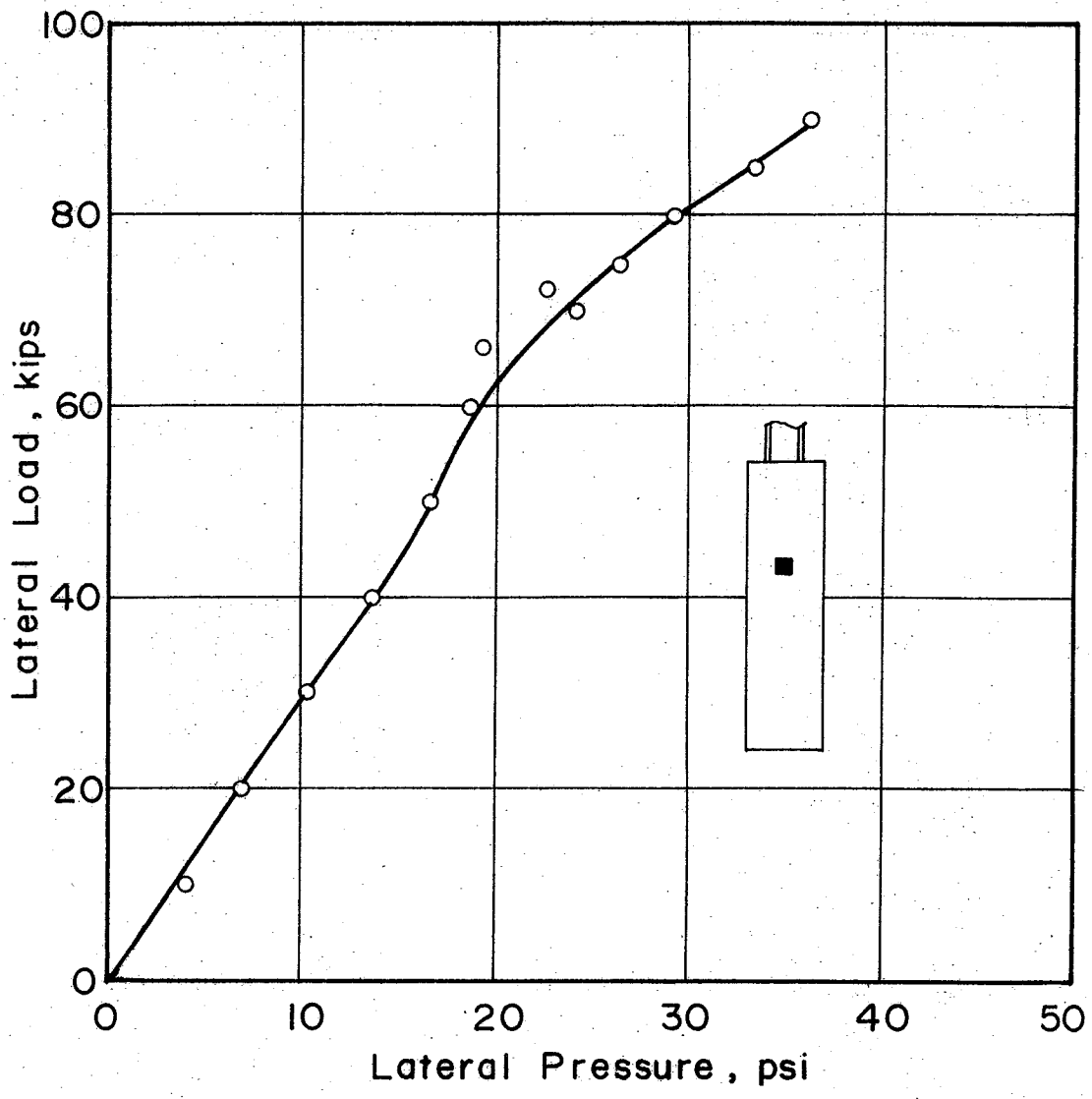

FIG. 24 - Lateral Load Versus Lateral Pressure, Cell 887 (1 kip = 4.45 kN; 1 psi = 6.89 kn/m^2)

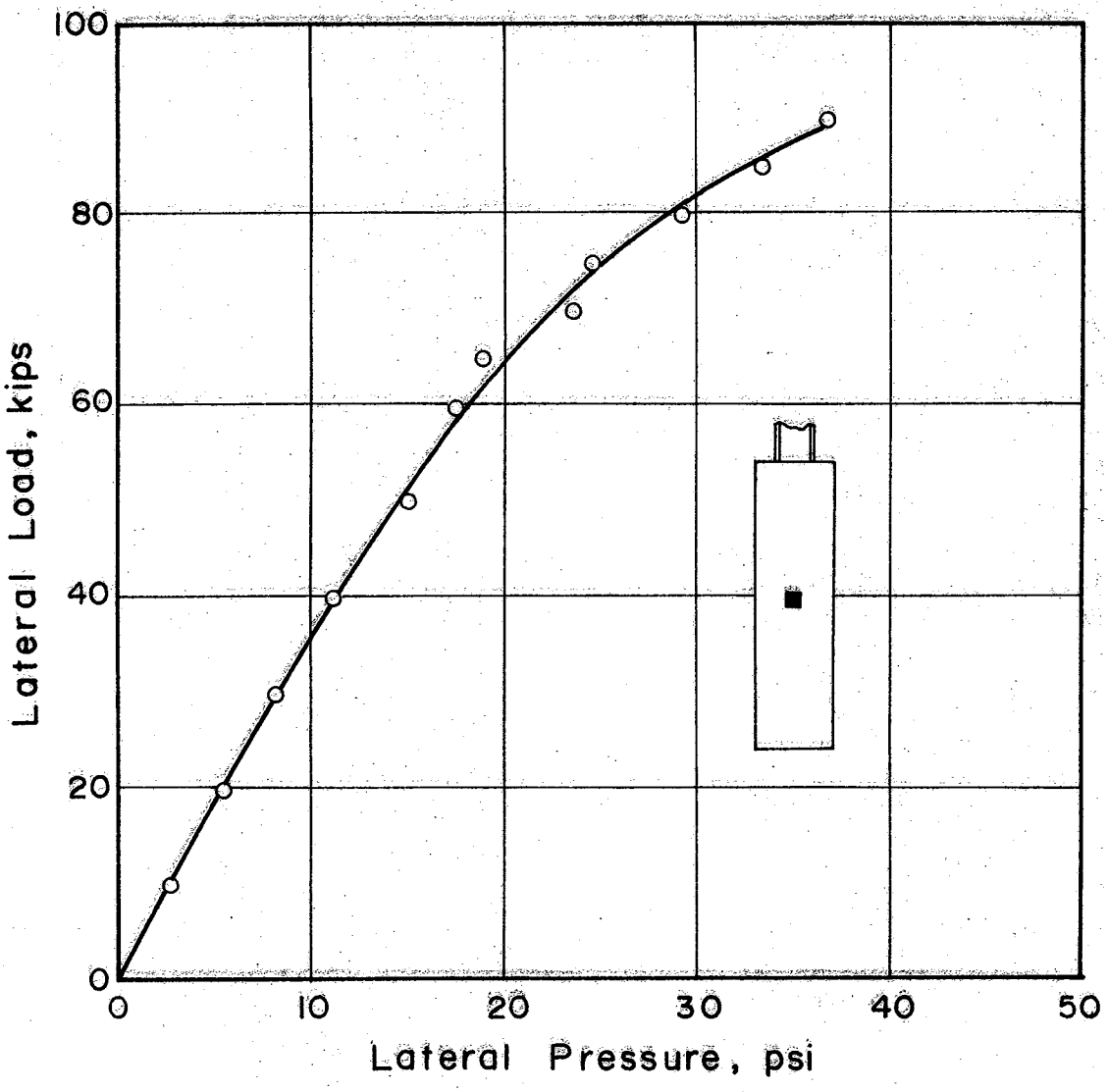

FIG. 25 - Lateral Load Versus Lateral Pressure, Cell 895 (1 kip = 4.45 kN; 1 psi = 6.89 kN/m^2)

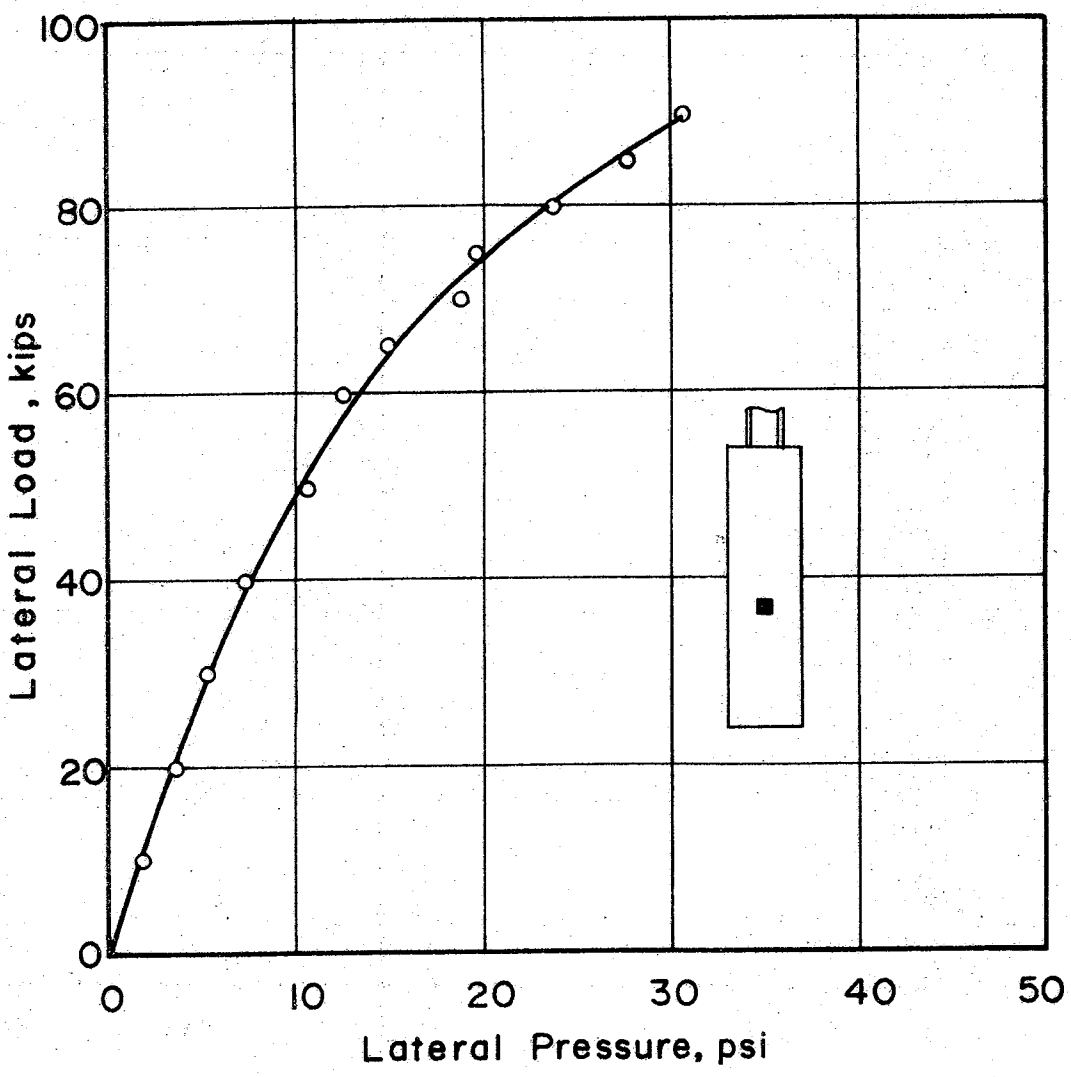

FIG. 26 – Lateral Load Versus Lateral Pressure, Cell 911
(1 kip = 4.45 kN; 1psi = 6.89 kN/m^2)

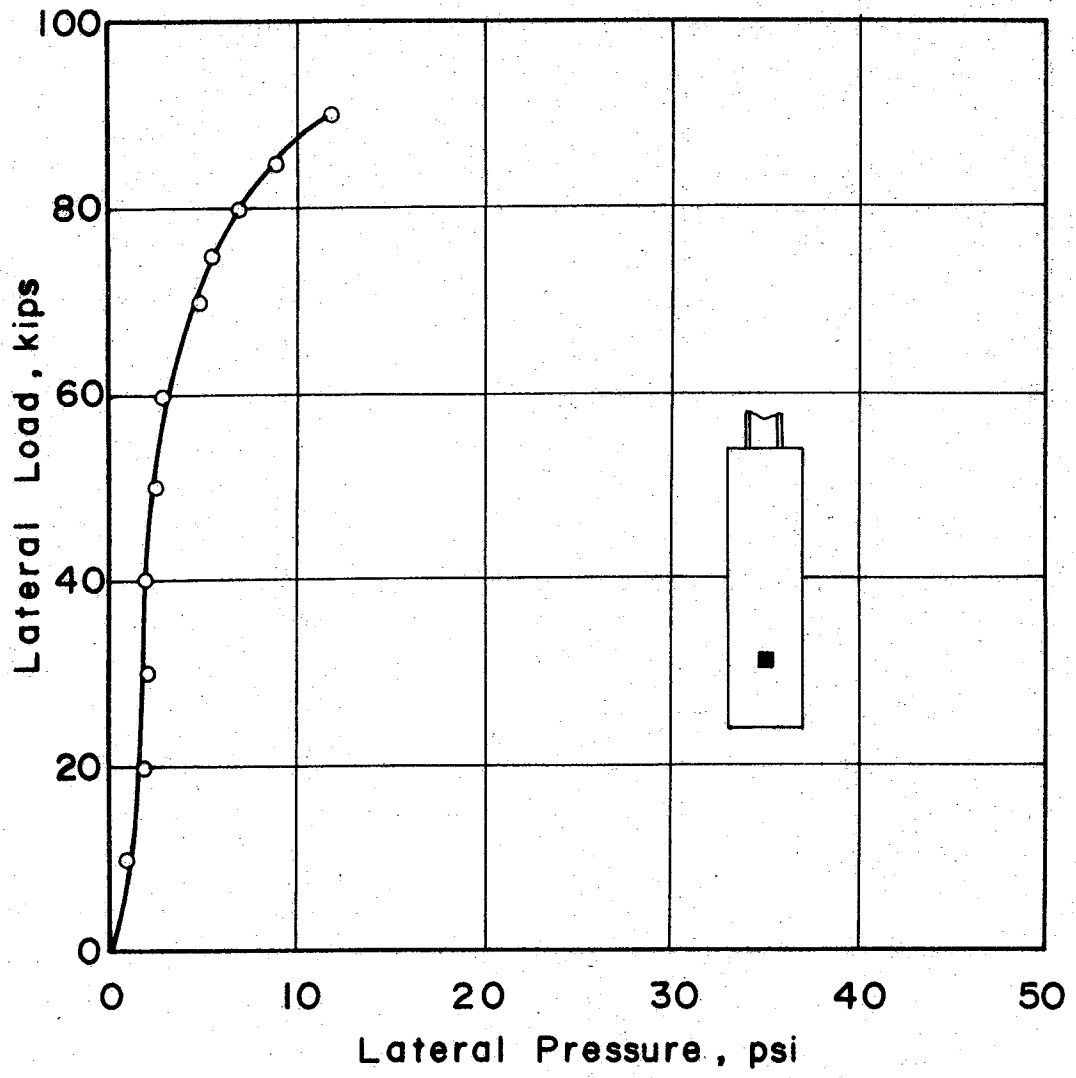

FIG. 27 — Lateral Load Versus Lateral Pressure, Cell 897
(1 kip = 4.45 kN ; 1 psi = 6.89 kN/m^2)

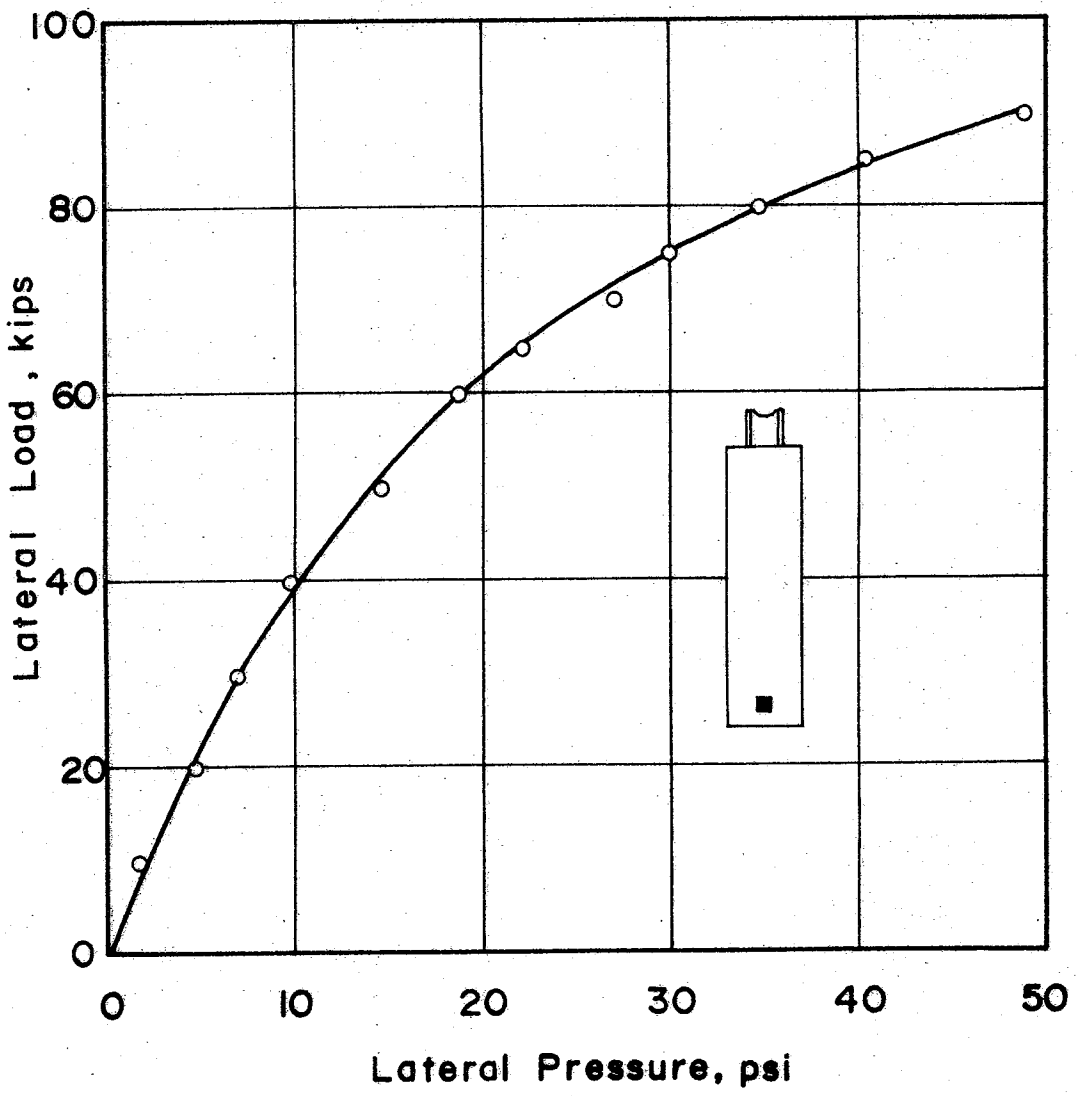

FIG. 28 – Lateral Load Versus Lateral Pressure, Cell 909

(1 kip = 4.45 kN; 1 psi = 6.89 kN/m^2)

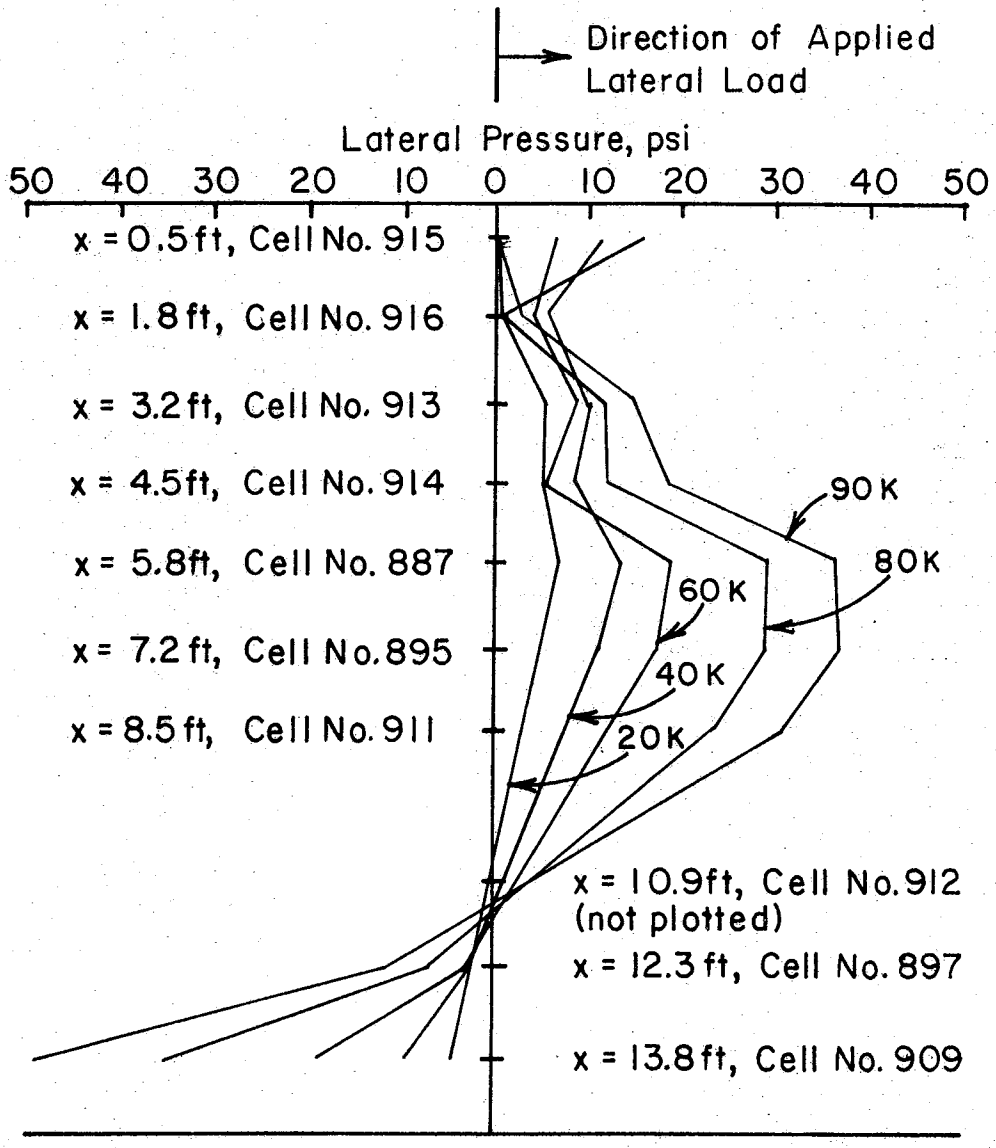

FIG. 29.—Lateral Pressure Versus Depth For Final Test Shaft. x = Depth Below Groundline (1 ft = 0.3048 m, 1 kip = 4.45 kN, 1 psi = 6.89 kN/m^2)

removed from the ground. It was then noticed that the fluid within cell 915 had escaped due to a leak in the line connecting the cell with the transducer (see Fig. 14). Referring to Fig. 20, it appears that cell 915 was functioning properly until the 60 kip (267 kN) load level. It was also observed that cell 914 was reading 3 psi (20.7 kN/m^2) low. Therefore, a correction of 3 psi (20.7 kN/m^2) was applied accordingly to the raw data taken from the field. The remainder of the cells appeared to be functioning properly.

In an attempt to determine if the recorded pressures were valid, the static equilibrium of the shaft was checked. This was accomplished by assuming that the pressures acted uniformly over the projected diameter of the shaft and by summing moments about the point of zero lateral stress. The static analysis showed that the shaft was not in equilibrium based on the recorded pressures, and that, in order to achieve equilibrium, the lateral pressures in the upper portion of the shaft would have to be increased substantially.

From the one additional soil boring taken for the final test it was noted that the shear strength of the soil had decreased in the upper soil strata due to abnormally large amounts of rain. This could possibly account for the low pressure readings acquired in the upper cells. However, the soil strength decrease, as compared to the other two previous test shafts, is not significantly lower. Therefore, it is concluded that the pressure distribution in the upper portion of the shaft (above cell 887) is not representative of the actual soil reaction which occurred during the final load test.

Considering the results shown in Fig. 29 it is possible to draw

some general conclusions about the shape of the lateral soil pressure distribution. Disregarding the upper four pressure cells, the lateral pressure distribution in the lower portion of the shaft seems to take the form of a parabolic function. The absence of a pressure cell near the 10 ft (3.0 m) depth made it necessary to interpolate in order to obtain pressures between cell 911 and 897. Consequently the distribution is not as well defined in this region. Also, based on the stress distribution, the point of zero lateral stress or the point of rotation is located at a depth below the ground surface equal to approximately 0.7 times the embedment depth of the shaft. This location lies in the range which has been reported and documented by other researchers (12, 14, 15, 17, 20).

Rotation Point

Many of the proposed theories for the design and analysis of rigid drilled shafts assume a fixed position for the point of rotation. As indicated in the introduction of this report, this is not always the case. The location of the point of rotation for this test shaft was obtained in two ways: (1) from inclinometer or rotation data, assuming a rigid shaft exists; and (2) from the lateral earth pressure distribution along the length of the shaft, assuming the point of rotation lies at the point of zero lateral stress.

Based on the inclinometer readings, the point of rotation was obtained by dividing the measured deflection of the shaft by the tangent of the rotation angle. During the analysis of these data, it was realized that deflection of the steel column due to the applied

lateral load would introduce error into the computed values. Therefore, a correction was applied based on the amount of deflection experienced by the steel column. The measured and corrected rotation points are presented in Table 2. The data given in Table 2 indicate that the exact location of the point of rotation of the shaft is not precisely defined. However, the values lie in a range close to the two-thirds embedment depth as shown by other researchers (14, 15, 19, 33, 34). Also, there seems to be a trend for the point to shift downward with increasing lateral load as proposed by Hays et al. (12).

Conflicting results exist between the location of the point of rotation found by the pressure cell distribution and by the inclinometer. Use of the lateral pressure distribution seems to indicate that the rotation point lies in the range of 10.6 ft (3.23 m) to 11.8 ft (3.60 m) below the ground surface, while the corrected inclinometer results indicate that the shaft was rotating at a shallower depth in the range of 7.44 ft (2.27 m) to 11.11 ft (3.39 m). Both methods show that the rotation point shifted downward from some point below the middle of the shaft for light loads, to a point approximately three quarters of the embedment depth for maximum loads. Analytical studies performed by Hays et al. (12) also suggested this type of behavior.

Soil Reaction

In order for a rational and orderly prediction of the static resistance of a laterally loaded drilled shaft to be computed, an estimate of the soil deformation characteristics should be known.

TABLE 2. - Rotation Points Based on Inclinometer Data

Load, in Kips	Measured Rotation Point, in feet	Corrected Rotation Point, in feet
20	6.87	7.44
25	7.88	8.63
30	8.16	8.96
35	8.09	8.79
40	8.08	8.71
45	8.57	9.17
50	8.62	9.21
55	8.82	9.39
60	8.96	9.49
65	9.17	9.66
70	9.71	10.16
75	10.38	10.76
80	10.72	11.11
85	10.61	10.97

NOTE: 1 kip = 4.45 kN; 1 ft = 0.305 m

Instrumentation with pressure cells enabled soil pressure measurements to be made at any load on the test shaft. Thus it is possible to convert field soil pressures into soil reaction quantities by multiplying the soil pressure by the diameter of the shaft.

Several different theories have been proposed by Rankine (37), Hansen (11), Matlock (24), Reese (25), and Hays (12) to compute the soil reaction, p, which is the force per unit length of the shaft. The equations used by the various researchers are:

$$\text{Rankine:} \quad p = (\gamma X + 2\, C_u)\, B \quad \ldots\ldots\ldots\ldots\ldots \quad (2)$$

$$\text{Hansen:} \quad p = K_c\, C_u\, B \quad \ldots\ldots\ldots\ldots\ldots\ldots \quad (3)$$

$$\text{Matlock:} \quad p = \left\{3 + \gamma X/C_u + \frac{0.5X}{B}\right\} C_u\, B \quad \ldots\ldots\ldots \quad (4)$$

$$\text{Reese:} \quad p = \left\{3 + \gamma X/C_u + \frac{2.83X}{B}\right\} C_u\, B \quad \ldots\ldots\ldots \quad (5)$$

$$\text{Hays:} \quad p = 2\eta\, C_u\, B + \alpha X \quad \ldots\ldots\ldots\ldots\ldots \quad (6)$$

where p = soil reaction

γ = unit weight of the overburden material

X = depth below the groundline

C_u = undrained cohesive shear strength

B = shaft diameter

K_c = theoretical earth pressure coefficient

η = soil strength reduction factor

α = slope of the soil reaction curve

All of the above theories, except for Rankine's, incorporate a limiting value for the soil reaction at a critical depth below the groundsurface. The limiting value for Matlock's, Reese's, and Hays'

theory is 9 C_u B, while Hansen defined the limit at 8.14 C_u B.

If a value of 92 kips (409 kN) is taken as the ultimate load, then the soil pressures at this load level can be used to determine ultimate soil reaction. The lateral soil pressure which was recorded by cell 895 (see Fig. 29) in the direction of the applied 92 kip (409 kN) lateral load was 36.8 psi (254 kN/m^2). The corresponding value of lateral soil pressure in the direction away from the applied lateral load was recorded by cell 909 (see Fig. 29) with a measured value of 49.1 psi (339 kN/m^2). The soil pressures recorded by cells 895 and 909 for the 92 kip (409 kN) load were used to construct the test shaft soil reaction curve. A plot of soil reaction versus depth, as determined by different theories and by field measurements, is presented in Fig. 30.

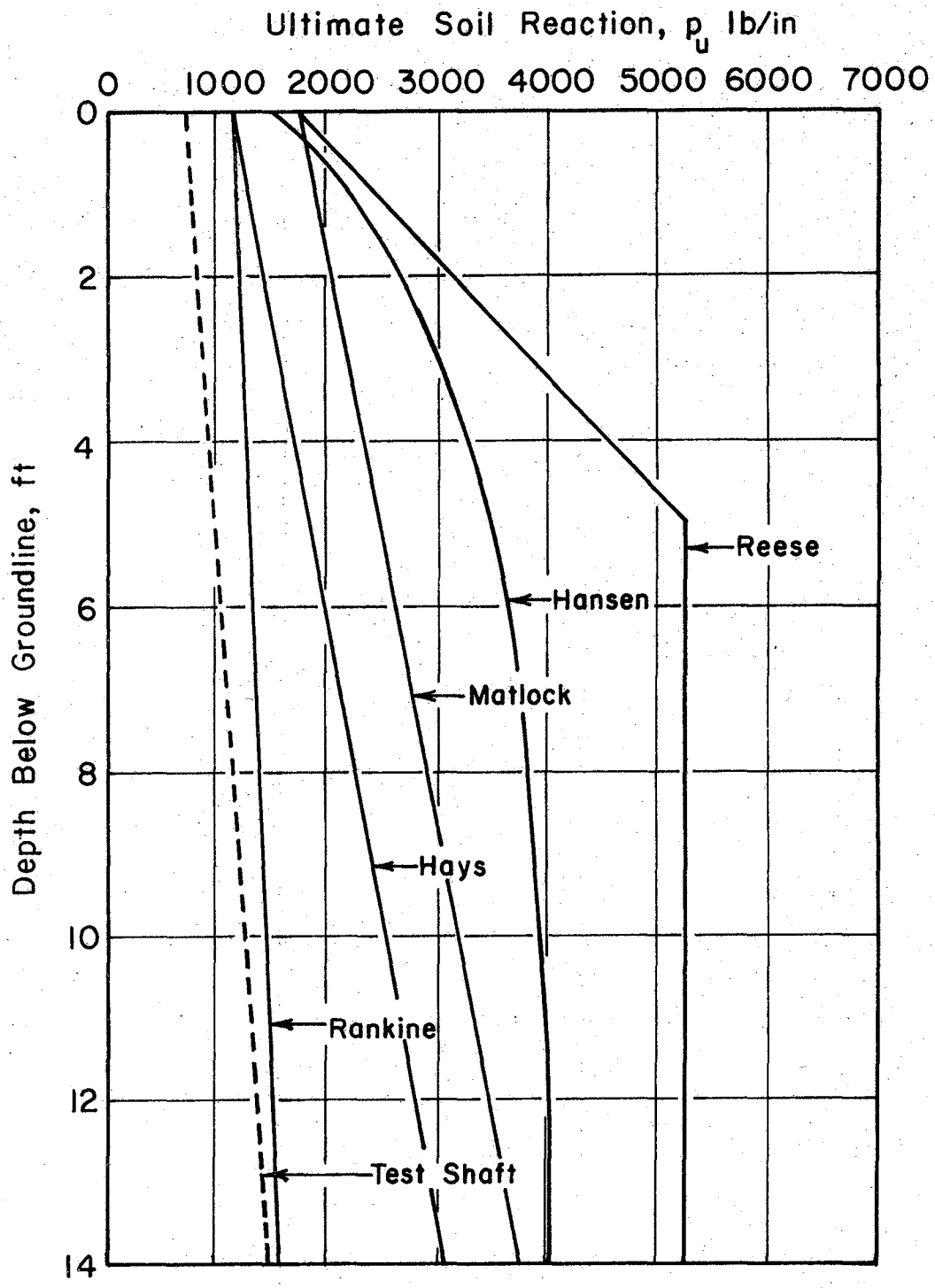

FIG. 30.— Ultimate Soil Reaction Versus Depth For Final Test Shaft (1 ft = 0.3048 m, 1 lb/in = 1.75 N/cm)

SUMMARY OF ALL FIELD LOAD TEST RESULTS

The prediction of the behavior of laterally loaded drilled shafts involves the determination of the shaft and soil interaction. In order to rationally study the soil-structure interaction and develop meaningful relationships, several different size shafts founded in different types of soil conditions should be investigated. The optimum situation in developing such relationships would involve a full range of shaft sizes founded in all types of soils. However, this is not economically feasible from a testing program, nor does the literature furnish sufficient information to make it possible. This section of the report contains a summary of the soil-structure interaction for a number of shaft sizes founded in several different types of soil conditions.

Load-Deflection and Load-Rotation Characteristics

The measured values of lateral load versus groundline deflection for the three load tests conducted during this research study are presented in Fig. 31. In all three test shafts, deflection readings were taken in the same manner as for the final test. From Fig. 31 it is seen that all three test shafts yielded a characteristically shaped load-deflection curve. The 1977 and 1978 test shafts experienced the same amount of resistance for a given deflection up to the 30 kip (134 kN) load. The 1979 test shaft, however, has a much flatter slope in the lower load region. One possible explanation for this is the time-dependent response of the soil when sustained loads are applied. However, it is difficult to determine the actual effect of

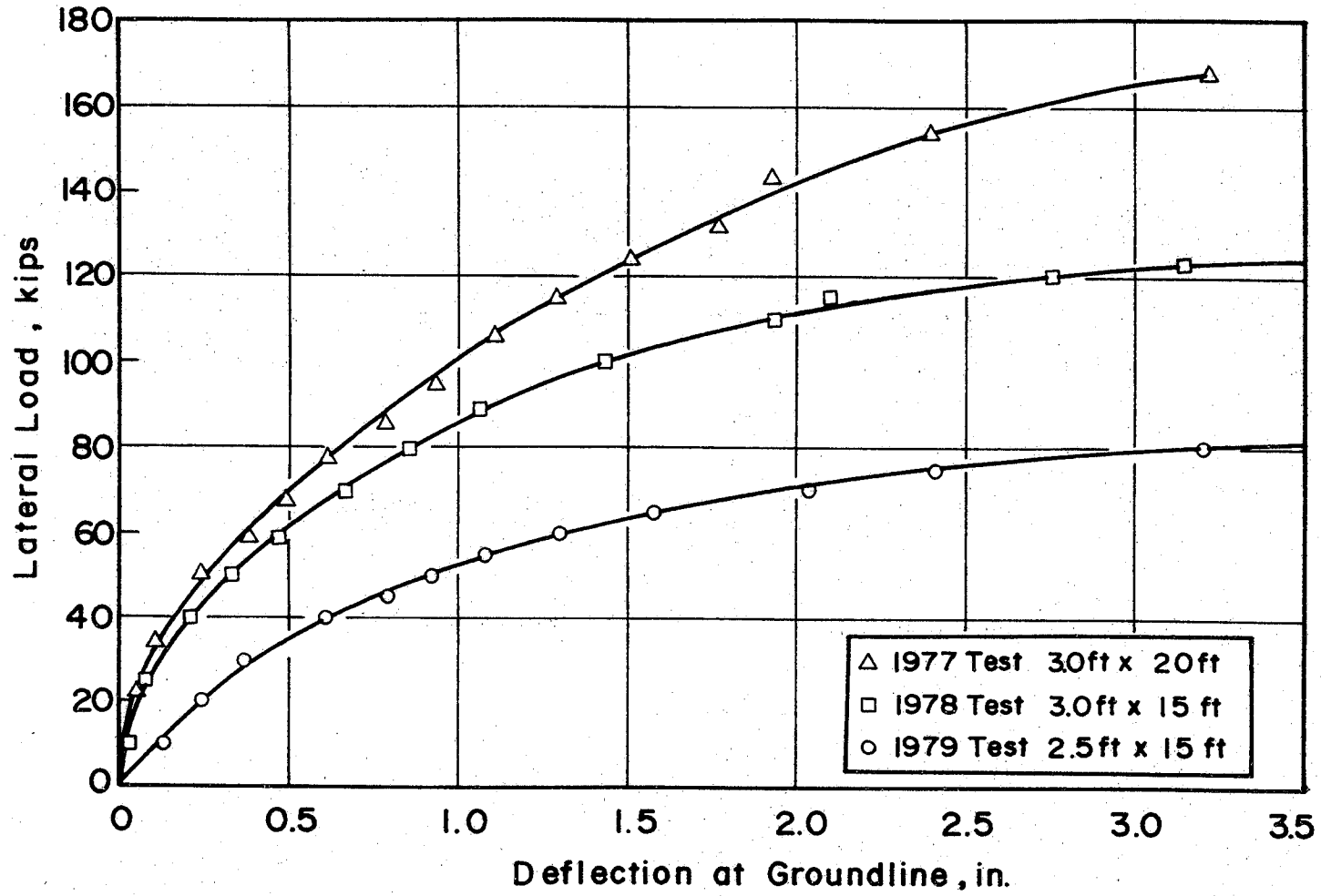

FIG. 31 - Lateral Load Versus Deflection at Groundline (TTI-Project 2211 Test Shafts) (1 kip = 4.45 kN; 1 in. = 2.54 cm; 1 ft = 0.3048 m)

long-term sustained loading without comparing load-deflection characteristics to a test shaft of the same dimensions, founded in the same soil, and subjected to short-term loading.

The load-rotation characteristics for the three test shafts are shown in Fig. 32. The ultimate lateral load capacity for drilled shafts in this study will be defined on the basis of rotation. The load which corresponds to a rotation of 2 degrees will be defined as the ultimate of the test shaft. The load corresponding to a rotation of 2 degrees is not the absolute maximum capacity of the test shaft, and it is considerably less than the load at 5 degrees rotation which Ivey and Dunlap (19) indicated was needed to develop the ultimate soil resistance for minor service footings. However, based on the results reported from other recently conducted field load tests (1, 14, 20), it is believed that at this load level any slight increase in load will cause continued amounts of undesirable deflection and rotation to occur. The amount of deflection and rotation which occurs is important in regard to the serviceability of the supported structure. Also, the load at 2 degrees rotation is not ultra-conservative in the sense of under-utilization of the available capacity of the shaft.

Ultimate Load Ratio Versus Shaft Rotation Correlation

Using the results of the three load tests conducted in this research study (14, 20), two performed by Ivey and Dunlap (19) and four reported by Bhushan et al. (1), a plot relating ultimate lateral load to shaft rotation up to 2 degrees was developed as shown in Fig. 33. The test shafts used in the plot ranged in size from 2.17 ft (0.660 m)

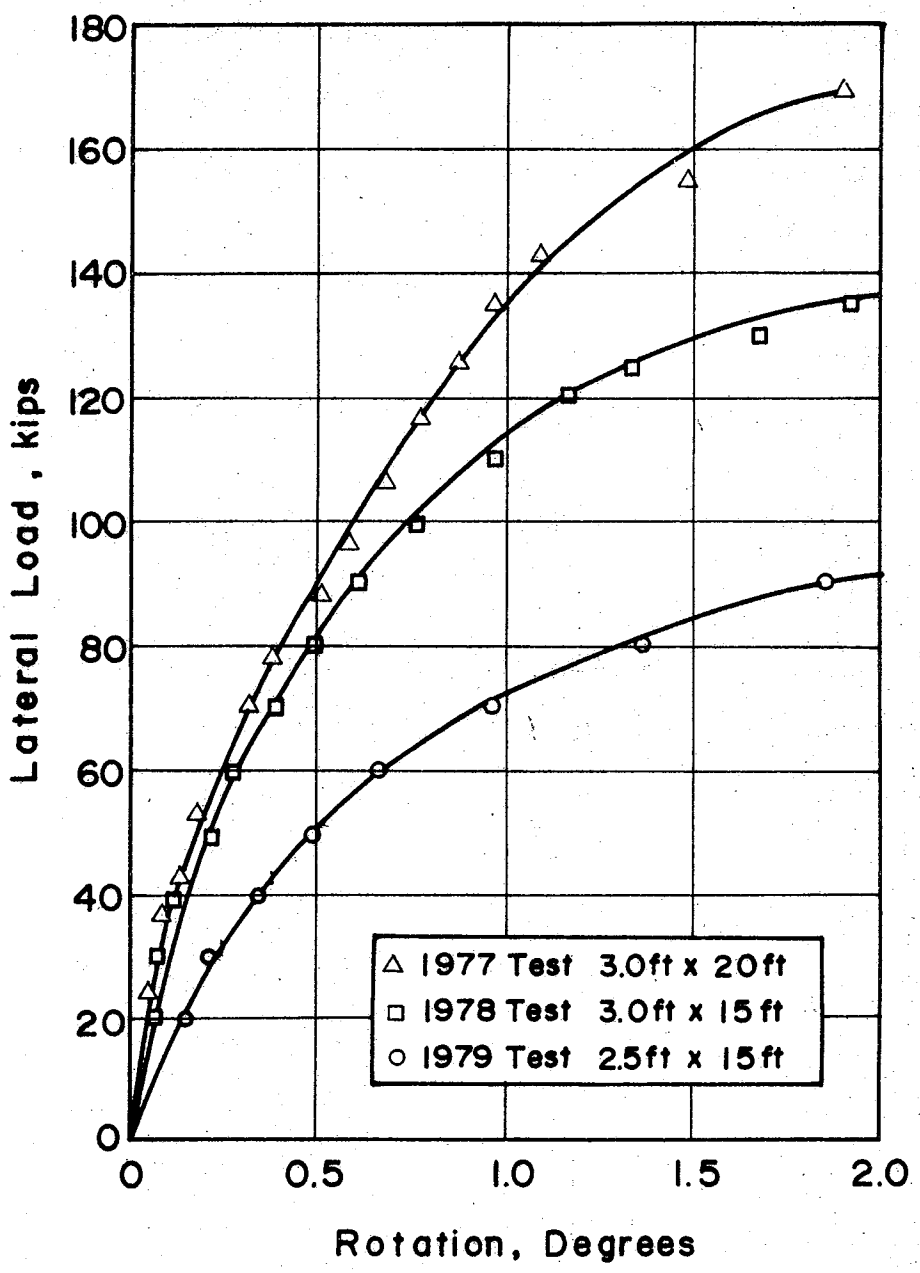

FIG. 32 – Lateral Load Versus Rotation (TTI - Project 2211 Test Shafts) (1 kip = 4.45 kN ; 1 ft = 0.3048 m)

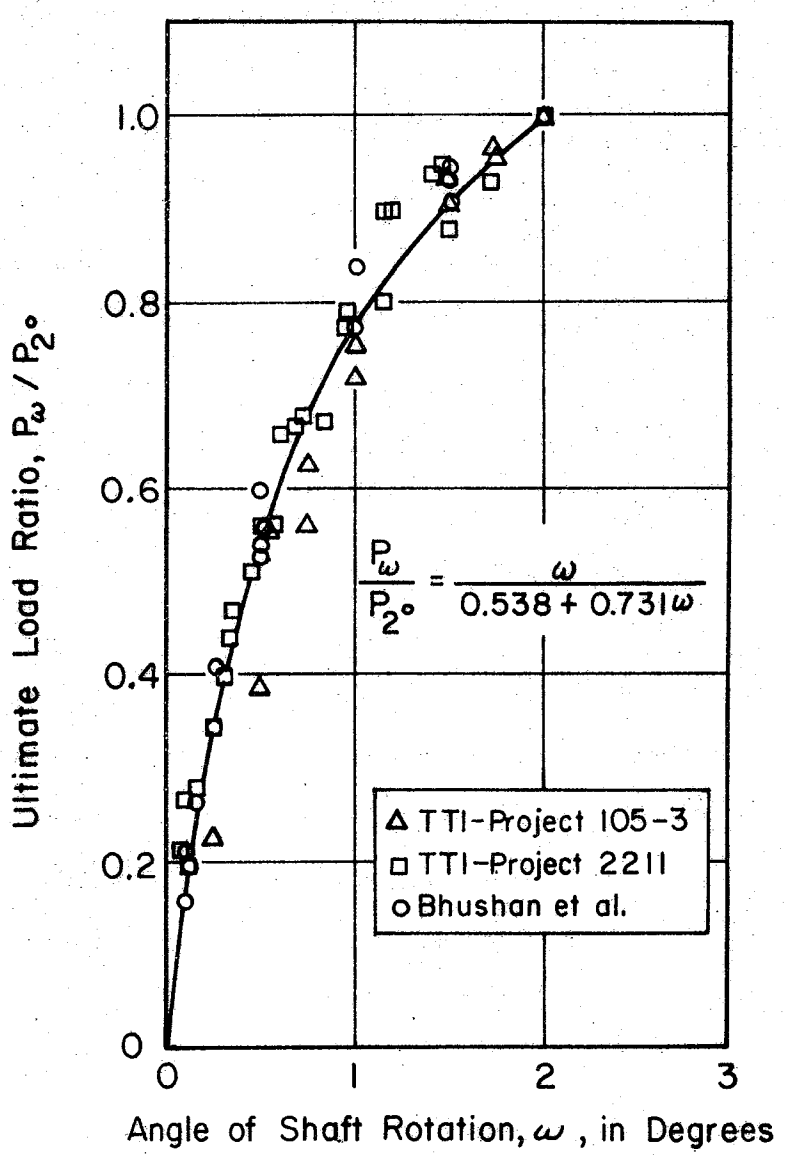

FIG.33— Ultimate Load Ratio Versus Shaft Rotation

in diameter by 6 ft (1.83 m) deep to 4 ft (1.22 m) in diameter by 15.5 ft (4.73 m) deep. The D/B ratio expressing the shaft rigidity varied from 2.77 to 7.75 and the undrained cohesive shear strengths ranged from 0.58 tsf to 2.75 tsf (55 kN/m^2 to 263 kN/m^2).

Ivey and Dunlap (19) developed a similar curve but defined ultimate lateral load capacity at a shaft rotation of 5 degrees. In the development of the plot, the load corresponding to 2 degrees rotation for each load test was assigned the value of 1.0. Each intermediate load corresponding to some rotation between 0 and 2 degrees is then expressed as a ratio of the 2 degree load. The plot by Ivey and Dunlap (19) was based on data from both model and full-scale load tests founded in soils including both sands and clays (18).

For this research study, rather than selecting a curve to conservatively represent the data, numerical methods were employed in the formulation of a best fit curve. The deviation of the plotted points from the selected correlation curve is remarkably small considering the wide range of shaft sizes and soil strengths represented by the data. The curve is described by the following equation:

$$\frac{P_\omega}{P_2o} = \frac{\omega}{0.538 + 0.731\ \omega} \quad \ldots\ldots\ldots\ldots\ldots\ldots \quad (7)$$

where P_ω = any intermediate load corresponding to an arbitrary shaft rotation, ω, between 0 and 2 degrees,

P_2o = the lateral load at a rotation of 2 degrees (ultimate load)

ω = shaft rotation between 0 and 2 degrees, and

P_ω/P_2o = ultimate load ratio

After the ultimate capacity of a given shaft has been determined, this equation can be used to predict a load-rotation curve. The equation can also be incorporated in a design procedure as a safety factor against undesirable rotation. Both of these aspects will be elaborated upon in a later section on design procedure.

Pressure Cell Data

Lateral soil pressures as a function of depth resulting from applied lateral loads for four test shafts are presented in this report. All of the test shafts described herein were instrumented with pressure cells on the front and back of the cylindrical test shaft to give a complete picture of the pressure distribution along the full length of the shaft. Results of these field measurements are shown in Figs. 29, 34, 35, and 36. The results for the final load test are presented in Fig. 29, Holloway et al. (14) in Fig. 34, Kasch et al. (20) in Fig. 35, and Ismael and Klym (15) in Fig. 36.

Considering these results, it is possible to draw some general conclusions about the shape of the lateral pressure distribution for drilled shafts in a relatively homogeneous cohesive soil. The point of zero lateral stress is considered as the point of rotation. For the test shafts presented, the point of rotation is located between 0.6 D and 0.75 D, where D is the depth of embedment of the shaft. This agrees well with the rotation point found from rotation-deflection data, where the location was determined to lie at approximately two-thirds of the embedment depth. It was also observed that the point of rotation

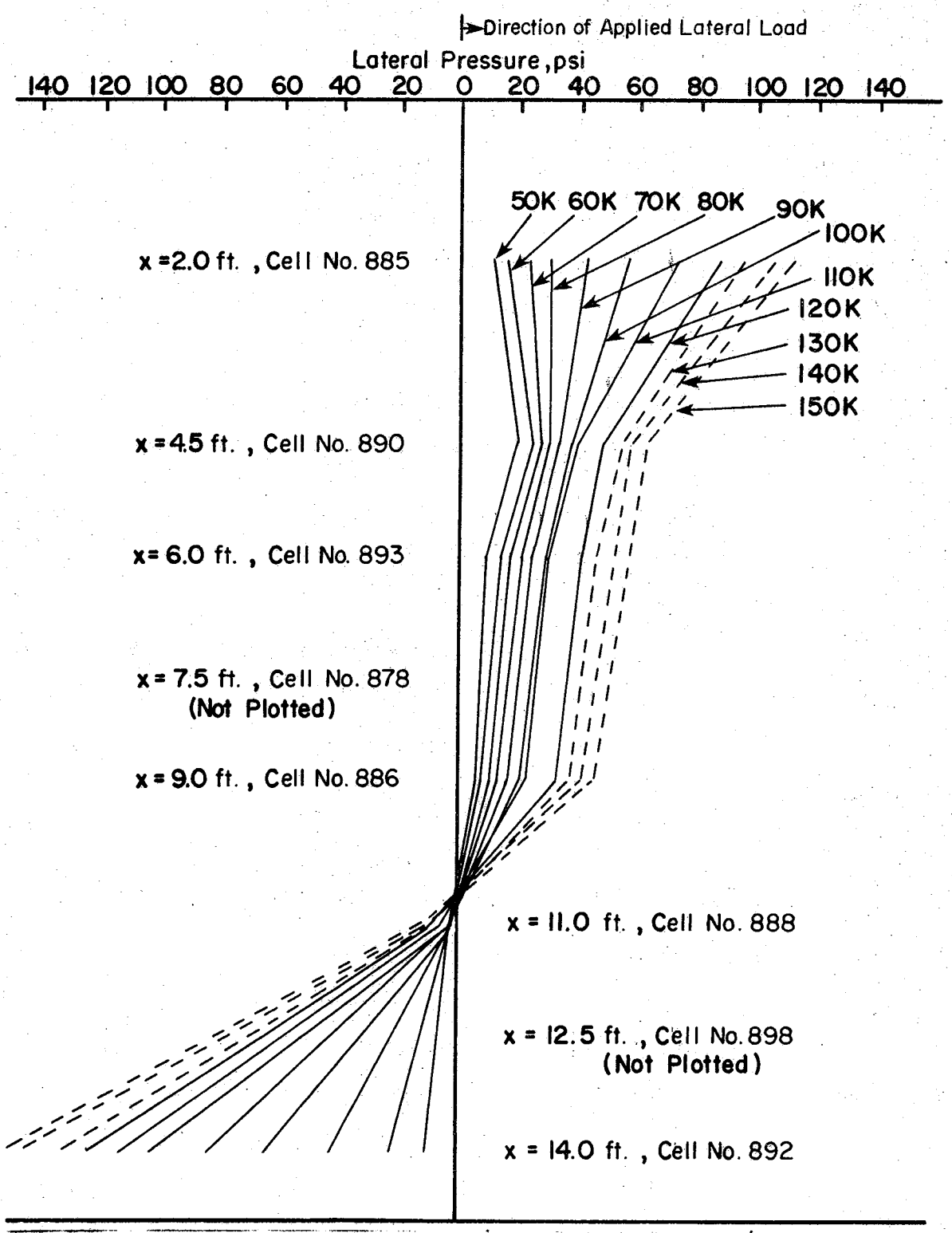

FIG. 34.– Lateral Pressure Versus Depth (After Holloway et al.)
x = Depth Below Groundline (1ft=0.3048m, 1kip=4.45kN, 1psi=6.89kN/m^2)

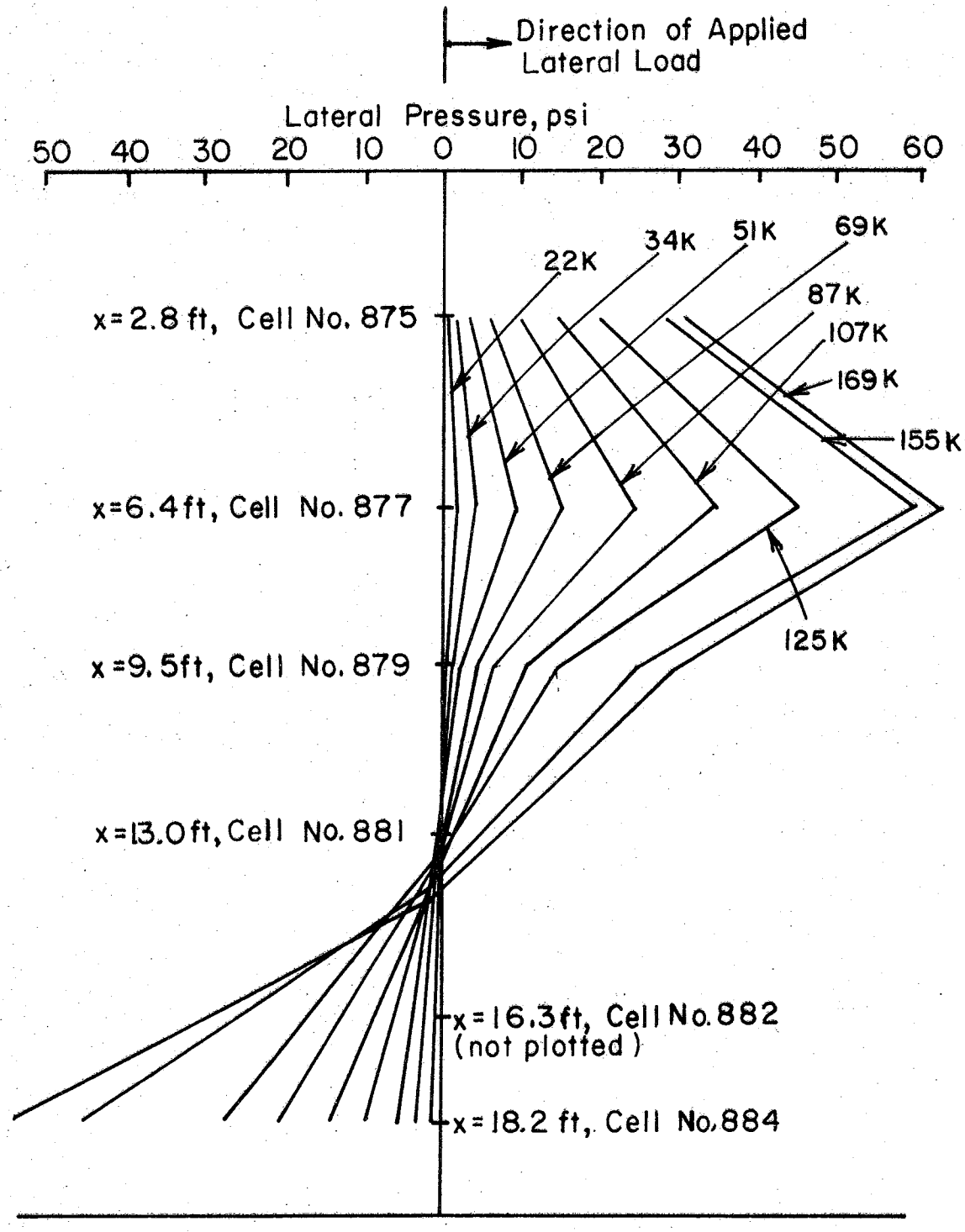

FIG. 35.— Lateral Pressure Versus Depth (After Kasch et al.)
x = Depth Below Groundline (1 ft = 0.3048 m, 1 kip = 4.45 kN, 1 psi = 6.89 kN/m^2)

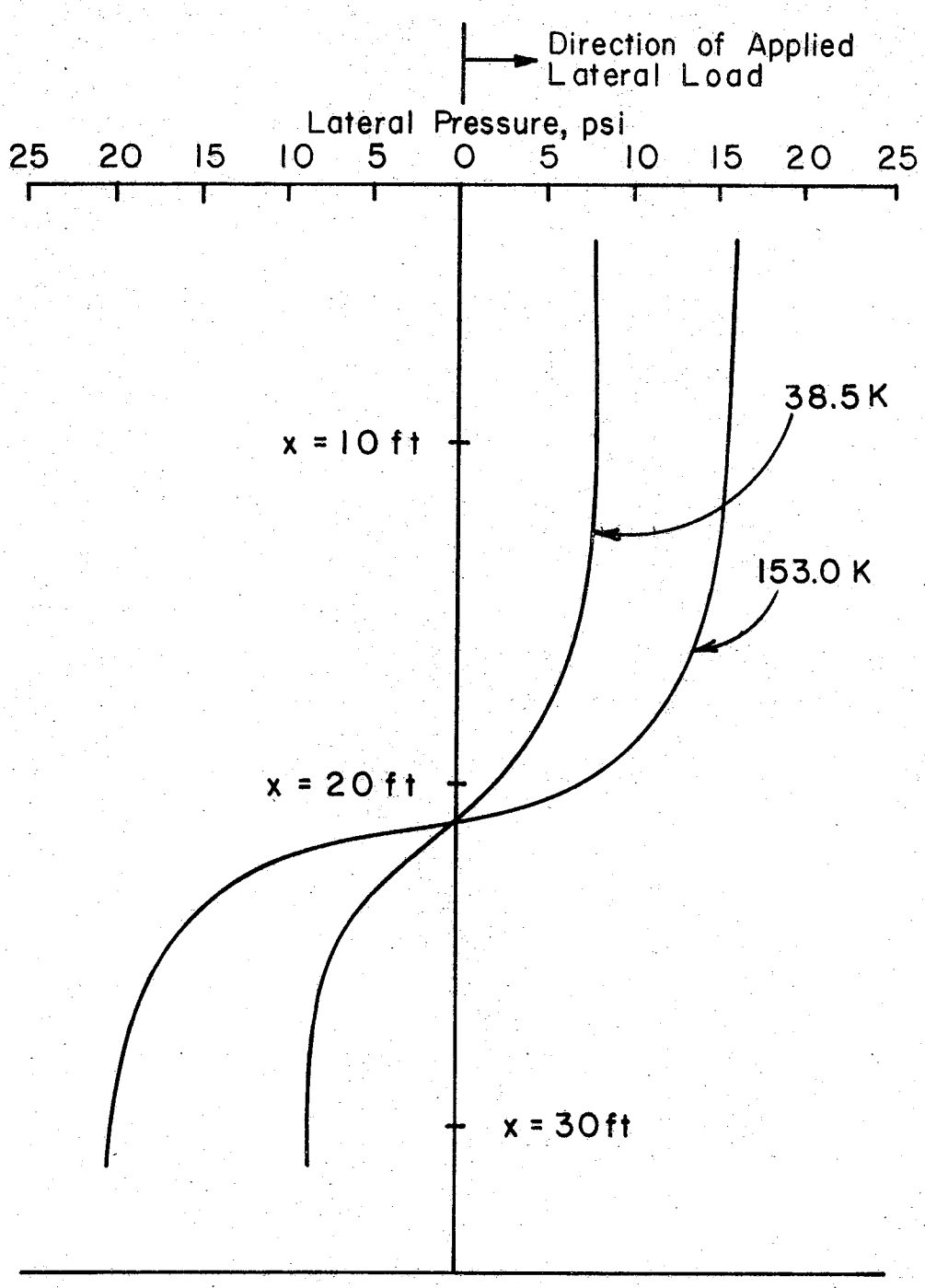

FIG. 36.— Lateral Pressure Versus Depth (After Ismael and Klym) (1ft = 0.3048m, 1 psi = 6.89 kN/m^2, 1 kjp = 4.45 kN)

shifted downward with increasing lateral load. Analytical studies conducted by Hays et al. (12) indicated similar behavior in rotation point movements. Conflicting results were reported by Kasch (20) in regard to the rotation point location. Based on shaft rotation data, Kasch determined the rotation point to lie at 0.4 times the embedment depth. However, a structural failure occurred in his test shaft, and it is possible to conclude that the shaft was experiencing flexural rather than rigid rotation.

A characteristic shape of the lateral pressure distribution is formed for each of the four test shafts. The distribution reported by Kasch (19)(see Fig. 35) and the final test (see Fig. 29) seem to have more of a parabolic shape, while the distributions reported by Holloway (14)(see Fig. 34) and Ismael and Klym (15)(see Fig. 36) indicate a shape similar to that proposed by Hays (12). For all distributions the soil resistance at the ground surface appears to be some value in excess of zero. This conflicts with an assumption made by Broms (2). Broms assumes that the soil resistance to a depth of 1.5 times the pile diameter below the ground surface should be neglected. A similar assumption was made by Ivey and Hawkins (16). Ivey and Hawkins assumed a parabolic stress distribution with zero soil reaction at the ground surface. The assumption of zero soil reaction at the ground surface is valid for cohesionless soils. However, for cohesive soils this does not appear to be the case.

Holloway (14), in addition to measuring pressures developed in the vertical direction along the face of the shaft, measured pressures developed in the horizontal plane. This was accomplished by placing

two pressure cells at horizontal angles of 30 degrees and 45 degrees from the direction of the applied load. These results are presented in Fig. 37 and the plot clearly illustrates the fact that the lateral pressures begin to drop significantly beyond an angle of 30 degrees. This same type of behavior was observed by Reese and Cox (46) from an analysis of tests performed on uninstrumented piles subjected to lateral loading.

Ultimate Soil Reaction

Plots of ultimate soil reaction versus depth for the four instrumented test shafts are presented in Figs. 30, 38, 39 and 40. The soil reaction for the final load test is presented in Fig. 30, Holloway et al. (14) in Fig. 38, Kasch et al. (20) in Fig. 39, and Ismael and Klym (15) in Fig. 36. The soil reaction curves illustrated were constructed by using theories proposed by Rankine (37), Hansen (11), Matlock (24), Reese (25), and Hays (12) and field soil pressure measurements converted to soil reaction. The equations proposed by the various theories to develop the soil reaction curves have been presented previously (Eqs. 2, 3, 4, 5 and 6).

During the test conducted by Kasch (20) a structural failure occurred before the load test was completed. However, based on the previously defined ultimate load corresponding to 2 degrees rotation, Kasch did verify that the theory proposed by Rankine was conservative, as shown in Fig. 39. The soil reaction curve was constructed by Kasch using the soil pressures obtained from cells 877 and 884 as shown in Fig. 35. Referring to Fig. 39, it is observed that the computed field

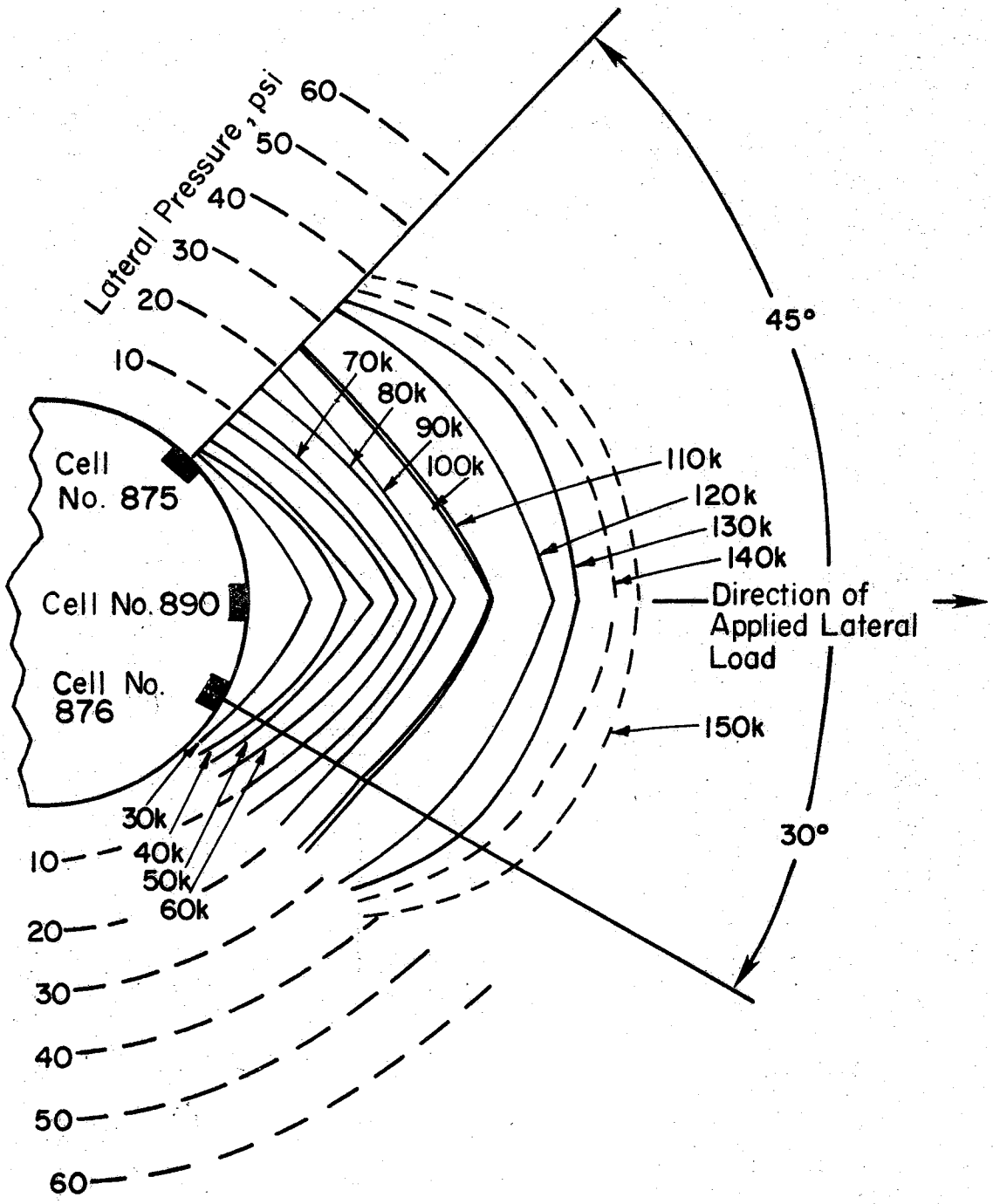

FIG. 37 — Horizontal Pressure Versus Lateral Load (After Holloway et al.)(1 kip = 4.45kN, 1 psi = 6.89kN/m^2)

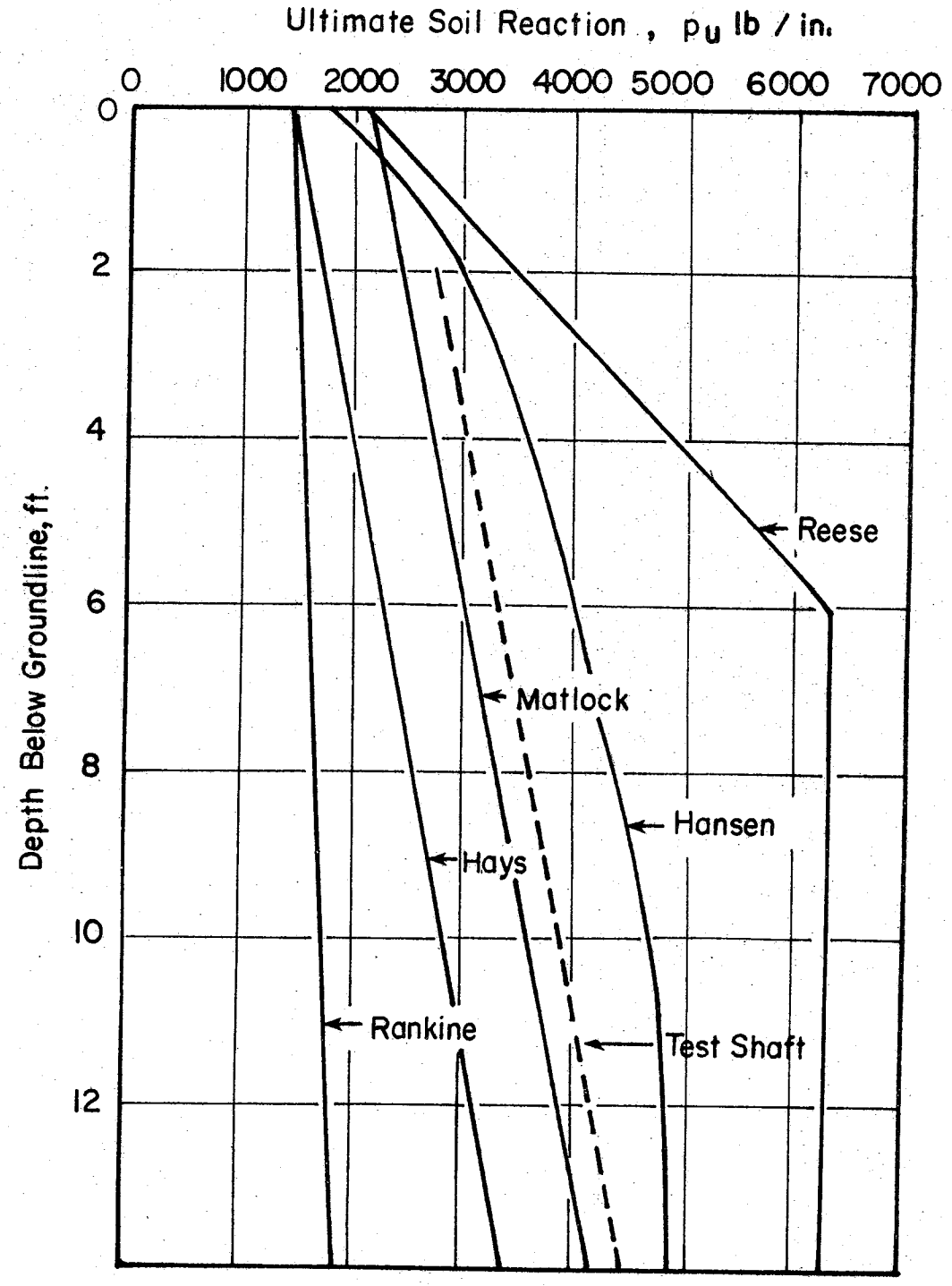

FIG. 38.— Ultimate Soil Reaction Versus Depth(After Holloway et al.) (1ft=0.3048m, 1 lb/in.=175 N/m)

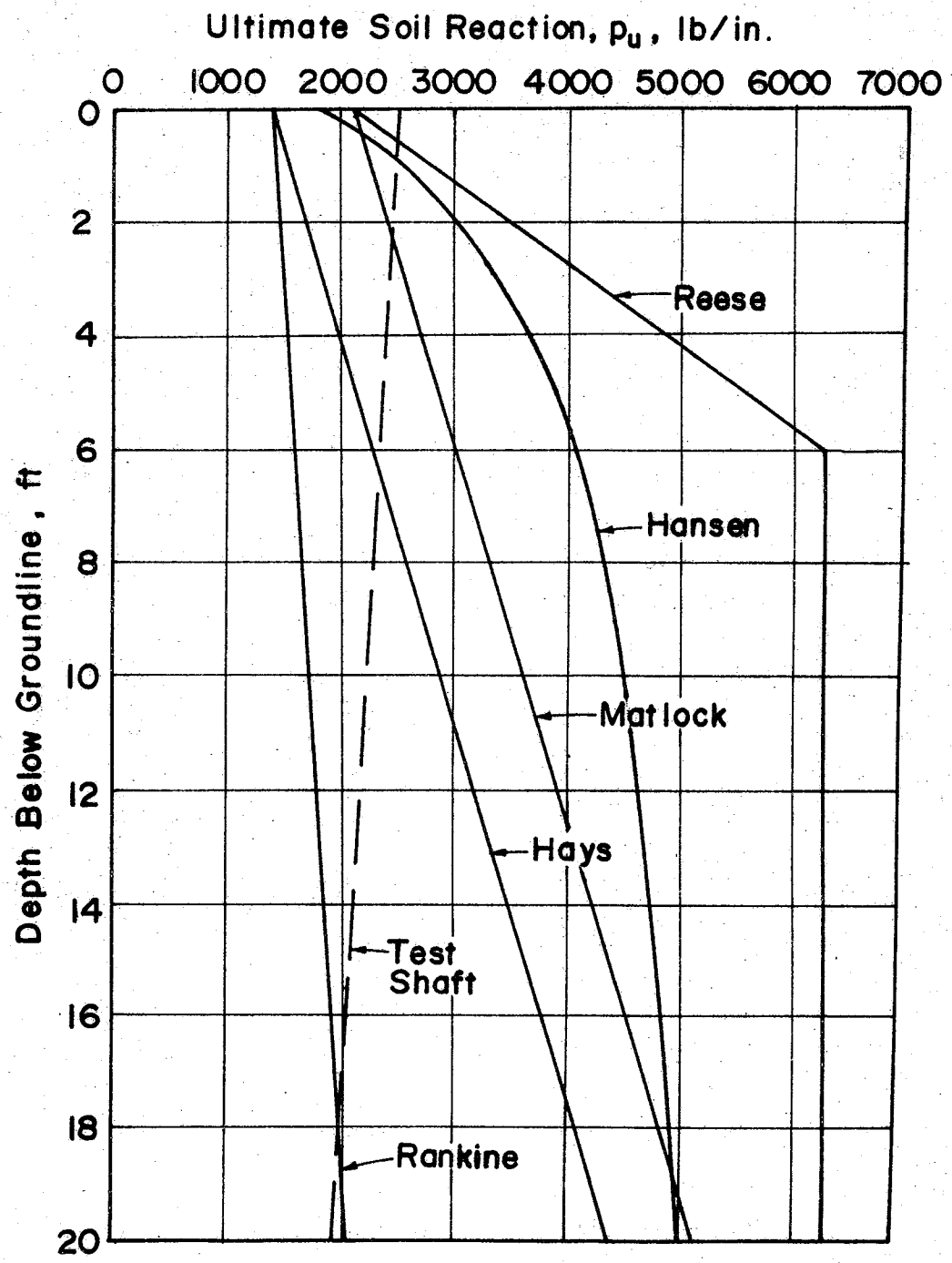

FIG. 39 – Ultimate Soil Reaction Versus Depth (After Kasch et al.) (1 ft = 0.3048 m; 1 lb/in. = 1.75 N/cm)

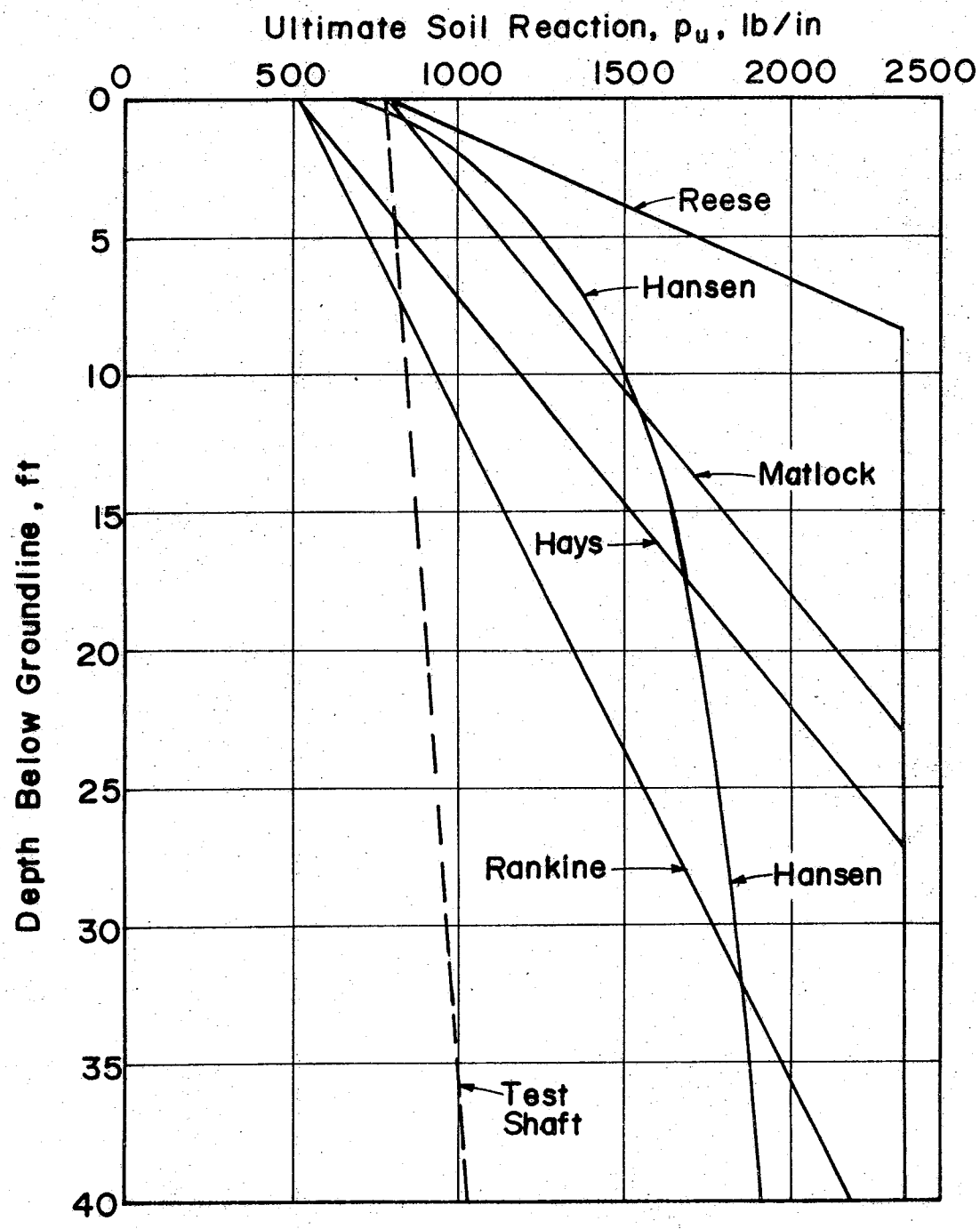

FIG. 40 – Ultimate Soil Reaction Versus Depth (After Ismael and Klym). Note: Test Shaft Values are not Ultimate Values (1 ft = 0.3048 m; 1 lb/in. = 1.75 N/cm)

reaction curve slopes in the positive sense, while the soil reaction curves proposed by the various theories slope in the negative direction, increasing soil reaction with depth. A possible explanation for this difference could be the fact that the Kasch test shaft experienced flexible behavior. The computed location of the point of rotation, 0.4 times the embedment depth, and a D/B ratio of 6.67 suggests that some flexibility probably existed in this test shaft.

Pressures recorded by Ismael and Klym (15) on a pressure cell instrumented shaft were converted to soil reaction and are plotted in Fig. 40. However, the computed field soil reaction curve is not at the defined ultimate load, but at some intermediate value. The soil reaction in the region directly below the groundsurface suggests that Rankine's and Hays' criteria are conservative.

For the final load test (Fig. 30) and the results obtained by Holloway et al., (Fig. 38) the general slope of the field soil reaction curve is almost identical to those determined from both the Matlock and Hays theory. The equation used by Hays is basically the same as that used by Matlock, except that Hays proposes a factor of two times the pile diameter for the ultimate soil reaction at the surface, whereas Matlock proposed a factor of three. This factor is defined as the ultimate resistance coefficient and is denoted by the symbol, N_p. By adjusting the factor N_p used to define the soil reaction at the surface, it is possible that the field measurements could be correlated with the theory postulated by Matlock. Also, it is possible to conclude that from the data presented and studies reported by Matlock (24) and Reese (27, 39) that the Reese (25) method may

represent an upper bound for ultimate soil reaction.

Ultimate Load on Rigid Shafts

Most problems in soil mechanics involving load capacity of soils are handled by consideration of ultimate strength characteristics. Failure in rigid shafts takes place when the lateral earth pressure resulting from applied lateral loads exceeds the ultimate lateral resistance of the supporting soil along the full length of the member.

Various methods have been previously presented which can be used to predict the ultimate capacity of laterally loaded drilled shafts. These methods were used to calculate the predicted ultimate load for various test shafts at 2 degrees of rotation. Comparisons were then made between measured lateral capacities at 2 degrees of rotation with those predicted by the various methods for several test shafts. The results are summarized in Table 3. For the Bhushan test shafts 2, 4, and 5 presented in Table 3, a load rotation curve had to be developed based upon a reported load-deflection curve. This was accomplished by assuming the shaft was rigid and rotated about a point located at 0.67 times the embedment depth. All of the shafts involved in the comparison conformed to the D/B rigidity requirements of less than six.

Inspection of Table 3 shows that some of the methods consistently yield conservative predictions, while others yield unconservative predictions. Broms' (2) method yields highly unconservative predictions in the lower shear strength soils (TTI Project 2211) and conservative results in the higher strength soils (Bhushan et al. (1)).

TABLE 3. - Comparison of Measured Ultimate Load With Predicted Ultimate Loads

Method	Load Test Results, in kips								Average Percent Deviation
						Bhushan, Haley, Fong (1)			
	Project 2211 (Final Test)	Project 2211 (1978 Test)	Project 2211 (1977 Test)	Project 105 (Galves-ton)	Project 105 (Bryan)	Shaft 2	Shaft 4	Shaft 5	
Measured Load @ 2°	92	137	172	4.35	11.5	500	375	450	-
Ivey & Dunlap $\phi = 0$	48	94	130	1.35	8.72	315	250	263	39%
Ivey & Hawkins	58	62	89	0.96	5.94	179	138	175	57%
Broms	157	171	260	1.55	9.54	315	228	304	41%
Hays	108	125	191	4.34	12.59	320	223	287	20%
Hansen	135	183	271	2.02	12.4	528	446	518	31%
Lytton	240	337	538	3.75	13.75	NA	1800	2933	216%

NOTE: 1 kip = 4.45 kN

The design method proposed by Lytton (21) produces highly unconservative results for the larger size shafts and relatively good predictions for the smaller size shafts (19). It should be noted that the design procedure proposed by Lytton is based on field load test results for minor service type foundations (19).

The average percentage differences between actual and predicted load capacity for each method are also tabulated in Table 3. Examination of the averages shows that the method proposed by Hays (12) produced the best correlation with measured field loads. Individual examination of the percentages for each load test shows that the Hays method yields good results in the lower to medium shear strength soils (0.58 tsf - 188 tsf)(55 kN/m^2 - 180 kN/m^2) and became less accurate, but conservative in the stiffer soils (2.38 tsf - 2.75 tsf)(228 kN/m^2 - 263 kN/m^2). It is possible that the equation which Hays uses for soil reaction is inappropriate for stiff clays. This possibility was investigated and, as will be shown in the next section a correlation was developed which accounts for variations in soil shear strength.

Ultimate Resistance Coefficient Versus Soil Strength Correlation

The most difficult aspect of the soil-structure interaction problem for drilled shafts is the relationship between soil reaction and soil shear strength. The design method for laterally loaded drilled shafts proposed by Hays (12) will be the basis upon which a relation between soil reaction and soil shear strength will be developed. However, before the relation is developed an explanation of the criteria proposed by Hays is appropriate.

The lateral soil resistance distribution assumed by Hays (12) is shown in Fig. 41. The distribution and magnitude of the soil resistance is based on studies conducted by Matlock (24). Matlock determined that the ultimate soil resistance, p_u, for clays under static loading varies linearly from the ground surface to some depth where the resistance reaches a maximum. The ultimate resistance per unit length of shaft was expressed as:

$$p_u = N_p C_u B \quad \ldots\ldots\ldots\ldots\ldots\ldots\ldots\ldots \quad (8)$$

where N_p = a nondimensional ultimate resistance coefficient,
C_u = the undrained cohesive shear strength, and
B = the shaft diameter.

Equation (8) is well known and has been used by many researchers (2, 22, 35, 31). The general concensus of the investigators appears to be that, for clay soils at a considerable depth below the ground surface, the factor N_p equals 9. Matlock (24) reported that very near the surface the soil in front of the pile will fail by shearing forward and upward. Consequently, the value of N_p reduces to the range of 2 to 4. Matlock believed a value of 3 to be appropriate for cylindrical pipe piles. This aspect of Matlock's soil reaction criteria was modified in the design method proposed by Hays. For reasons of conservatism, Hays assumed a value of 2 for N_p at the ground surface.

From the ground surface, the resistance reaches its maximum ($N_p = 9$) at some depth, x_r, which is termed the depth of reduced

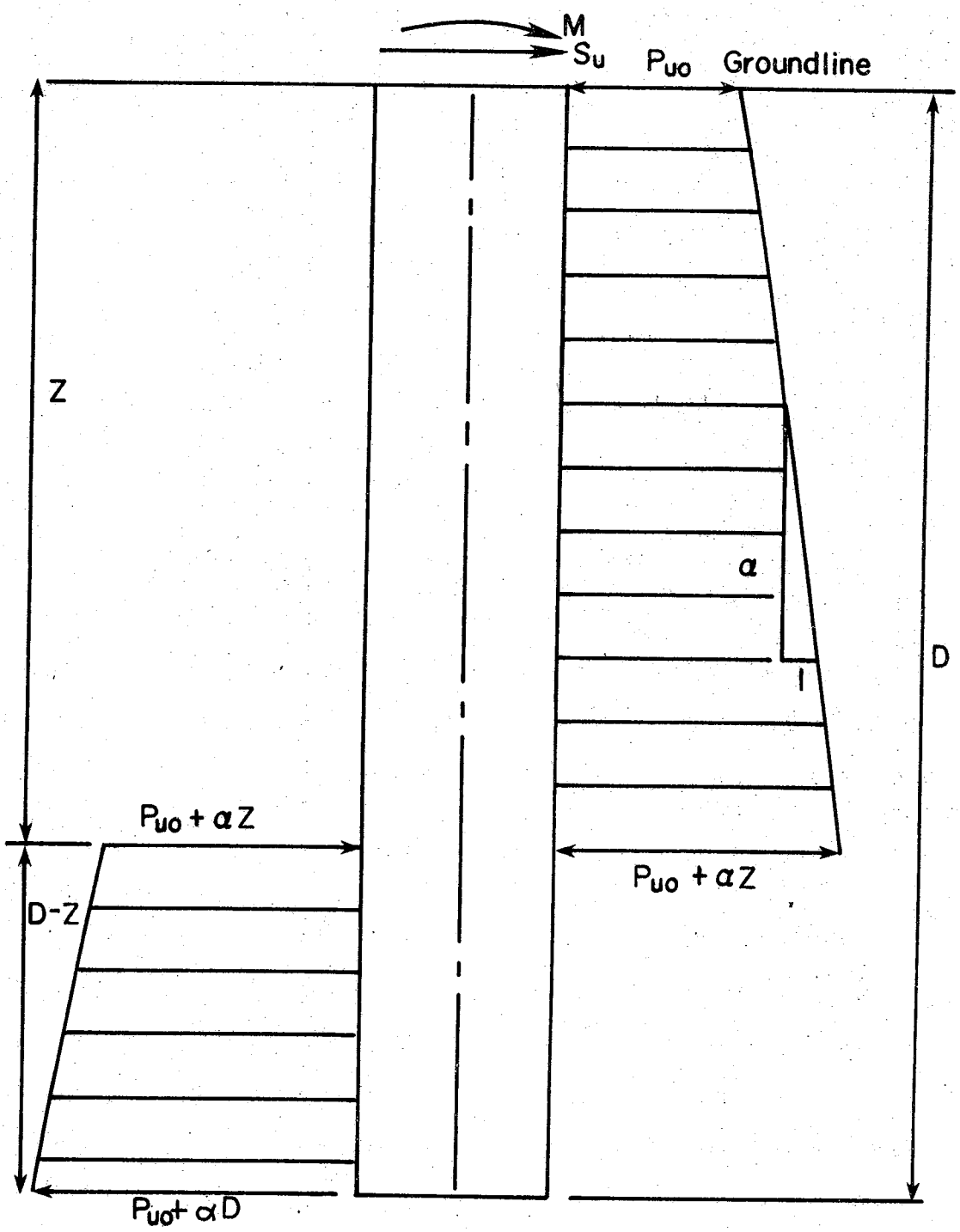

FIG. 41— Ultimate Lateral Soil Resistance For Cohesive Soils (After Hays et al.). S_u= Lateral Load; Z = Distance to Rotation Point; M = Moment; D = Embedded Depth; P_{uo}= Ultimate Soil Resistance at Groundline; α = Slope of Soil Resistance Diagram

resistance. Based on N_p equal to 9, Matlock (24) formulated the following equation for the depth of reduced resistance:

$$x_r = \frac{(9-N_p)C_u B}{(\gamma B + \frac{C}{2})} \quad \ldots\ldots\ldots\ldots\ldots\ldots\ldots\ldots \quad (9)$$

Thus, knowing the value of the ultimate soil reaction at the ground surface and the depth x_r where the maximum resistance is reached, the change of soil resistance with depth can be determined. Similarly, Hays assumed a linear increase in soil resistance with depth, the slope being designated as α as shown in Fig. 41.

It has been shown that the Hays method yielded good predicted lateral loads for the lower shear strength soils, and conservative results for the stiffer soils. Since discrepancies exist among various researchers (11, 24, 31) in the value choosen for N_p at the ground surface, an empirical relationship was developed between N_p and C_u. The correlation, shown in Fig. 42 was developed by calculating values of N_p for eight different test shafts at lateral loads corresponding to the ultimate load as defined previously. All safety factors suggested by Hays in the design method were disregarded in the formulation of the correlation. It should be pointed out that the test shafts involved in this correlation were field load tested at five different sites, with a broad range of soil strength, and the D/B ratio varied from 2.77 to 6.67.

Referring to Fig. 42, it is observed that for the stiffer soils the value of N_p increases, while for the lower shear strength soils, the N_p value consistently lies in the range of 2. Matlock (24)

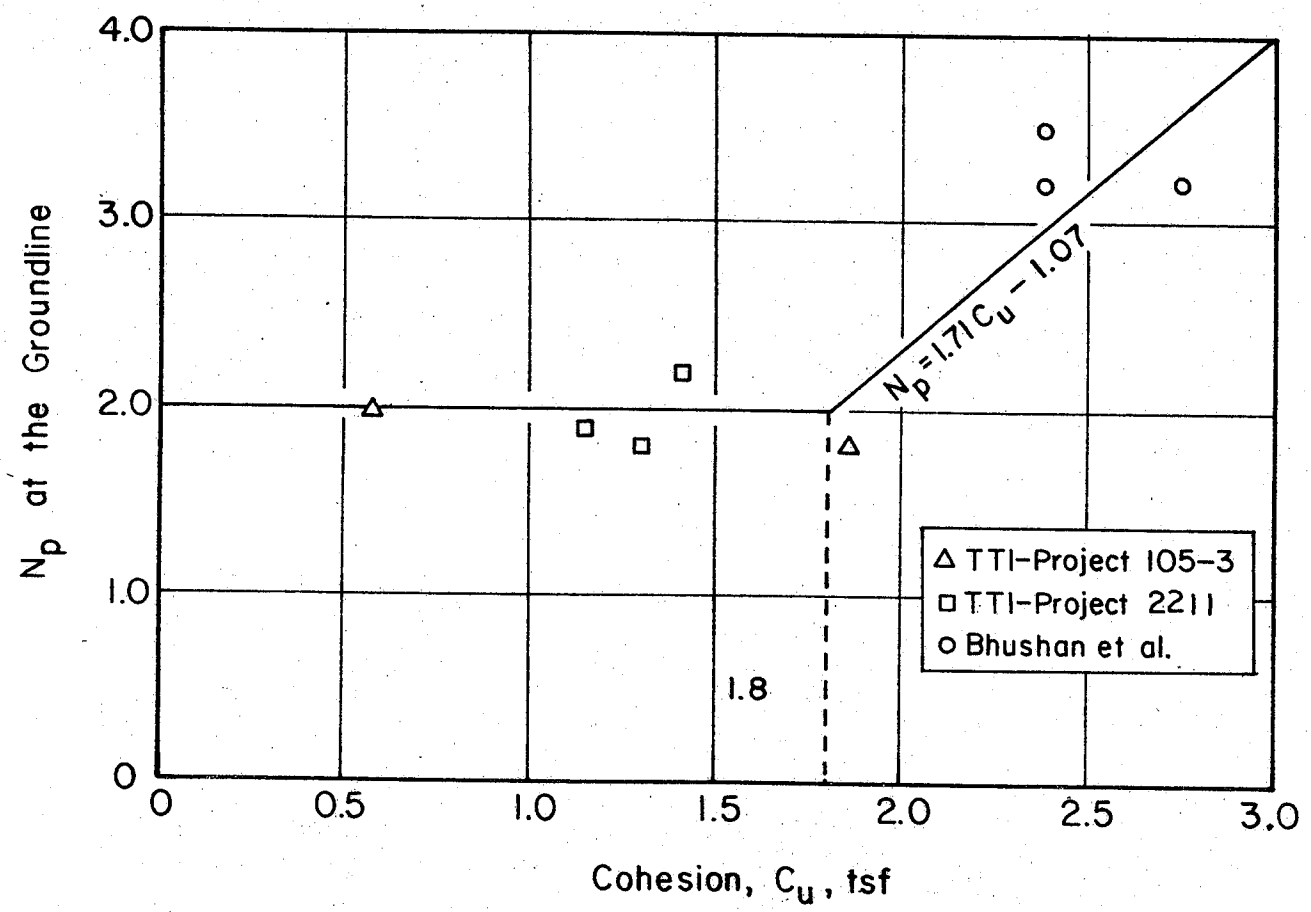

FIG. 42. — Ultimate Resistance Coefficient, N_p, at the Groundline Versus Undrained Cohesive Shear Strength, C_u, (1 tsf = 95.8 kN/m^2)

empirically determined that the value of N_p at the ground surface for piles was in the range between 2 and 4. Reese (25) and Rankine (37) analytically established a value of 2, while Hansen (11) theoretically determined a value of 2.6 for N_p. Therefore, N_p approximates a limiting value of 2 in the lower shear strength soils. This value has a theoretical basis as well as an empirical one.

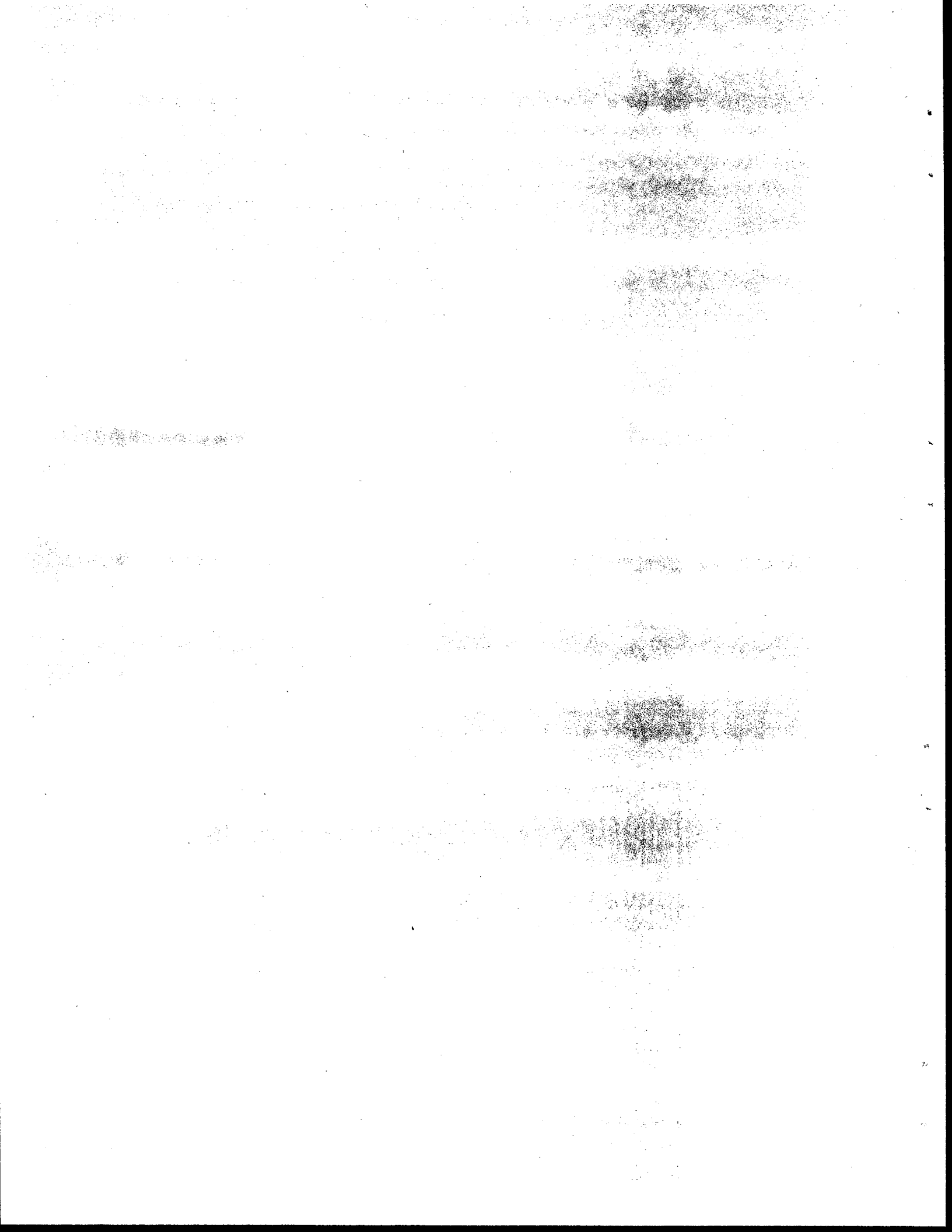

RECOMMENDED DESIGN PROCEDURE

In highway construction, drilled shafts are used extensively for foundations of bridges, highway interchanges, and retaining structures. When designing drilled shafts to support precast panel retaining walls, it is probably appropriate to use shafts which behave as rigid elements. However, it is possible that loads may be encountered in the highway industry which require a shaft of such large magnitude that flexible behavior is experienced by the member. In order to be reasonably assured of rigid foundation behavior, the depth to diameter ratio, D/B, of the shaft should be limited to about six or less (20, 40).

Before the design depth and diameter of a shaft can be determined, several design parameters must be obtained. These parameters include the resultant force acting on the retaining wall, the point of application of the resultant force, the allowable shaft rotation, soil creep potential and the undrained cohesive shear strength of the soil.

Force Acting on Retaining Wall

The force acting on a retaining wall is the resultant of the lateral pressure in the backfill. Based on the results of a study conducted on an instrumented precast panel retaining wall, Wright et al. (41) developed an equation to predict the resultant force for a level cohesionless backfill with no surcharge, acting on a retaining wall. The equation developed to predict this force is:

$$Fr = 0.25\ \gamma h^2 L\ (Ka + 0.8) \quad \ldots\ldots\ldots\ldots\ldots\ldots \quad (10)$$

where h is the height of the wall and L is the length of the panel, pilaster to pilaster. The term γ has been defined in Eq. 2 (p. 60). The expression for Ka is the Rankine coefficient of active earth pressure, and is defined as follows:

$$Ka = \cos \zeta \left[\frac{\cos \zeta - \sqrt{\cos^2 \zeta - \cos^2 \phi'}}{\cos \zeta + \sqrt{\cos^2 \zeta - \cos^2 \phi'}} \right] \quad \ldots\ldots \quad (11)$$

where ζ is the angle of the slope of the backfill to the horizontal and ϕ' is the effective angle of shearing resistance of the backfill material.

Application Point of Resultant Force

Wright et al. (41) also developed an equation to calculate the location of the point of application of the resultant force, Fr, of a level backfill with no surcharge. The equation is:

$$H = \frac{h}{2} \left(\frac{Ka + 0.267}{Ka + 0.8} \right) \quad \ldots\ldots\ldots\ldots\ldots\ldots \quad (12)$$

where H is the distance from the ground surface to the point where the force is applied above the base of the retaining wall. The terms h and Ka were defined in Eqs. 10 and 11, respectively.

Shaft Rotation

If excessive rotation of the drilled shaft were allowed to occur, objectionable deflection of the panel retaining wall in terms of aesthetics and possibly serviceability would result. It is

therefore desirable to be able to use the design criteria to guard against this potential problem.

In the section covering ultimate load ratio versus shaft rotation the following equation was developed:

$$\frac{P_\omega}{P_{2^o}} = \frac{\omega}{0.538 + 0.731\ \omega} \quad \ldots\ldots\ldots\ldots\ldots\ldots \quad (7)$$

The equation expresses the lateral load at some intermediate rotation between 0 and 2 degrees as a percentage of the ultimate load defined at a 2 degree rotation. This allows the engineer to predict a load-rotation curve for a particular size shaft up to a rotation of 2 degrees.

The above equation can be rearranged and used to compute a design load based on a limiting angle of rotation. If the terms are redefined to coincide with the notation used in the design criteria, the following equation is obtained:

$$S_d = \frac{0.538 + 0.731\ \theta}{\theta}\ F_r \quad \ldots\ldots\ldots\ldots\ldots\ldots \quad (13)$$

where S_d = design load

F_r = resultant force transmitted from the wall to the drilled shaft, and

θ = the desired limiting angle of rotation

Determination of the necessary limiting value for the angle of rotation should be based on the importance of the particular structure and sound engineering judgement.

Soil Creep

The time-dependent deformation behavior of a soil mass under a given set of sustained stress is referred to as soil creep. At the present time, no general theory or method exists which can adequately predict the time-dependent deformation of cohesive soils. The creep phenomenon is rather complex and is a function of several variables, including soil type, soil structure, and stress history (8). Since drilled shafts used for almost any type of structure may be subjected to long-term or sustained loads, the creep potential of the supporting soil must be considered.

Dunlap et al. (8) conducted a study investigating the effects of long-term loading on shaft behavior for minor service structures. On the basis of their research, the following conservative conclusions were made in regard to the effects of sustained loads for various cohesive soil types:

Cohesive Soil Type	Safety Factor
Soft clay	3
Stiff, non-fissured clays	2
Stiff, fissured clays	3

These safety factors are applied to the design lateral load. Also, they are based on an ultimate capacity corresponding to a shaft rotation of 5 degrees, whereas, in this study the ultimate load has been defined as the load at a 2 degrees rotation.

Based on the results seen in recently conducted field load tests and data presented in the literature, it is believed that these safety

factors are highly conservative. Bhushan et al. (1) indicated from load tests performed on 12 drilled shafts that, under sustained load, deflections increased on the order of 0 to 20% over short-term loading. The Bhushan field load tests were conducted in stiff clays where undrained shear strengths varied from 2.38 tsf (228 kN/m^2) to 2.75 tsf (263 kN/m^2). Data from the final shaft tested in this research study show that it is difficult to accurately determine the effect of sustained loading. It would be necessary to compare data from shaft subjected to short-term static loading with data obtained in this study. However, it is felt that the effects of soil creep are not as detrimental as Dunlap et al. (8) indicated, but more on the order of the values presented by Bhushan et al. (1).

It is obvious that in soft clays the effects of creep would be much more pronounced than in a stiff highly overconsolidated clay. Therefore, engineering judgement and the importance of the supported structure should be the controlling criteria in choosing an appropriate safety factor.

For retaining walls it has been shown that the highest pressures applied to the wall occurred during the backfilling process (41). The pressures reached a peak value at that time and then decreased with time. Thus, for retaining wall purposes, the loads applied to the drilled shaft are not truly sustained and the soil creep phenomena may not be critical.

Soil Shear Strength

The State Department of Highways and Public Transportation often

uses the Texas Cone Penetrometer Test as the primary means of determining soil shear strength in routine subsurface investigations. Laboratory testing to determine soil shear strength is often omitted because of the additional expense involved. The TCP test consists of driving a 3.0 in. (7.6 cm) diameter cone attached to a drill rod, with a 170 lb (77.1 kg) hammer. The hammer is dropped 2 ft (0.61 m) for each blow. The cone is seated with 12 blows and the number of blows, N, required to produce the next foot of penetration is recorded (7).

An improved correlation between the TCP blow count, N, and the undrained shear strength has recently been reported by Duderstadt et al. (7). The correlation has been reported for highly plastic homogeneous clays (CH) and for homogeneous clays of low to medium plasticity (CL). The results were reported as:

$$\text{Homogeneous CH:} \quad C_u = 0.067N \quad \ldots\ldots\ldots\ldots\ldots \quad (14)$$

$$\text{Homogeneous CL:} \quad C_u = 0.053N \quad \ldots\ldots\ldots\ldots\ldots \quad (15)$$

If it is desired by the design engineer, a factor of safety may be applied to the shear strength, C_u. Also, the undrained shear strength can be obtained from unconfined compression tests, vane shear tests, or unconsolidated-undrained triaxial tests.

Design Criteria

The method proposed by Hays (12) with a soil reaction modification at the ground surface has been selected as the recommended design criteria. The results presented in Table 3 and the correlation

established between the ultimate resistance coefficient, N_p, and soil shear strength, C_u, presented in Fig. 42 are the basis upon which this decision was made.

The assumed soil resistance distribution used by Hays has been presented in Fig. 41. By applying static equilibrium to the assumed soil resistance distribution, equations for the ultimate applied lateral load, S_u, and bending moment, M, were developed in terms of the soil parameters, the pile embedment depth, D, and an unknown distance, Z, to the point of rotation. The two equations of static equilibrium are:

$$S_u = P_{u_o} (2Z-D) + \frac{\alpha}{2} (2Z^2-D^2) \quad \ldots\ldots\ldots\ldots\ldots \quad (16)$$

$$M = P_{u_o} (Z^2 - \frac{D^2}{2}) - \frac{\alpha}{3} (2Z^3-D^3) \quad \ldots\ldots\ldots\ldots\ldots \quad (17)$$

where α = the slope of the soil resistance diagram

P_{u_o} = the ultimate soil reaction at the ground surface

By defining a variable K as the ratio of Z over D, and introducing a nondimensional variable beta:

$$\beta = \alpha \frac{D}{P_{u_o}} \quad \ldots\ldots\ldots\ldots\ldots\ldots\ldots\ldots \quad (18)$$

equations 16 and 17 can be modified into nondimensional form as follows:

$$\frac{S_u}{P_{u_o} D} = 2K - 1 + \beta (K^2 - \frac{1}{2}) \quad \ldots\ldots\ldots\ldots\ldots \quad (19)$$

$$\left(\frac{S_u}{P_{u_o} D}\right)\left(\frac{H}{D}\right) = -K^2 \times \frac{1}{2} - \frac{\beta}{3}(2K^3 - 1) \quad \ldots\ldots\ldots \quad (20)$$

where H is the height above the ground surface to the point where the lateral load is applied. This gives two equations with four unknowns, $\frac{S_u}{P_{u_o} D}$, $\frac{H}{D}$, K and β. The dimensionless design chart shown in Fig. 43 was developed for different values of K and β, relating $\frac{S_u}{P_{u_o} D}$ and $\frac{H}{D}$, in order to expedite the design process. The procedure is iterative, with the designer choosing a trial diameter and embedment depth and then checking his solution to see if it has adequate strength, converges quickly.

Design Procedure

The following step by step procedure is recommended for the design of drilled shafts to support precast panel retaining walls:

1. Use Eq. 10 and Eq. 11 to calculate the force, F_r, that will be applied to the shaft by the retaining wall.
2. Use Eq. 12 to calculate the point of application, H, of the force, F_r.
3. If a limit on rotation is desired, use Eq. 13 to calculate the design lateral load, S_d.
4. Apply an appropriate Factor of Safety for creep, if desired.
5. Determine the undrained shear strength, C_u, of the soil by use of Eq. 14 or 15. A factor of safety may be applied if desired.
6. Enter Fig. 42 with C_u and obtain the value for N_p.
7. Choose a trial value for shaft diameter, B and embedment

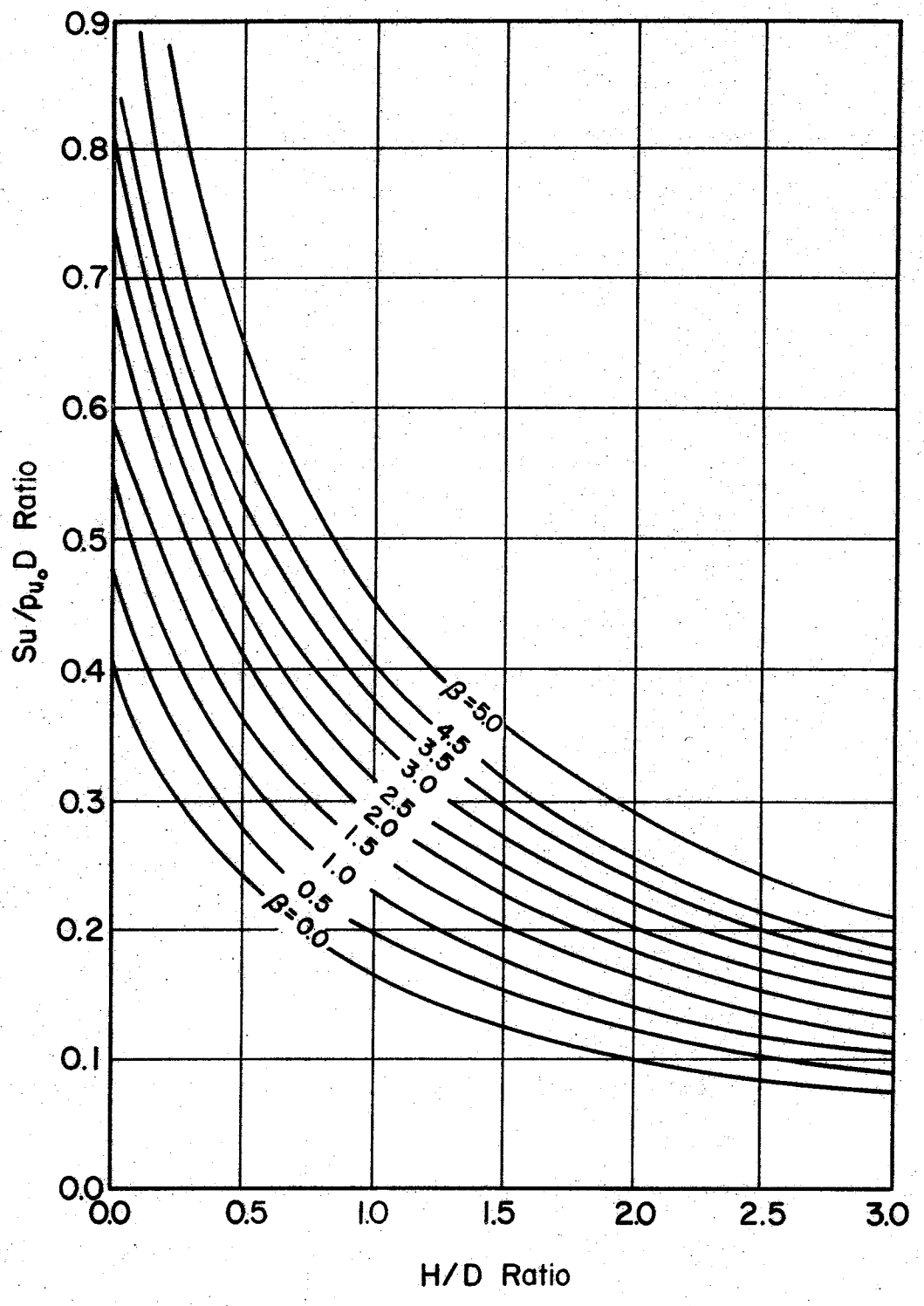

FIG. 43 - Design Chart for Cohesive Soils (After Hays et al.)

depth, D.

8. Use Eq. 9 to calculate the depth of reduced resistance, x_r.
9. Calculate α using the following equations:

$$\alpha = (9 - N_p)\, C_u B/x_r \text{ for } D < x_r$$

$$\alpha = (9 - N_p)\, C_u B/D \text{ for } D > x_r$$

The first equation given represents the actual slope of the soil resistance. If the required embedment depth is greater than x_r, the second equation conservatively extends the slope of the soil resistance.

10. Use Eq. 8 to determine the soil reaction at the ground surface, P_{u_o}.
11. Use Eq. 18 to calculate the nondimensional variable, β.
12. Determine the ratio of the height of the applied force, H, to the depth of the shaft, D.
13. Enter the design chart (Fig. 43) with β and H/D to obtain the ratio $\frac{S_u}{P_{u_o}D}$.
14. Multiply the ratio $\frac{S_u}{P_{u_o}D}$ by P_{u_o} to obtain the ultimate lateral load, S_u.
15. Repeat Steps 7-14 until the value calculated for S_u equals or exceeds the design load, S_d, calculated in Step 3.

Example Problem

The following example illustrates the use of the above procedure

for the design of precast panel retaining wall foundations. A drilled shaft foundation is to be designed for the following situation:

A retaining wall is to consist of panels having a depth of 11 ft (3.35 m) and a length of 20 ft (6.1 m). The backfill material will be clean sand having an effective angle of shearing resistance, ϕ', equal to 36 degrees and unit weight, γ, equal to 115 pcf (18.1 kN/m^3). The backfill will have no additional surcharge and will have a horizontal slope. The subsoil at the construction site has been classified as a non-fissured CH. The average N value obtained from the TCP test conducted at the site is 17. The unit weight of the subsoil is 130 pcf (20.4 kN/m^3). The limiting angle of rotation, θ, is 1 degree.

Step 1:

Using Eq. 11.

$$K_a = \text{Cos } 0^o \left[\frac{\text{Cos } 0^o - \sqrt{\text{Cos}^2(0)^o - \text{Cos}^2(36^o)}}{\text{Cos } 0^o + \sqrt{\text{Cos}^2(0)^o - \text{Cos}^2(36^o)}} \right] = 0.260$$

Using Eq. 10.

$$F_r = 0.25(.115 \text{ kcf})(11 \text{ ft})^2(20 \text{ ft})(0.260 + 0.8) = 73.7 \text{ kips}$$

Step 2:

Using Eq. 12.

$$H = \frac{11}{2} \frac{0.26 + 0.267}{0.26 + 0.8} = 2.73 \text{ ft}$$

Step 3:

Using Eq. 13.

$$S_d = \frac{0.538 + 0.731(1^o)}{1^o} \quad 73.7 \text{ kips} = 94^K$$

Step 4:

No Factor of Safety is applied for creep.

Step 5:

Calculate undrained cohesive shear strength using Eq. 14.

$C_u = (0.067)(17) = 1.14$ tsf = 2.28 ksf (No Factor of Safety is applied).

Step 6:

Enter Fig. 42 with $C_u = 1.14$ tsf and obtain the value for $N_p = 2.0$.

Step 7:

Choose trial depth, D, and diameter, B.

Try B = 2.5 ft

D = 10 ft

Step 8:

Calculate x_r using Eq. 9.

$$x_r = \frac{(9-2)(2.28 \text{ ksf})(2.5 \text{ ft})}{0.130 \text{ kcf}(2.5 \text{ ft}) + 0.5(2.28 \text{ ksf})} = 27.2 \text{ ft}$$

Step 9:

Calculate α; the slope of the soil reaction curve.

since $D < x_r$ then

$$\alpha = \frac{(9-2)(2.28 \text{ ksf})(2.5 \text{ ft})}{27.2 \text{ ft}} = 1.47 \text{ k/ft}^2$$

Step 10:

Calculate P_{u_o} ; the soil reaction at the surface using Eq. 8.

$$P_{u_o} = (2.0)(2.28 \text{ ksf})(2.5 \text{ ft}) = 11.4 \text{ k/ft}$$

Step 11:

Using Eq. 18 calculate β.

$$\beta = \frac{(1.47 \text{ k/ft}^2)(10 \text{ ft})}{11.4 \text{ k/ft}} = 1.29$$

Step 12:

Compute H/D ratio.

$$H/D = \frac{2.73 \text{ ft}}{10 \text{ ft}} = 0.273$$

Step 13:

Enter Design Chart (Fig. 43) with H/D ratio and β to determine

$$\frac{S_u}{P_{u_o} D} .$$

$$\frac{S_u}{P_{u_o} D} = 0.44$$

Step 14:

Solve for the ultimate load, S_u.

$$S_u = (0.44)(11.4 \text{ k/ft})(10 \text{ ft}) = 50^k$$

$S_u = 50^k < S_d = 94^k$ $\therefore$ This solution is not valid.

Step 15:

Since $S_u < S_d$ repeat Steps 7-14:

TRIAL 2:

Step 7:

Choose a new trial depth, D.

Try B = 2.5 ft

D = 15 ft

Step 8:

Calculate x_r using Eq. 9.

$$x_r = \frac{(9-2)(2.28 \text{ ksf})(2.5 \text{ ft})}{0.130 \text{ kcf}(2.5 \text{ ft}) + 0.5(2.28 \text{ ksf})} = 27.2 \text{ ft}$$

Step 9:

Calculate α.

since $D < x_r$ then

$$\alpha = \frac{(9-2)(2.28 \text{ ksf})(2.5 \text{ ft})}{27.24 \text{ ft}} = 1.47 \text{ k/ft}^2$$

Step 10:

Calculate P_{u_o} using Eq. 8.

$$P_{u_o} = (2.0)(2.28 \text{ ksf})(2.5 \text{ ft}) = 11.4 \text{ k/ft}$$

Step 11:

Calculate β using Eq. 18.

$$\beta = \frac{(1.47\ k/ft^2)(15\ ft)}{11.4\ k/ft} = 1.93$$

Step 12:

Calculate H/D.

$$H/D = \frac{2.73\ ft}{15\ ft} = 0.18$$

Step 13:

Enter Design Chart (Fig. 43).

$$\frac{S_u}{\beta_{u_o} D} = 0.55$$

Step 14:

Solve for S_u.

$$S_u = (0.55)(11.4\ k/ft)(15\ ft) = 94^k$$

$S_u = 94^k \geq S_d$ $\therefore$ The solution is valid

For purposes of comparison, the example problem was deliberately set up so that the results would match the load-rotation data obtained for the final field load test. Referring to the example problem and the load-rotation curve presented in Fig. 19, it is observed that the working load, F_r = 73.7 kips, is approximately equal to the field load at a rotation of 1 degree, and the ultimate load, S_u = 94 kips, is approximately equal to the field load at a rotation of 2 degrees. This verifies that for the size shaft chosen in the example problem at a lateral load of 73.7 kips, 1 degree of rotation can be expected. However, if 2 degrees of rotation is not objectionable the shaft has

the capacity to carry a load of S_u equal to 94 kips, which is the defined ultimate. This comparison verifies the reliability of the recommended design procedure. Further verification of the reliability of the recommended design criteria is shown in the next section.

Comparison of Predictions

Since the reliability of any type of design procedure can only be based upon the results it produces, comparisons of predicted capacities with those obtained in the field become a necessary exercise for the formulation of a positive conclusion. Therefore, the validity of the recommended design procedure was evaluated by comparing predicted ultimate loads with those observed in the field. The predicted capacities were compared with those obtained in the field corresponding to degrees of rotation between 0 and 2 degrees. The comparisons made for shafts involved in the empirical relationships are shown in Table 4. Table 5 presents the results of predictions for shafts not involved in any of the correlations. No safety factors were applied in the design criteria for the predictions shown.

Ratios of predicted to observed loads for the available drilled shaft data based on the new design procedure are plotted versus shaft rotation in Fig. 44. This plot shows that a majority of the loads predicted by the new design procedure are within 10 percent of the observed capacity. Only five points deviate more than 20 percent from the line of equality. Four of the five points which deviate beyond the 20 percent range are conservative predictions. The general trend of the points suggests a tendency for conservatism where large

TABLE 4. - Comparisons of Predicted and Observed Loads For Shafts Involved in Empirical Relationships

Test Shaft	Shaft Rotation, in Degrees	Predicted Load, in kips	Observed Load, in kips	Predicted Load / Observed Load
TTI Project 2211 (1977 Test)	2.0	187	172	1.09
	1.5	171	160	1.07
	1.0	147	135	1.09
	0.5	103	91	1.13
TTI Project 2211 (1978 Test)	2.0	126	137	0.92
	1.5	115	130	0.88
	1.0	99	115	0.86
	0.5	69	82	0.84
TTI Project 2211 (Final Test)	2.0	96	92	1.04
	1.5	87	84	1.03
	1.0	75	72	1.04
	0.5	53	50	1.06
Bhushan et al. Shaft 2	2.0	555	500	1.11
	1.5	507	475	1.07
	1.0	435	390	1.11
	0.5	305	280	1.09
Bhushan et al. Shaft 4	2.0	335	375	0.90
	1.5	309	335	0.92
	1.0	272	275	0.98
	0.5	197	200	0.98
Bhushan et al. Shaft 5	2.0	432	450	0.96
	1.5	399	400	1.00
	1.0	349	360	9.97
	0.5	254	250	1.02
TTI Project 105-3 (Galveston)	2.0	4.3	4.4	1.00
	1.5	4.0	4.0	1.00
	1.0	3.4	3.2	1.08
	0.5	2.4	1.7	1.42
TTI Project 105-3 (Bryan)	2.0	13.4	11.5	1.15
	1.5	12.1	10.8	1.12
	1.0	10.4	8.8	1.18
	0.5	7.3	6.4	1.14

NOTE: 1 kip = 4.45 kN

TABLE 5. - Comparisons of Predicted and Observed Loads For Shafts Not Involved in Empirical Relationships

Test Shaft	Shaft Rotation, in Degrees	Predicted Load, in kips	Observed Load, in kips	Predicted Load / Observed Load
Dow (32) TS-2	0.72	23.1	23.2	1.00
	0.57	20.6	21.2	0.97
	0.43	17.7	18.6	0.95
Bhushan et al. Shaft 1	1.0	431	425	1.01
	0.5	303	280	1.08
Bhushan et al. Shaft 3	1.5	294	350	0.84
	1.0	252	320	0.79
	0.5	177	230	0.77
Bhushan et al. Shaft 6	1.0	340	445	0.77
	0.5	240	260	0.92
Bhushan et al. Shaft 7	1.0	100	160	0.63
	0.5	70	100	0.70

NOTE: 1 kip = 4.45 kN

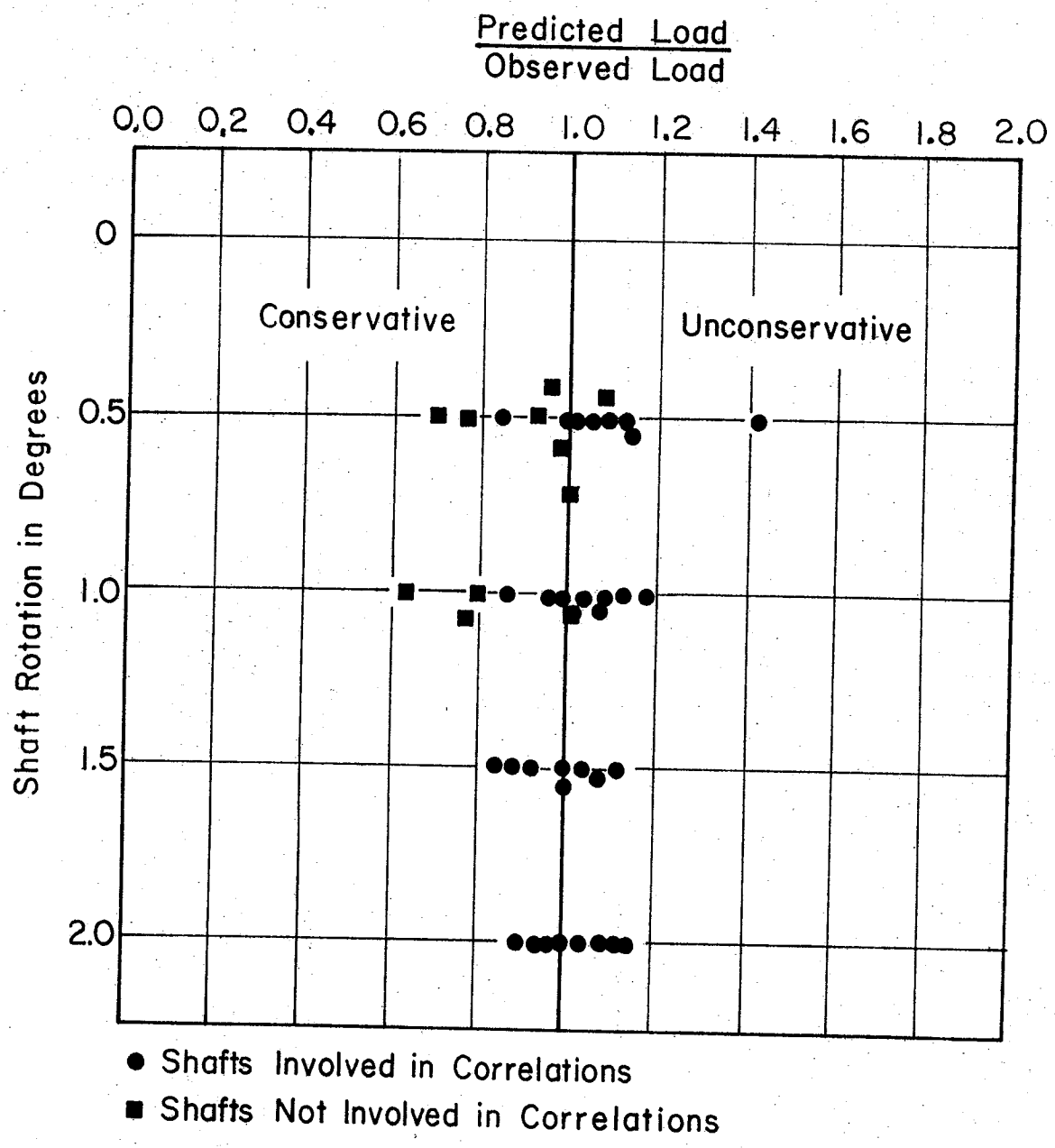

FIG. 44.– Comparison of Predicted and Observed Loads

deviations are involved. Considering the range of drilled shaft sizes involved and soil strengths represented by the data, the new design criteria predictions deviate rather insignificantly from observed capacities.

CONCLUSIONS AND RECOMMENDATIONS

Based upon the results and analysis of full-scale drilled shaft testing programs and comparisons made with existing lateral capacity prediction methods, the following conclusions and recommendations are made:

Conclusions

1. Based on the comparison between load tests shown in Table 3, it is concluded that the Ivey and Dunlap method (with ϕ equal to zero), and the Ivey and Hawkins method yield conservative predictions. On the other hand, the methods proposed by Hansen and Lytton consistently yield unconservative predictions for the larger sized shafts. Brom's method predicts unconservative results in the lower shear strength clays and conservative predictions in the stiffer clays.
2. Based on the same comparison of the measured versus predicted ultimate loads given in Table 3, the Hays method produces the best overall results for the different methods investigated. Therefore, the Hays method, with some modification was incorporated into a new design criteria.
3. The correlation shown in Fig. 42 relating undrained cohesive shear strength, C_u, and ultimate resistance coefficient, N_p, was developed for use with the Hay's method in the new design criteria.
4. An additional correlation was developed which makes it possible

to predict a load-rotation curve for rigid drilled shafts. This correlation, shown in Fig. 33, has also been incorporated in the recommended design procedure.

5. Based on the comparison presented in Table 4, Table 5, and Fig. 44 it is concluded that the use of this recommended design procedure produces excellent predictions.

Recommendations

1. Additional lateral load tests should be conducted on rigid drilled shafts of varying depths and diameters founded in a variety of soil types.
2. The effect of sustained loading on drilled shafts should be investigated by constructing shafts of identical geometry in the same soil and testing one under short term applied loads and testing the other under long-term loading conditions.
3. The effect of soil structure (i.e. soft, stiff, fissured or non-fissured) on the time-dependent behavior of drilled shafts should be investigated.
4. The correlation of undrained soil shear strength, C_u, versus ultimate resistance coefficient, N_p, at the ground surface, should be further refined and verified as additional data becomes available.
5. All future drilled shaft field load tests should be instrumented and conducted in such a manner that complete information is gathered and recorded. This complete information

should include the following:

a) Load-deflection data for all load levels.

b) Load-rotation data for all load levels.

c) Soil reaction measurements for the entire length of the shaft for all load levels.

d) Continue the test until it is certain that the ultimate capacity of the shaft has been obtained.

e) Accurate determination of soil shear strength as a function of depth.

6. The recommended design procedure should continue to be verified using future field load test data.

APPENDIX I. - REFERENCES

1. Bhushan, Kul, Haley, Steven C., and Fang, Patrick T., "Lateral Load Tests on Drilled Piers in Stiff Clays," Preprints 3248, ASCE Spring Convention and Exhibit, Pittsburgh, Pennsylvania, April 24-28, 1978.

2. Broms, Bengt B., "Lateral Resistance of Piles in Cohesive Soils," Journal of the Soil Mechanics and Foundation Division, ASCE, Vol. 90, No. SM2, Proc. Paper 3825, March 1964, pp. 27-63.

3. Corbett, David A., Coyle, Harry M., Bartoskewitz, Richard E., and Milberger, Lionel J., "Evaluation of Pressure Cells Used for Field Measurements of Lateral Earth Pressures on Retaining Walls," Research Report No. 169-1, Texas Transportation Institute, Texas A&M University, College Station, Texas, September 1971.

4. Czerniak, E., "Resistance to Overturning of Single Short Piles," Journal of the Structural Division, ASCE, Vol. 83, No. ST2, Proc. Paper 1188, March 1957, pp. 1188-1 - 1188-25.

5. D'Appolonia, Elio, D'Appolonia, David J., and Ellison, Richard D. "Drilled Piers," in Foundation Engineering Handbook, Winterkorn, Hans F., and Fang, Hsai-Yang (ed.), Van Nostrand Reinhold Co., New York, 1975, pp. 601-615.

6. Davisson, M. T., and Gill, H. L., "Laterally Loaded Piles in a Layered Soil System," Journal of the Soil Mechanics and Foundation Division, ASCE, Vol. 89, No. SM3, Proc. Paper 3509, May 1963, pp. 63-94.

7. Duderstadt, Franklin J., Coyle, Harry M., and Bartoskewitz, Richard E., "Correlation of the Texas Cone Penetrometer Test N-Value with Soil Shear Strength," Research Report 10-3F, Texas Transportation Institute, Texas A&M University, College Station, Texas, September 1970.

8. Dunlap, Wayne A., Ivey, Don L., and Smith, Harry L., "Long-Term Overturning Loads on Drilled Shaft Footings," Research Report 105-5F, Texas Transportation Institute, Texas A&M University, College Station, Texas, September 1970.

9. Feagin, L. B., "Lateral Pile Loading Test," Transactions, ASCE, Vol. 102, 1937, pp. 236-254.

10. Focht, John A., and Bramlette McClelland, "Analysis of Laterally Loaded Piles by Difference Equation Solution," Texas Engineer, Texas Section of American Society of Civil Engineers, September-November, 1955.

11. Hansen, J. Brinch, "The Ultimate Resistance of Rigid Piles Against Transversal Forces," Danish Geotechnical Institute, Bulletin 12, 1961.

12. Hays, C. O., Davidson, J. L., Hagan, E. M., and Risitano, R. R., "Drilled Shaft Foundation for Highway Sign Structures," Research Report D647F, Engineering and Industrial Experiment Station, University of Florida, Gainsville, Florida, December 1974.

13. Hetenyi, M., Beams on Elastic Foundation, University of Michigan Press, Ann Arbor, Michigan, and Oxford University Press, London, England, 1946.

14. Holloway, George L., Coyle, Harry M., Bartoskewitz, Richard E., and Sarver, William G., "Filed Test and Preliminary Design Method for Lateral Loaded Drilled Shafts in Clay," Research Report No. 211-2, Texas Transportation Institute, Texas A&M University, College Station, Texas, September 1978.

15. Ismael, Nabil F., and Klym, Tony W., "Behavior of Rigid Piers in Layered Cohesive Soils," Journal of the Geotechnical Engineering Division, ASCE, Vol. 104, No. GT8, August, 1978, pp. 1061-1074.

16. Ivey, Don L., and Hawkins, Leon, "Signboard Footings to Resist Wind Load," Civil Engineering, Vol. 36, No. 12, December 1966, pp. 34-35.

17. Ivey, Don L., "Theory, Resistance of a Drilled Shaft Footing to Overturning Loads," Research Report 105-1, Texas Transportation Institute, Texas A&M University, College Station, Texas, February 1968.

18. Ivey, Don L., Koch, Kenneth J., and Raba, Carl F., Jr., "Resistance of a Drilled Shaft Footing to Overturning Loads, Model Tests and Correlation with Theory," Research Report 105-2, Texas Transportation Institute, Texas A&M University, College Station, Texas, July 1968.

19. Ivey, Don L., and Dunlap, Wayne A., "Design Procedure Compared to Full-Scale Tests of Drilled Shaft Footings," Research Report 105-3, Texas Transportation Institute, Texas A&M University, College Station, Texas, February 1970.

20. Kasch, Vernon R., Coyle, Harry M., Bartoskewitz, Richard E., and Sarver, William G., "Design of Drilled Shafts to Support Precast Panel Retaining Walls," Research Report No. 211-1, Texas Transportation Institute, Texas A&M University, College Station, Texas, November 1977.

21. Lytton, Robert L., "Design Charts for Minor Service Structure Foundations," Research Report 506-1F, Texas Transportation

Institute, Texas A&M University, College Station, Texas, September 1971.

22. McClelland, Bramlette, and Focht, John A., Jr., "Soil Modulus for Laterally Loaded Piles," Journal of the Soil Mechanics and Foundation Division, ASCE, Vol. 82, No. SM4, Proc. Paper 1081, October 1956, pp. 1081-1 - 1081-22.

23. Matlock, Hudson, and Reese, Lymon C., "Generalized Solutions for Laterally Loaded Piles," Journal of the Soil Mechanics and Foundation Division, ASCE, Vol. 86, No. SM5, Part I, Proc. Paper 2626, October 1960, pp. 63-91.

24. Matlock, Hudson, "Correlations for Design of Laterally Loaded Piles in Soft Clay," Preprints, Second Annual Offshore Technology Conference, Paper No. OTC 1204, 1970, pp. 577-594.

25. Reese, Lymon C., Discussion of "Soil Modulus for Laterally Loaded Piles," by Bramlette McClelland and John A. Focht, Jr., Transactions, ASCE, Vol. 123, 1958, pp. 1071-1074.

26. Reese, Lymon C., and Cox, William R., "Soil Behavior from Analysis of Tests of Uninstrumented Piles Under Lateral Loading," ASTM Special Technical Publication 444, 1969, pp. 160-176.

27. Reese, Lymon C., Cox, William R., and Koop, Francis, D., "Field Testing and Analysis of Laterally Loaded Piles in Stiff Clay," Preprints, Seventh Annual Offshore Technology Conference, Paper No. OTC 2312, 1975, pp. 671-690.

28. Reese, Lymon C., and Welch, R. C., "Lateral Loading of Deep Foundations in Stiff Clay," Journal of the Geotechnical Division, ASCE, Vol. 101, No. 677, Proc. Paper 11456, July 1975, pp. 633-699.

29. Reese, Lymon C., O'Neill, M. W., and Touma, F. T., "Behavior of Drilled Piers Under Axial Loading," Journal of the Geotechnical Engineering Division, ASCE, Vol. 102, No. GT5, May 1976, pp. 493-510.

30. Reese, Lymon C., "Laterally Loaded Piles: Programming Documentation," Journal of the Geotechnical Engineering Division, ASCE, Vol. 103, No. GT4, Proc. Paper 12862, April 1977, pp. 287-305.

31. Reese, Lymon C., "Design and Construction of Drilled Shafts," Journal of the Geotechnical Engineering Division, ASCE, Vol. 104, No. GT1, January 1978, pp. 95-116.

32. "Report on Pier Loading Tests," unpublished report for Dow Chemical U.S.A., Plant A., Freeport, Texas, Prepared by Spencer J. Buchanan and Associates, Inc., Bryan, Texas, May 1977.

33. Seiler, J. F., "Effect of Depth of Embedment of Pole Stability," Wood Preserving News, Vol. 10, No. 11, November 1932, pp. 152-168.

34. Shilts, W. L., Graves, L. D., and Driscoll, G. G., "A Report of Field and Laboratory Tests on the Stability of Posts Against Lateral Loads," Proceedings, Second International Conference on Soil Mechanics and Foundation Engineering, Vol. 5, Rotterdam, Holland, 1948, pp. 107-122.

35. Skempton, A. W., "The Bearing Capacity of Clays," Proceedings, Building Research Congress, Division I, Part III, London, England, 1951, pp. 180-189.

36. Terzaghi, Karl, "Evaluation of Coefficients of Subgrade Reaction," Geotechnique, London, England, Vol. 5, No. 4, December 1955, pp. 297-326.

37. Terzaghi, Karl, and Peck, Ralph B., Soil Mechanics in Engineering Practice, 2nd ed., John Wiley & Sons, Ltd, New York, 1967, pp. 198-200.

38. Vesic, Aleksandar B., "Bending of Beams Resting on Isotropic Elastic Solid," Journal of the Engineering Mechanics Division, ASCE, Vol. 87, No. EM2, Proc. Paper 2800, April 1961, pp. 35-53.

39. Welch, Robert C., and Reese, Lymon C., "Lateral Load Behavior of Drilled Shafts," Research Report 89-10, Center for Highway Research, The University of Texas, Austin, Texas, May 1972.

40. Woodward, Richard, J., Gardner, William S., and Greer, David M., Drilled Pier Foundations, McGraw-Hill Book Co., New York, 1972.

41. Wright, William V., Coyle, Harry M., Bartoskewitz, Richard E., and Milberger, Lionel J., "New Retaining Wall Design Criteria Based on Lateral Earth Pressure Measurements," Research Report No. 169-4F, Texas Transportation Institute, Texas A&M University, College Station, Texas, August 1975.

APPENDIX II. - NOTATION

The following symbols are used in this thesis:

B = shaft diameter;

C_u = undrained cohesive shear strength;

D = embedded depth;

E = modulus of elasticity of foundation;

E_s = soil modulus;

EI = flexural stiffness of foundation;

F = applied lateral load;

F_r = resultant force transmitted from retaining wall to drilled shaft;

H = height of lateral load application;

h = height of retaining wall;

I = moment of inertia of foundation;

K_a = Rankine coefficient of active earth pressure;

K_c = theoretical earth pressure coefficient;

k = coefficient of lateral subgrade reaction;

L = length of precast panel;

M = applied moment;

N = blow count from TCP test;

N_p = ultimate resistance coefficient;

P_x = axial load on foundation;

P_ω = any intermediate load corresponding to an arbitrary shaft rotation, ω, between 0 and 2 degrees;

P_{2^o} = the lateral load at a rotation of 2 degrees;

P_ω/P_{2o} = ultimate load ratio;

P = soil reaction;

P_u = ultimate soil reaction;

P_{u_o} = ultimate soil reaction at groundline;

S_d = design load;

S_u = ultimate applied lateral load;

WF = wide flange;

X = depth below groundline;

X_r = depth of reduced resistance;

y = lateral deflection;

Z = depth to rotation point;

α = slope of Hays soil reaction curve;

β = nondimensional variable;

γ = unit weight of overburden material;

ζ = angle of slope of backfill to horizontal;

η = soil strength reduction factor;

θ = limiting angle of rotation;

ϕ = angle of shearing resistance;

ϕ' = effective angle of shearing resistance; and

ω = shaft rotation between 0 and 2 degrees.

NOTES